



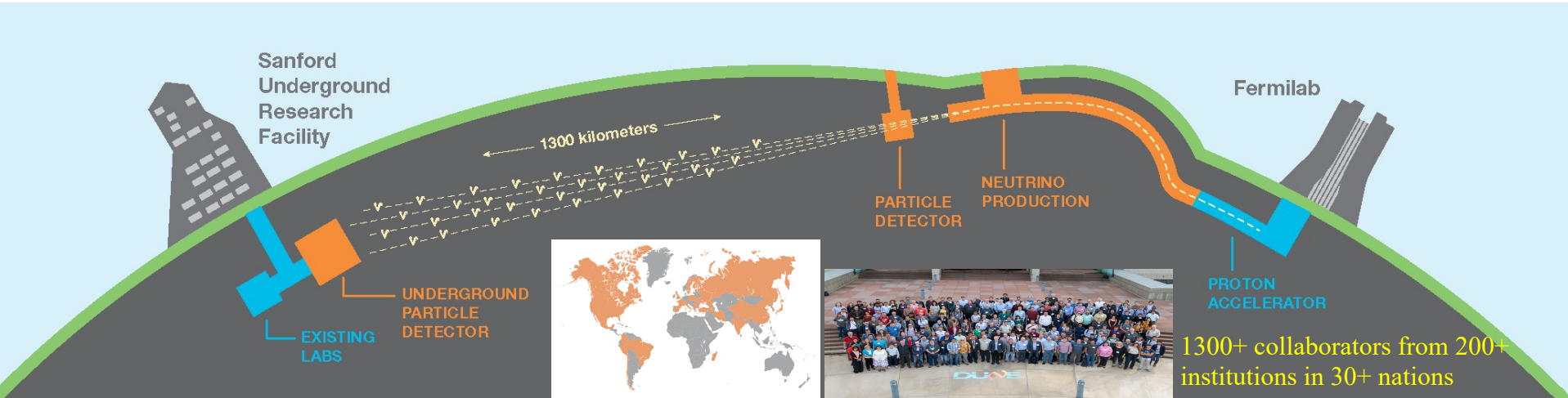
# The DUNE Neutrino Experiment

*Jianming Bian*  
*University of California,*  
*Irvine*

*08-24-2021*

*CCEPP Summer School 2021 on Neutrino Physics*

# DUNE DEEP UNDERGROUND NEUTRINO EXPERIMENT



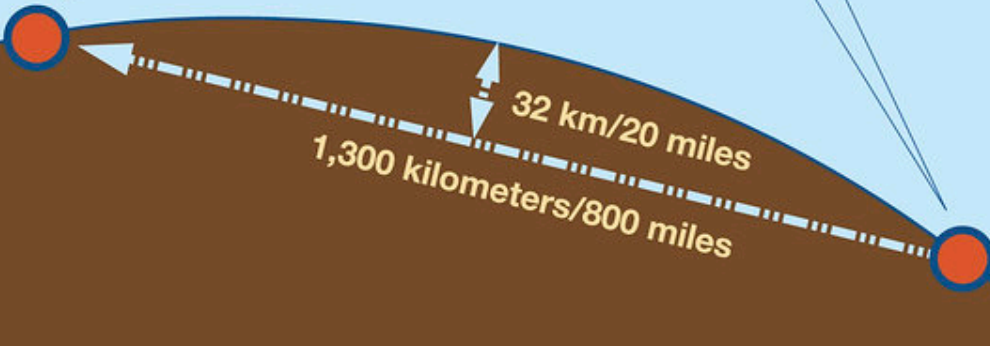
- New neutrino beam at Fermilab (1.2 MW@80 GeV protons, upgradeable to 2.4 MW), 1300 km baseline
- 70 kton Liquid Argon Time Projection Chamber (LArTPC) Far Detector at Sanford Underground Research Facility, South Dakota, 1.5 km underground
- Multiple technologies for the Near Detector (ND)
- $\nu_e$  appearance and  $\nu_\mu$  disappearance  $\rightarrow$  Neutrino mass ordering and CP violation
- Large detector, deep underground, high intensity beam  $\rightarrow$  Supernova burst neutrinos, atmospheric neutrinos, nucleon decay and other BSM, etc
- Excavation started in 2017, begin taking data in late 2020s

# DUNE DEEP UNDERGROUND NEUTRINO EXPERIMENT

## Deep Underground Neutrino Experiment

Sanford Underground  
Research Facility  
Lead, South Dakota

Fermi National  
Accelerator Laboratory  
Batavia, Illinois



- $\nu_e$  appearance and  $\nu_\mu$  disappearance  $\rightarrow$  Neutrino mass ordering and CP violation
- Large detector, deep underground, high intensity beam  $\rightarrow$  Supernova burst neutrinos, atmospheric neutrinos, nucleon decay and other BSM, etc
- Excavation started in 2017, begin taking data in late 2020s



# DUNE Collaboration

1300+ collaborators from 200+ institutions in 30+ nations



# Long-Baseline Neutrino Oscillation

$\nu_\mu$  disappearance:

$$P(\nu_\mu \rightarrow \nu_\mu) \approx 1 - \sin^2 2\theta_{23} \sin^2 \left( \frac{\Delta m_{32}^2 L}{4E} \right)$$

Provide high precision  $|\Delta m_{32}^2|$  and  $\sin^2 2\theta_{23}$

$\nu_e$  appearance:

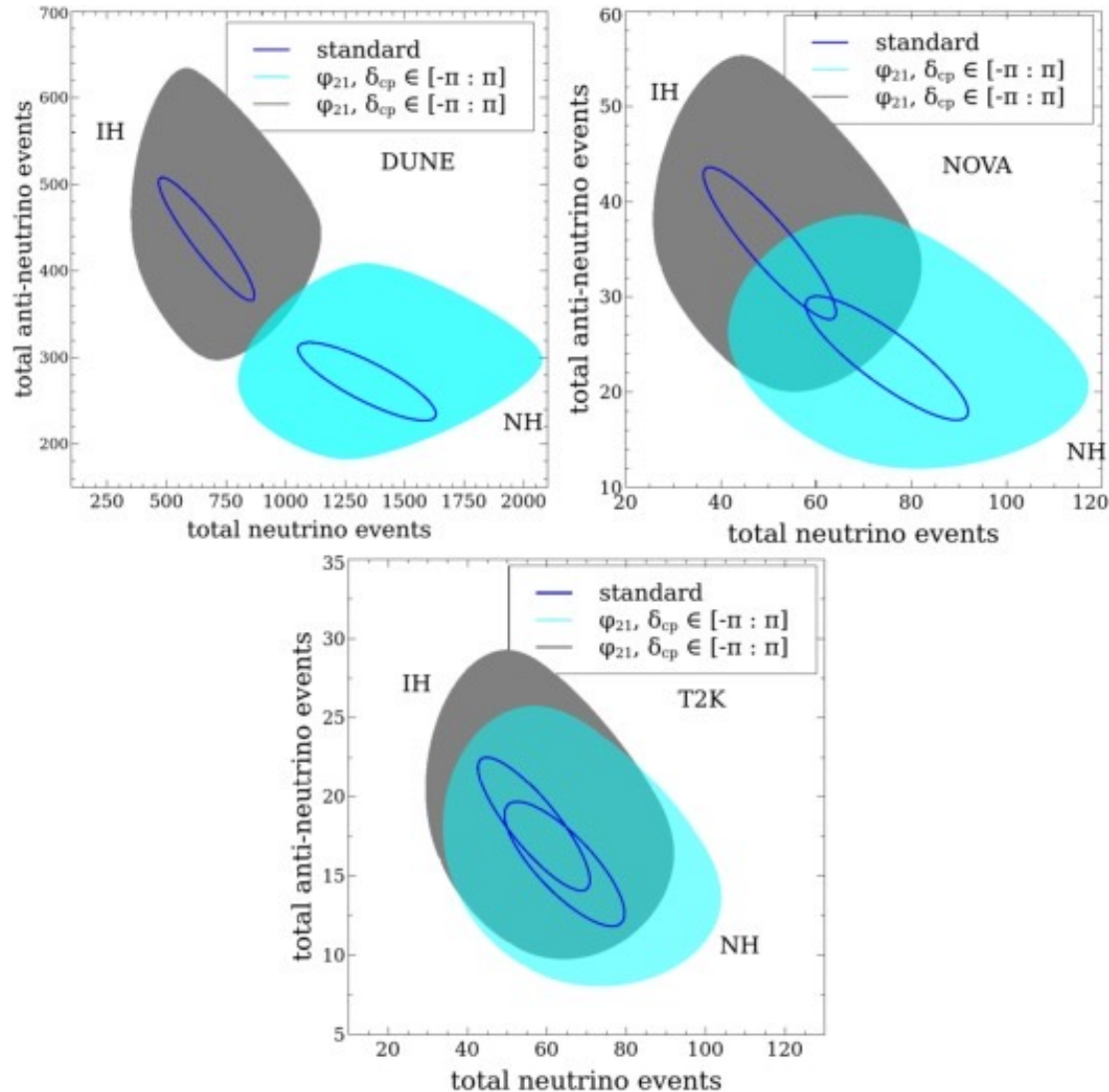
$$P(\nu_\mu \rightarrow \nu_e) \approx \sin^2 \theta_{23} \sin^2 2\theta_{13} \sin^2(\Delta m_{32}^2 L / 4E) + f(\delta_{CP}, \Delta m_{31}^2, \sin^2 2\theta_{23})$$

Measure mass ordering,  $\delta_{CP}$  and octant of  $\theta_{23}$

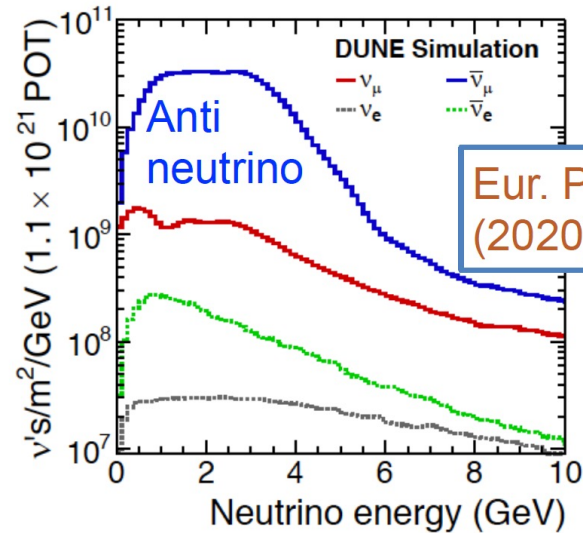
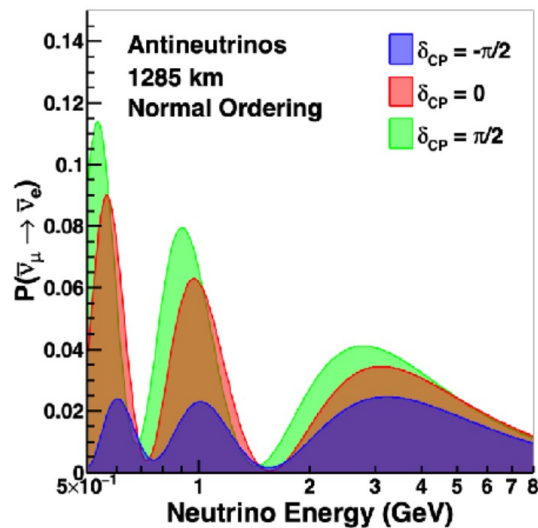
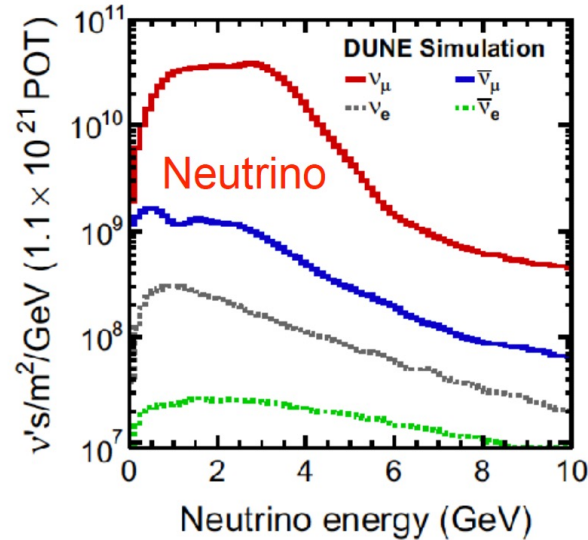
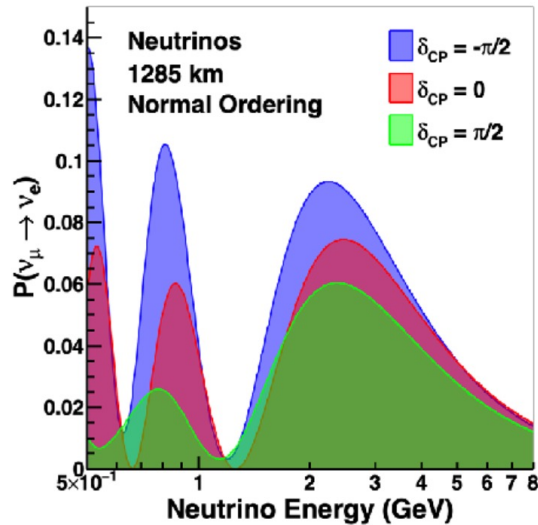
- $\sin^2 2\theta_{13}$  measured by reactor experiments
- $|\Delta m_{23}^2|$  and  $\sin^2 2\theta_{23}$  constraint by  $\nu_\mu$  disappearance
- $P(\nu_\mu \rightarrow \nu_e)$  difference between  $\Delta m_{31}^2 > 0$  and  $\Delta m_{31}^2 < 0$  enlarged by matter effect ( $\propto L$ )

*Matter effect is the correction to neutrino effective masses, when they travel through matter and scatter on electrons*

# $\nu_e$ appearance - $\bar{\nu}_e$ vs anti- $\nu_e$ events



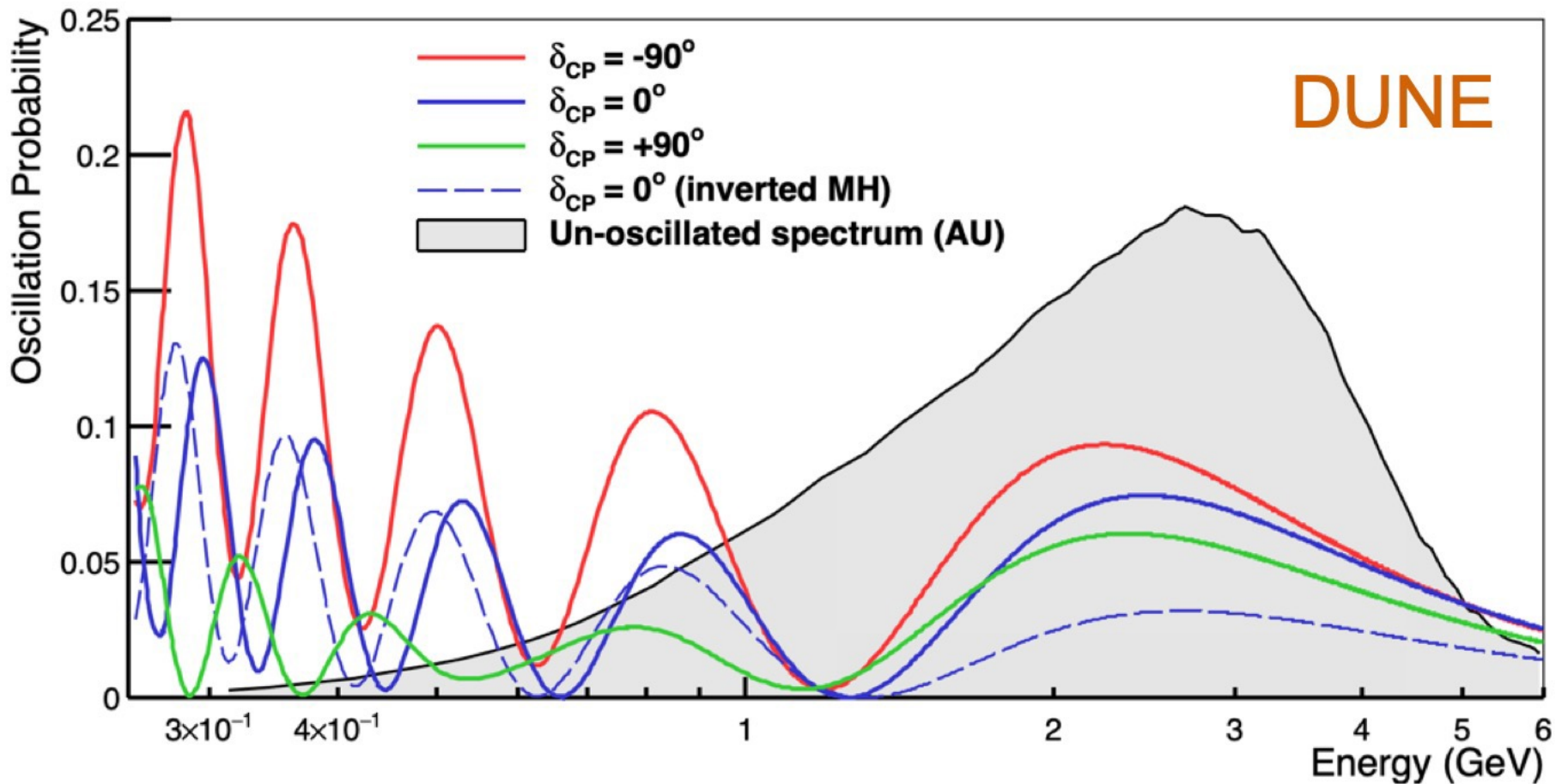
# $\nu_e$ appearance in DUNE



Eur. Phys. J. C  
(2020) 80:978

- On-axis wideband beam covering main oscillation features at 1295 km
- High performance detector to control beam backgrounds

# $\nu_e$ appearance in DUNE



- On-axis wideband beam covering main oscillation features at 1295 km
- High performance detector to control beam backgrounds

# Why Liquid Argon

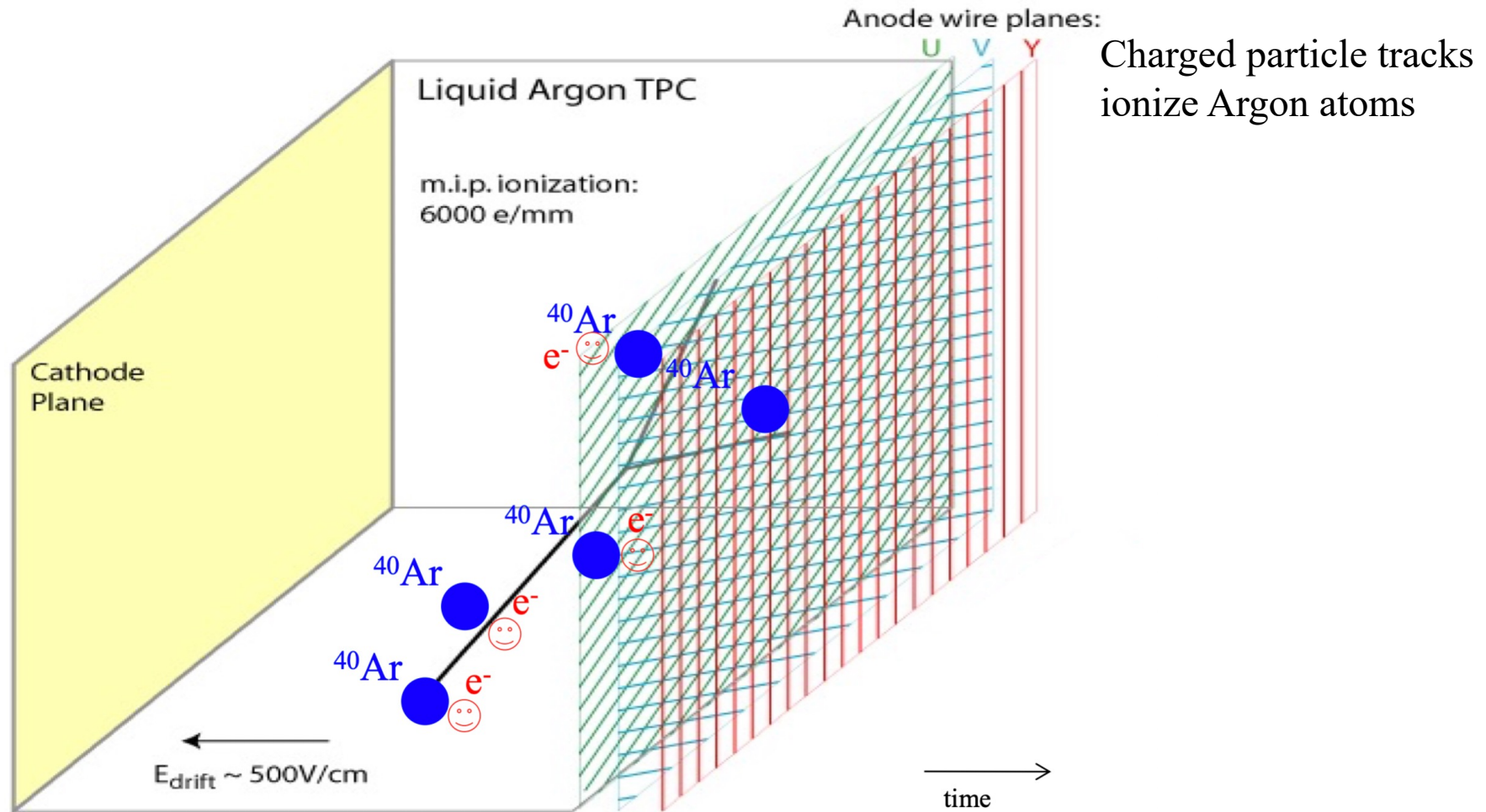
- Abundant ionization electrons and scintillation light can both be used for detection
- If liquids are highly purified ( $<0.1$ ppb), ionization can be drifted over long distances
- Excellent dielectric properties accommodate very large voltages
- Argon is relatively cheap and easy to obtain (1% of atmosphere)
- Noble liquids are dense, so they make a good target for neutrinos



Boiling Point [K] @ 1atm	4.2	27.1	87.3	120.0	165.0	373
Density [g/cm <sup>3</sup> ]	0.125	1.2	1.4	2.4	3.0	1
Radiation Length [cm]	755.2	24.0	14.0	4.9	2.8	36.1
dE/dx [MeV/cm]	0.24	1.4	2.1	3.0	3.8	1.9
Scintillation [ $\gamma$ /MeV]	19,000	30,000	40,000	25,000	42,000	
Scintillation $\lambda$ [nm]	80	78	128	150	175	
Price [\$/Liter]	~10	~100	~1	~300	~3000	~1

# Liquid Argon Time Projection Chamber (LArTPC)

The principle of LArTPC  
- 3D track reconstruction

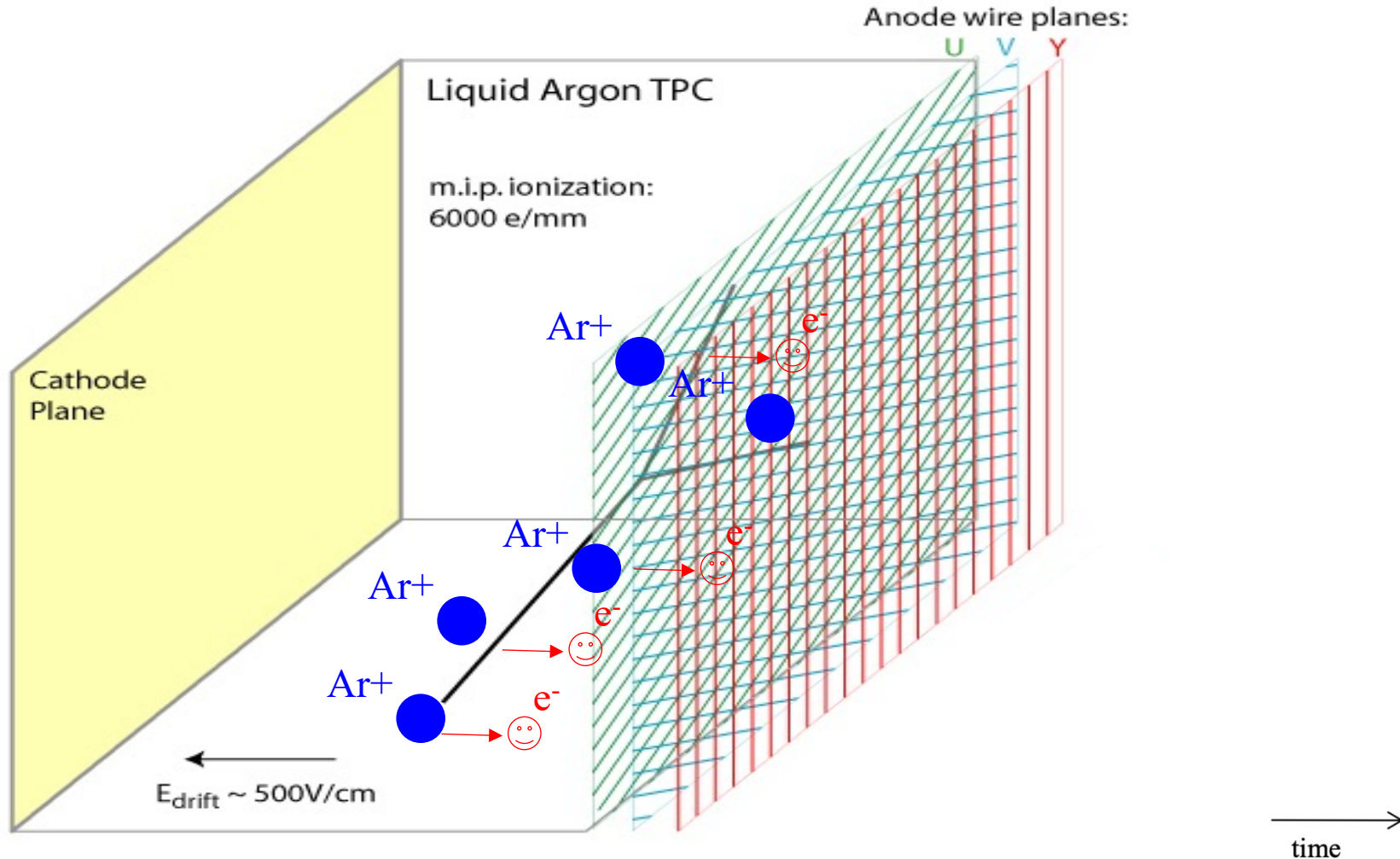




# Liquid Argon Time Projection Chamber (LArTPC)

The principle of LArTPC  
- 3D track reconstruction

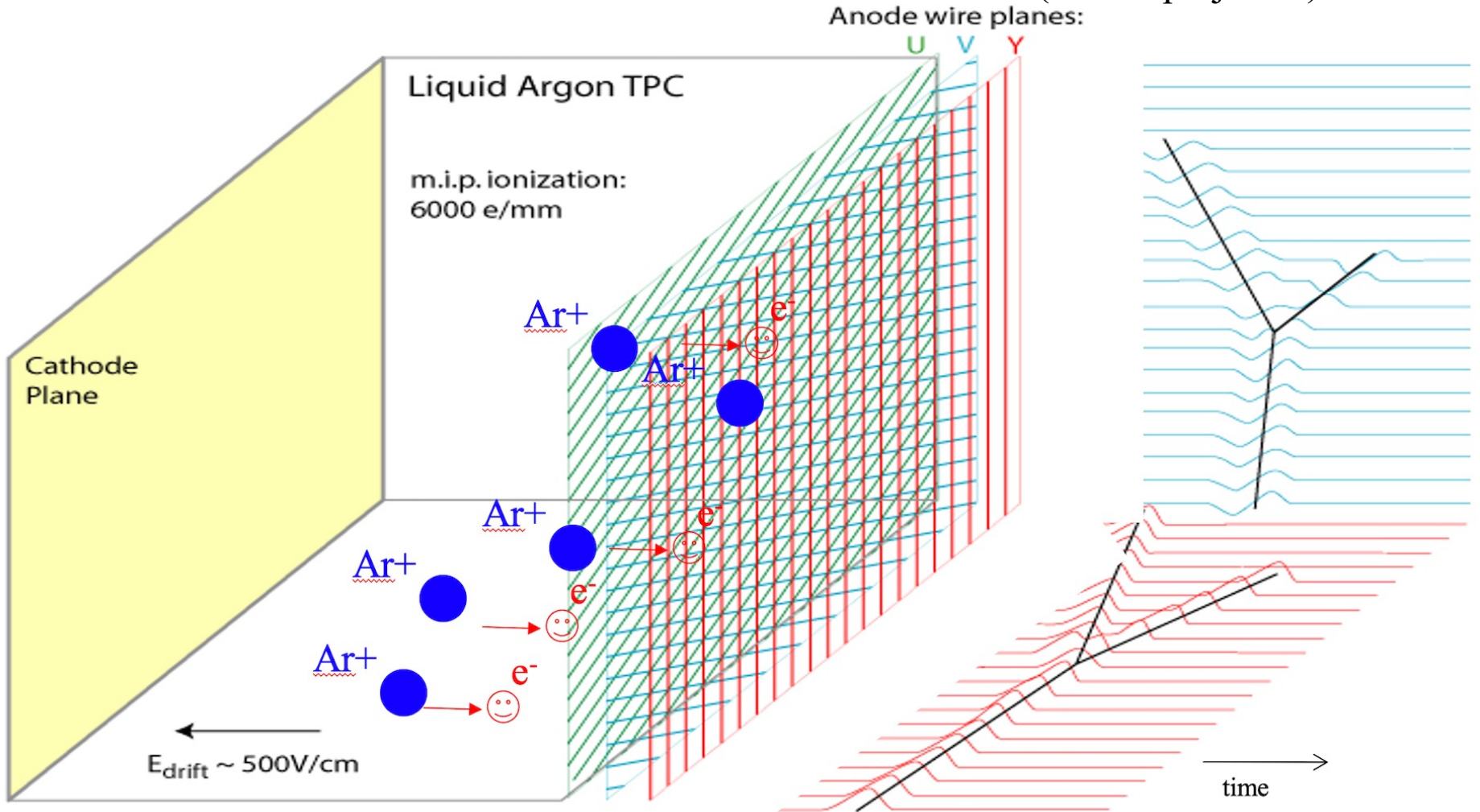
Electrons near the wires are collected first, and electrons far from the wires are collected last, so drift coordinate information is converted to electron drift time (time is projected)



# Liquid Argon Time Projection Chamber (LArTPC)

The principle of LArTPC  
- 3D track reconstruction

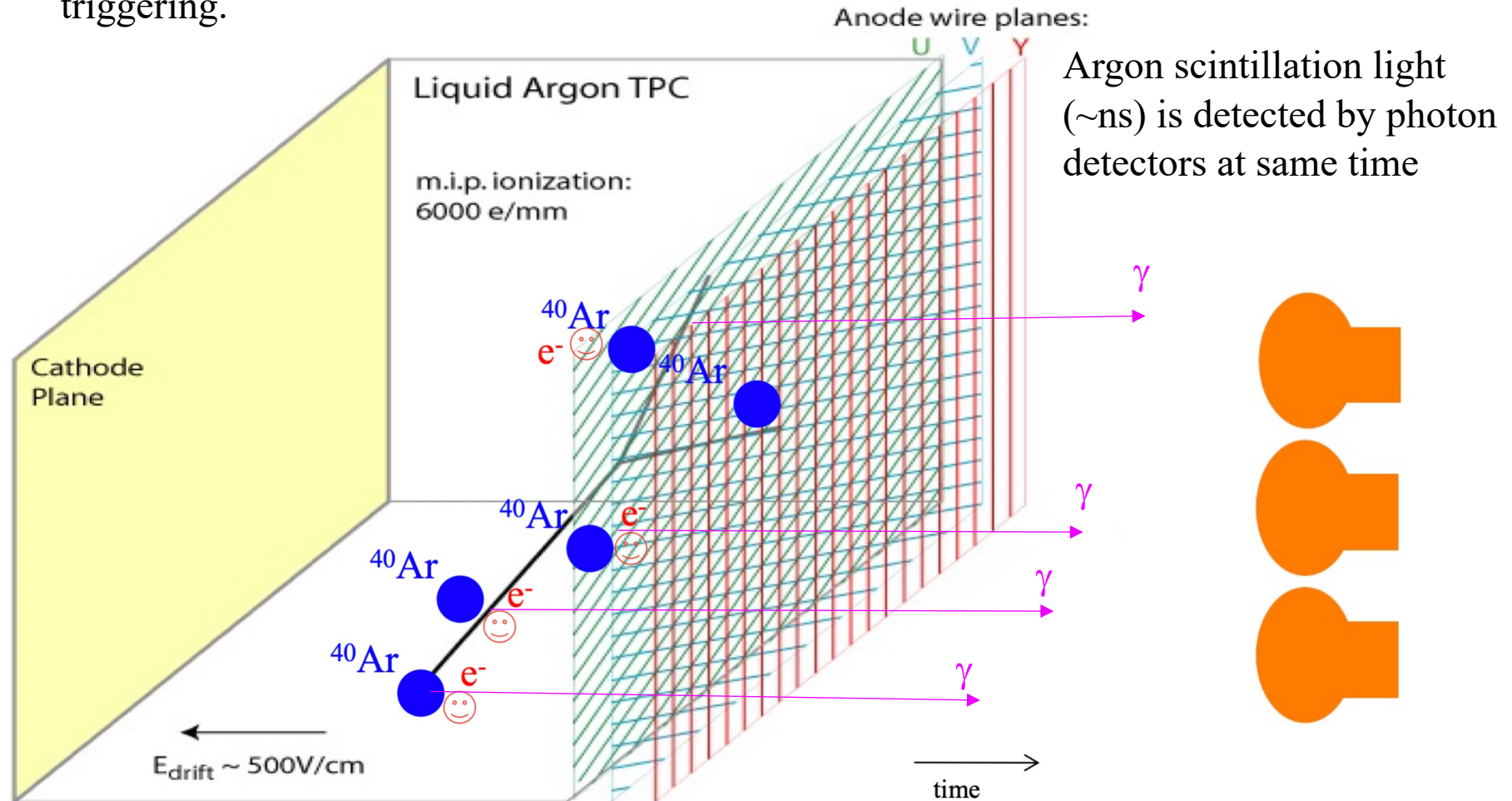
Electrons near the wires are collected first, and electrons far from the wires are collected last, so drift coordinate information is converted to electron drift time (time is projected).



# Liquid Argon Time Projection Chamber (LArTPC)

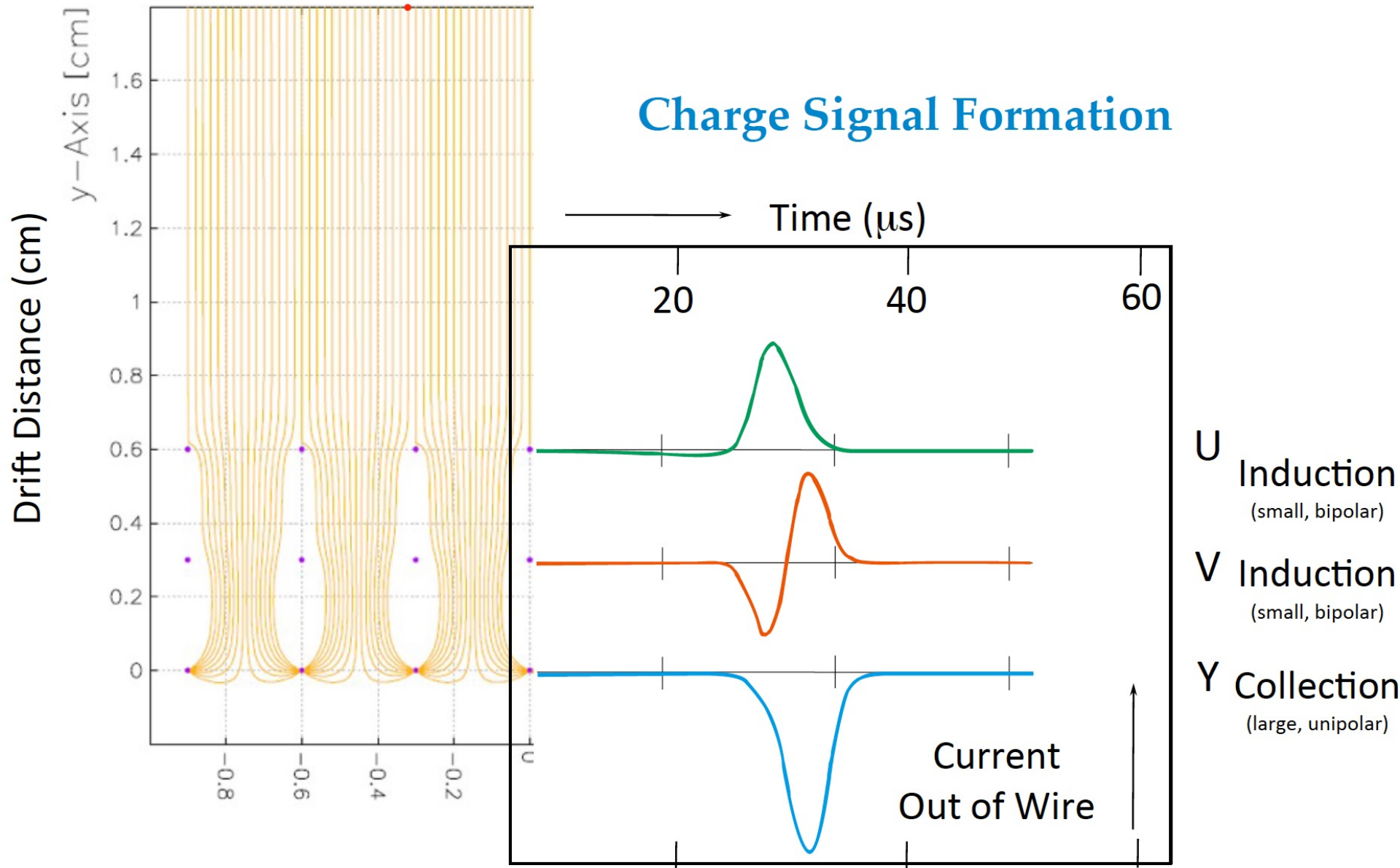
The principle of LArTPC

- 3D track reconstruction
- Abundant scintillation light, which LAr is transparent to, also available for collection and triggering.

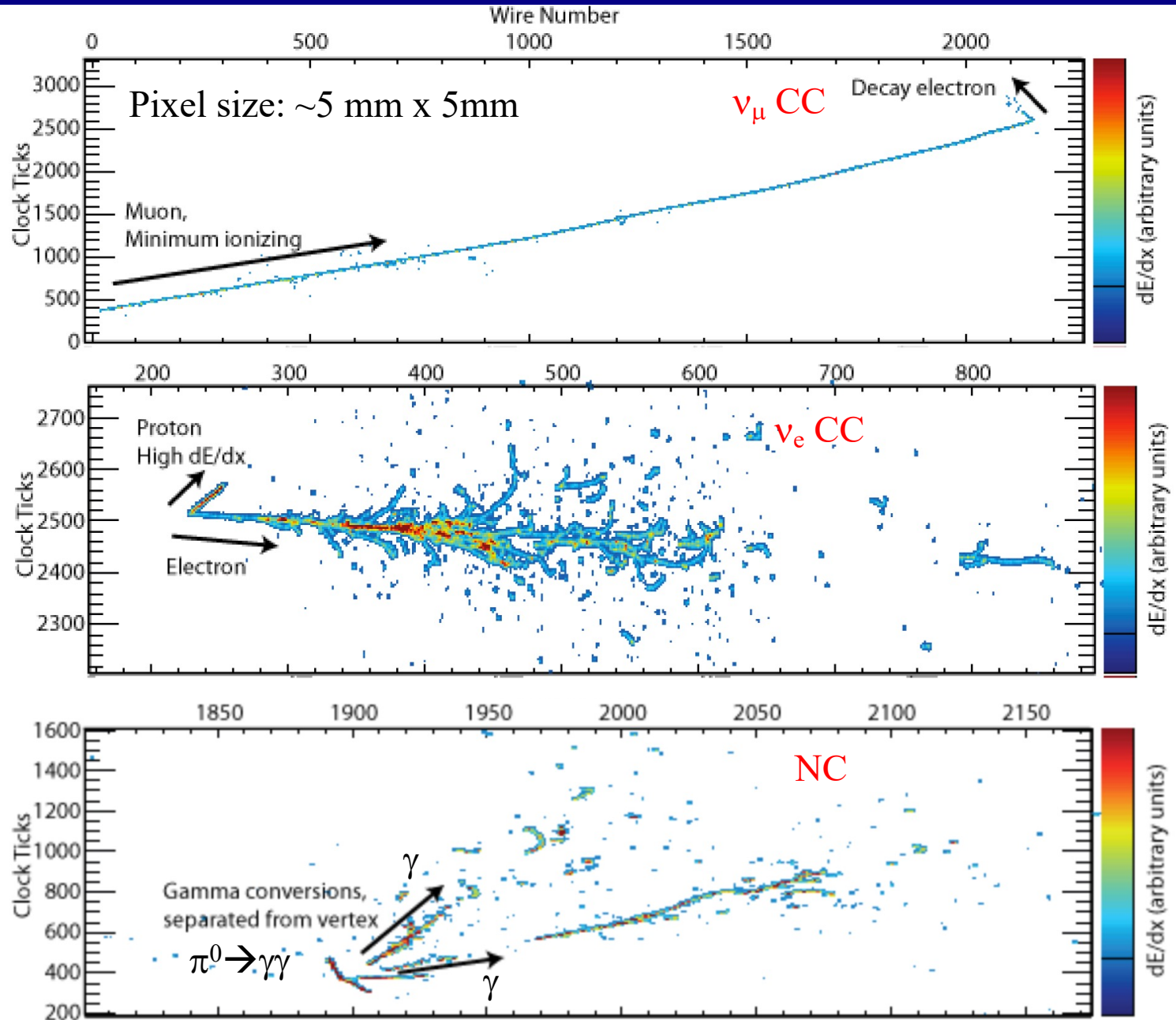


Argon scintillation light ( $\sim\text{ns}$ ) is detected by photon detectors at same time

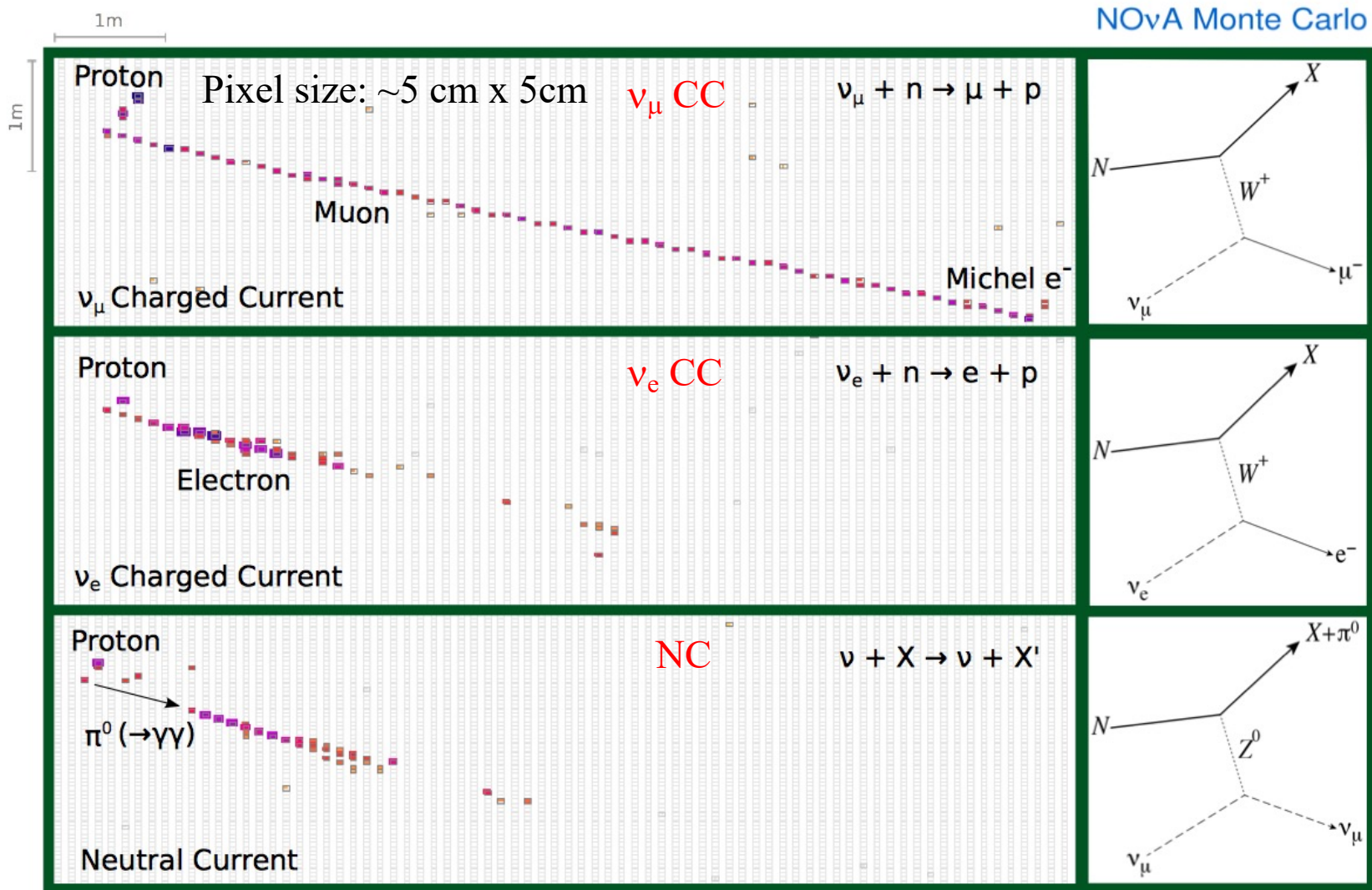
# Liquid Argon Time Projection Chamber (LArTPC)



# Neutrino Interaction in LArTPC (MicroBooNE)

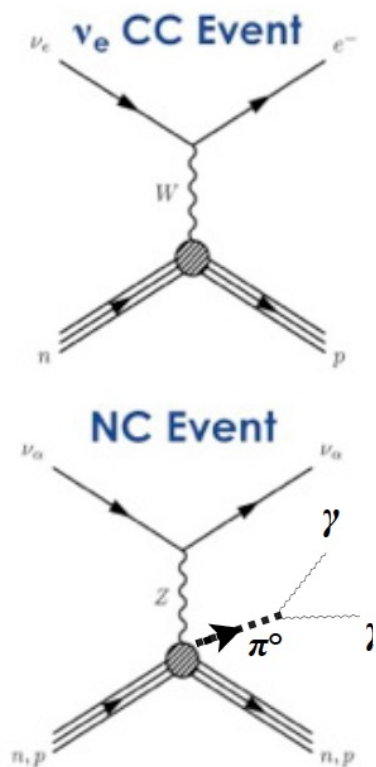


# Neutrino Interaction in scintillator detector (NOvA)

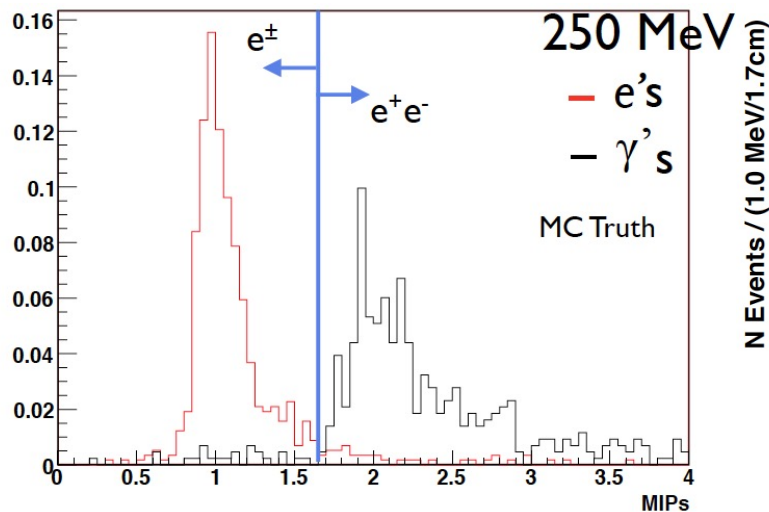


# e/ $\gamma$ separation in LArTPC

- Particle identification comes primarily from  $dE/dx$  (energy deposited) along track.
- Millimeter wire spacing plus appropriate sampling provides fine-grained resolution.
- $\nu_e$  appearance: Excellent signal (CC  $\nu_e$ ) efficiency and background (NC  $\pi^0$ ) rejection

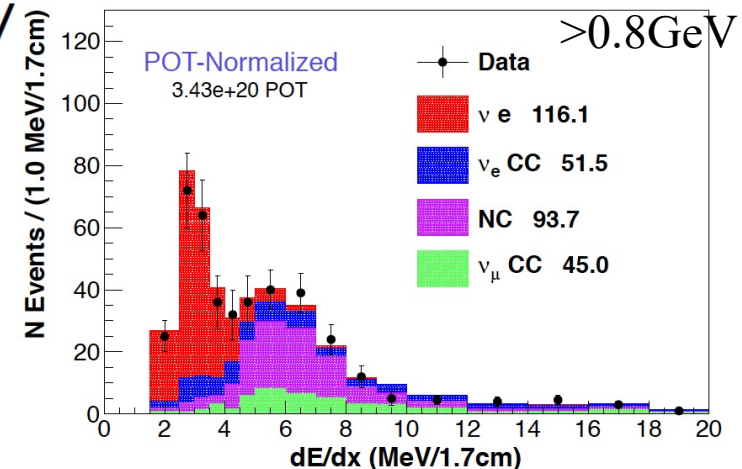


LArTPC (ArgoNeuT)  
Wire pitch  $\sim 4$  mm,  $X_0 \sim 14$  cm



$dE/dx$  for electrons and photons in the first 2.4 cm of track

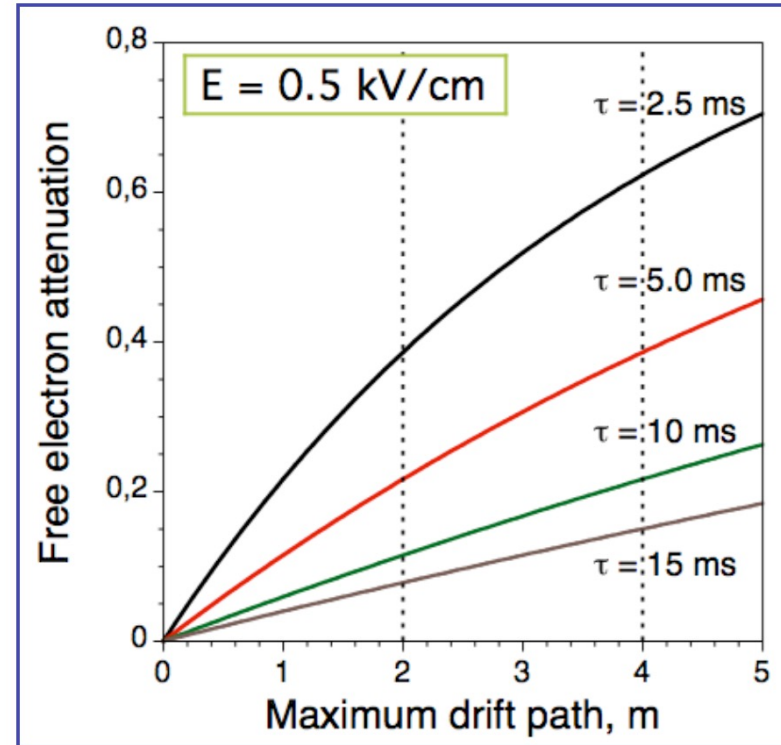
Liquid scintillator tracker (MINERvA)  
strip pitch  $\sim 1.7$  cm,  $X_0 \sim 40$  cm



$dE/dx$  for electrons and backgrounds in the first 6.8 cm of track

# LAr Purity for large LArTPC detectors

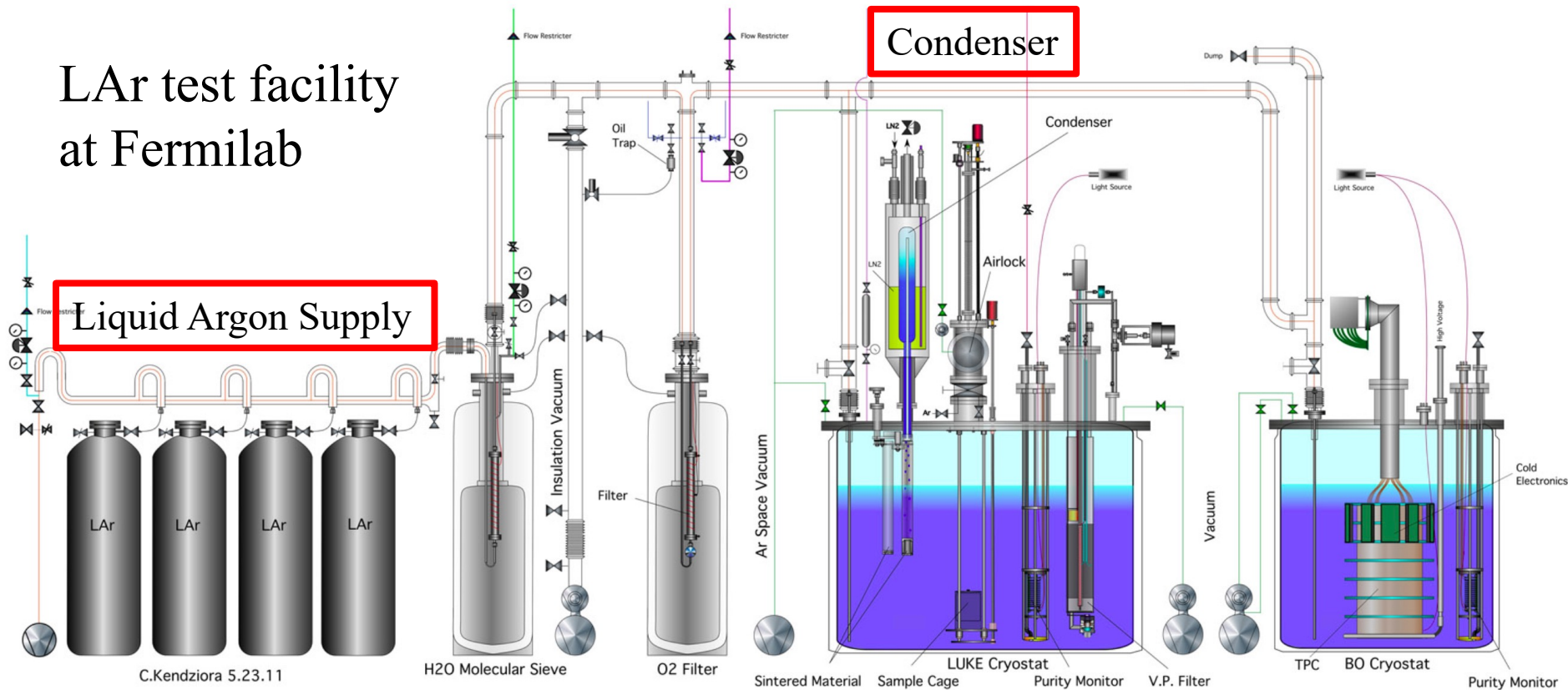
- The key component of LArTPC operation and calibration is the purity of liquid argon
- Signal charge attenuation caused by drift electrons captured by impurities such as  $O_2$  and  $H_2O$ .
- Electron drift lifetime is inversely proportional to the contamination.
- Requirement: less than 100 parts per trillion (ppt)  $O_2$  equivalent or electron lifetime  $> 3$  ms.
- Commercial liquid argon purity  $\sim 1$  ppm  $\rightarrow$  need high performance purification



# LAr Cryogenic and Cryostat

- LAr cryogenic system continuously purify and recirculate argon
- Commercial LAr passes through molecular sieve to remove water then activated copper to remove oxygen.
- Recirculate liquid/gaseous argon to actively remove impurities

LAr test facility  
at Fermilab



Liquid Argon Supply

Condenser

Argon Purification System

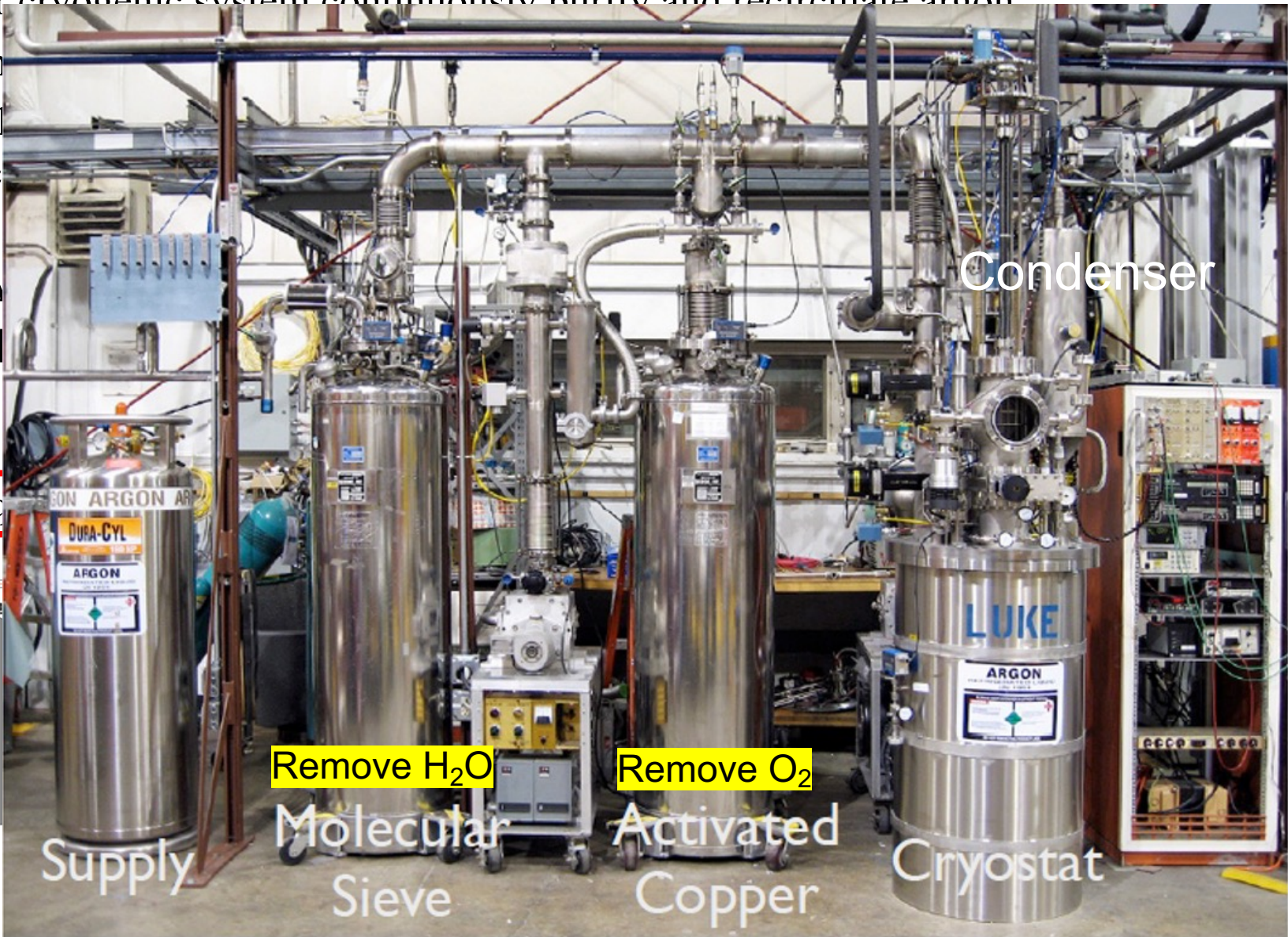
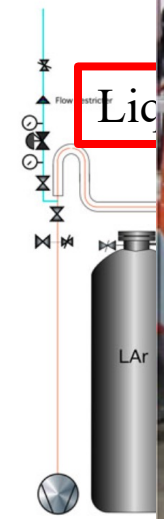
Luke – Cryostat for  
purity/material test

Bo – Cryostat for  
purity/TPC test

# LAr Cryogenic and Cryostat

- LAr cryogenic system continuously purify and recirculate argon
- Compressor
- Recirculation

LAr  
at L



Remove H<sub>2</sub>O

Remove O<sub>2</sub>

Supply

Molecular Sieve

Activated Copper

Cryostat

Condenser

Cold Electronics

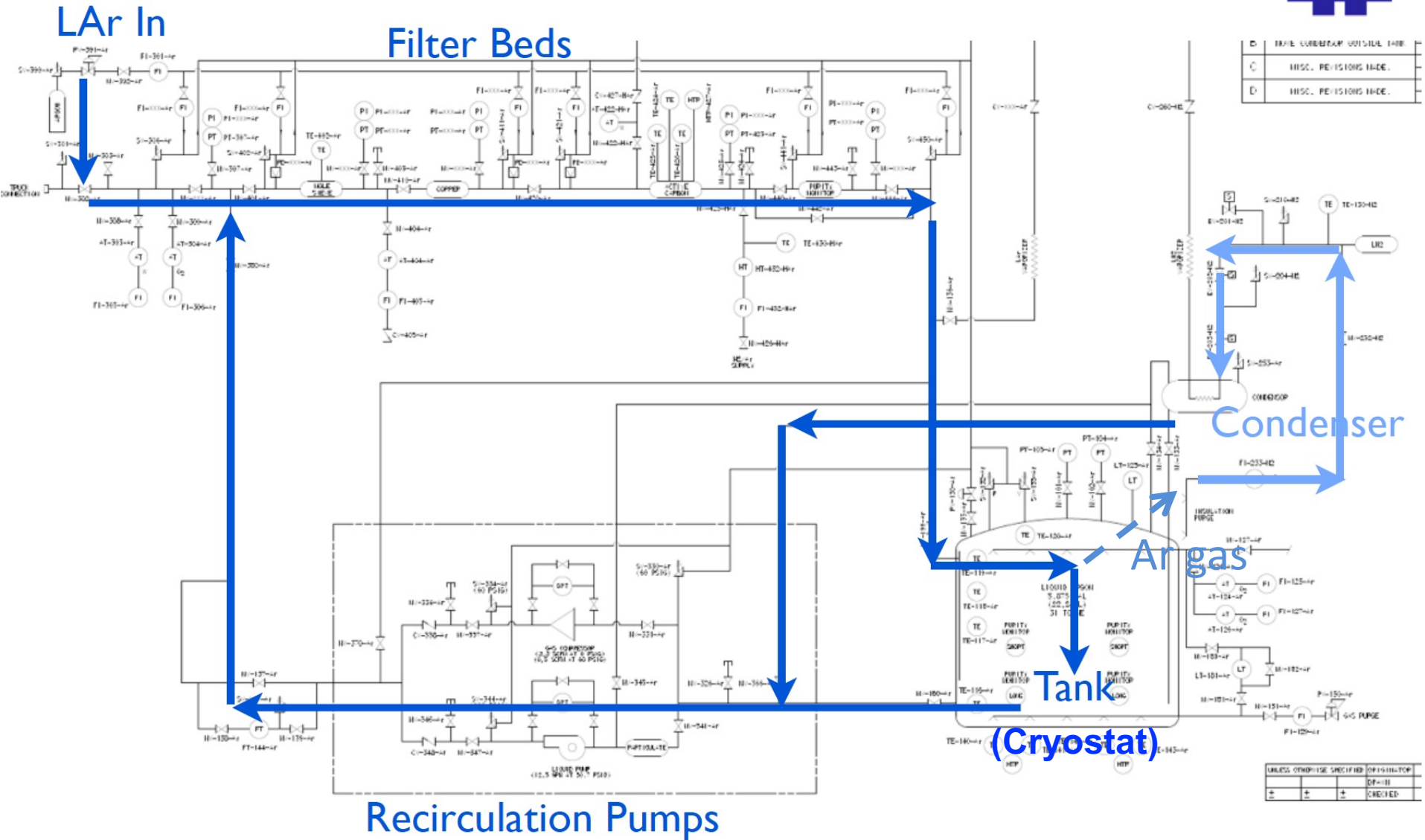
Purity Monitor

purity/material test

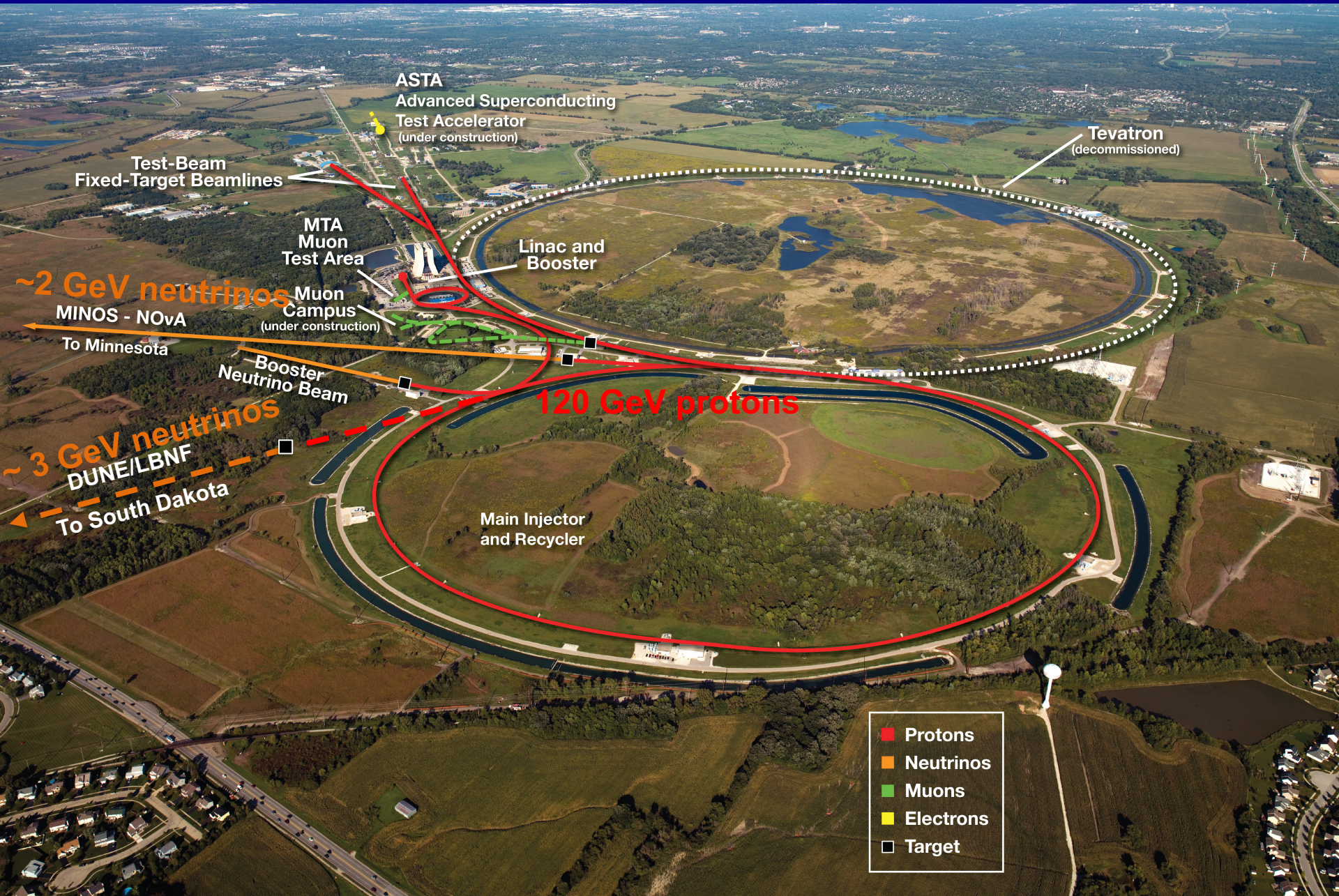
purity/IPC test

for

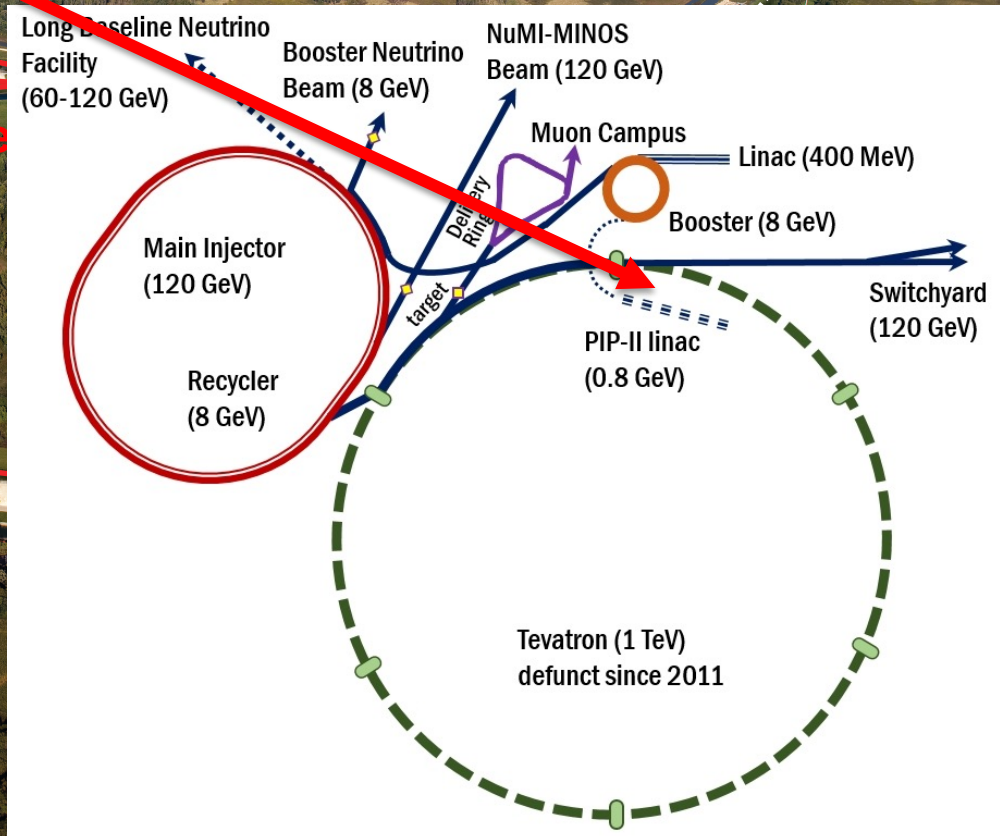
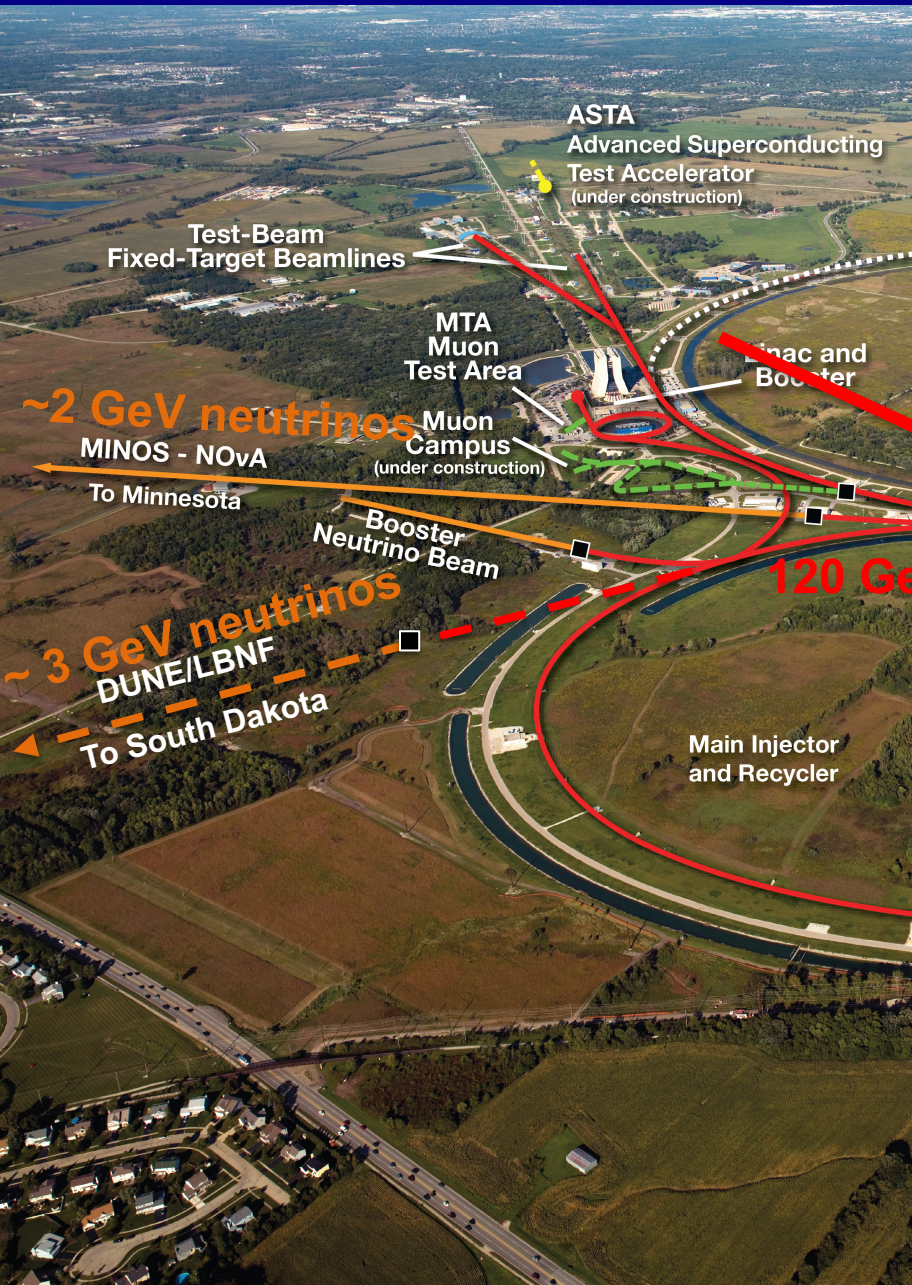
# LAr Cryogenic and Cryostat



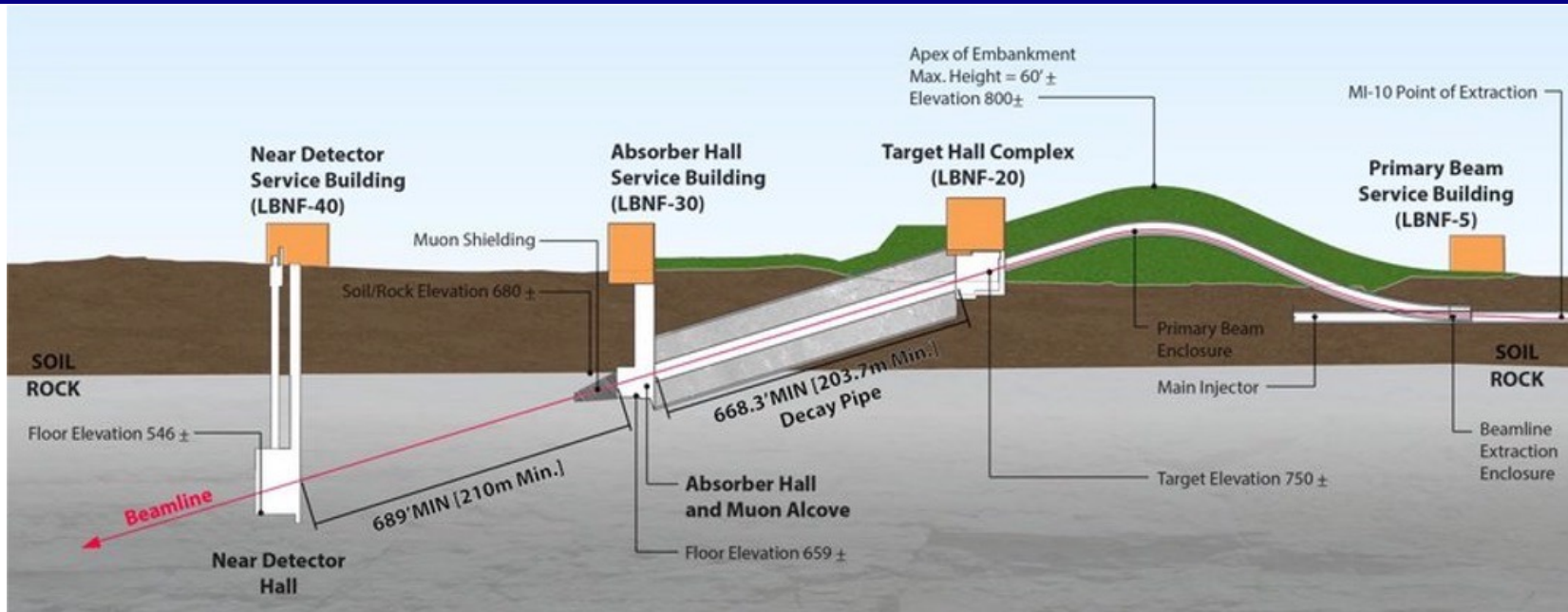
# Accelerator Neutrino Beams at Fermilab Near Chicago



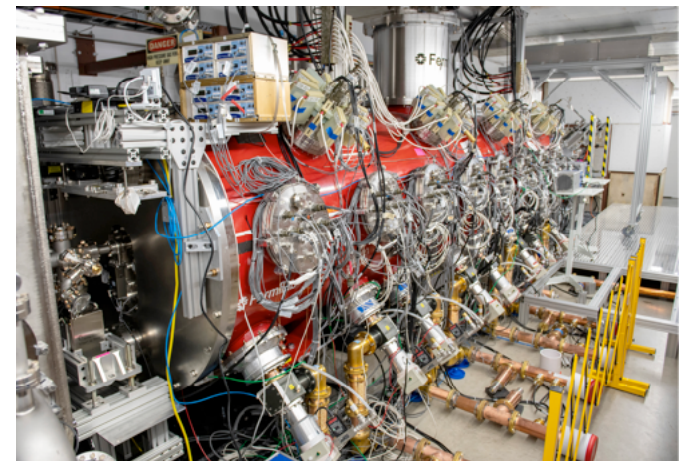
# Accelerator Neutrino Beams at Fermilab Near Chicago



# LBNF Beam for DUNE

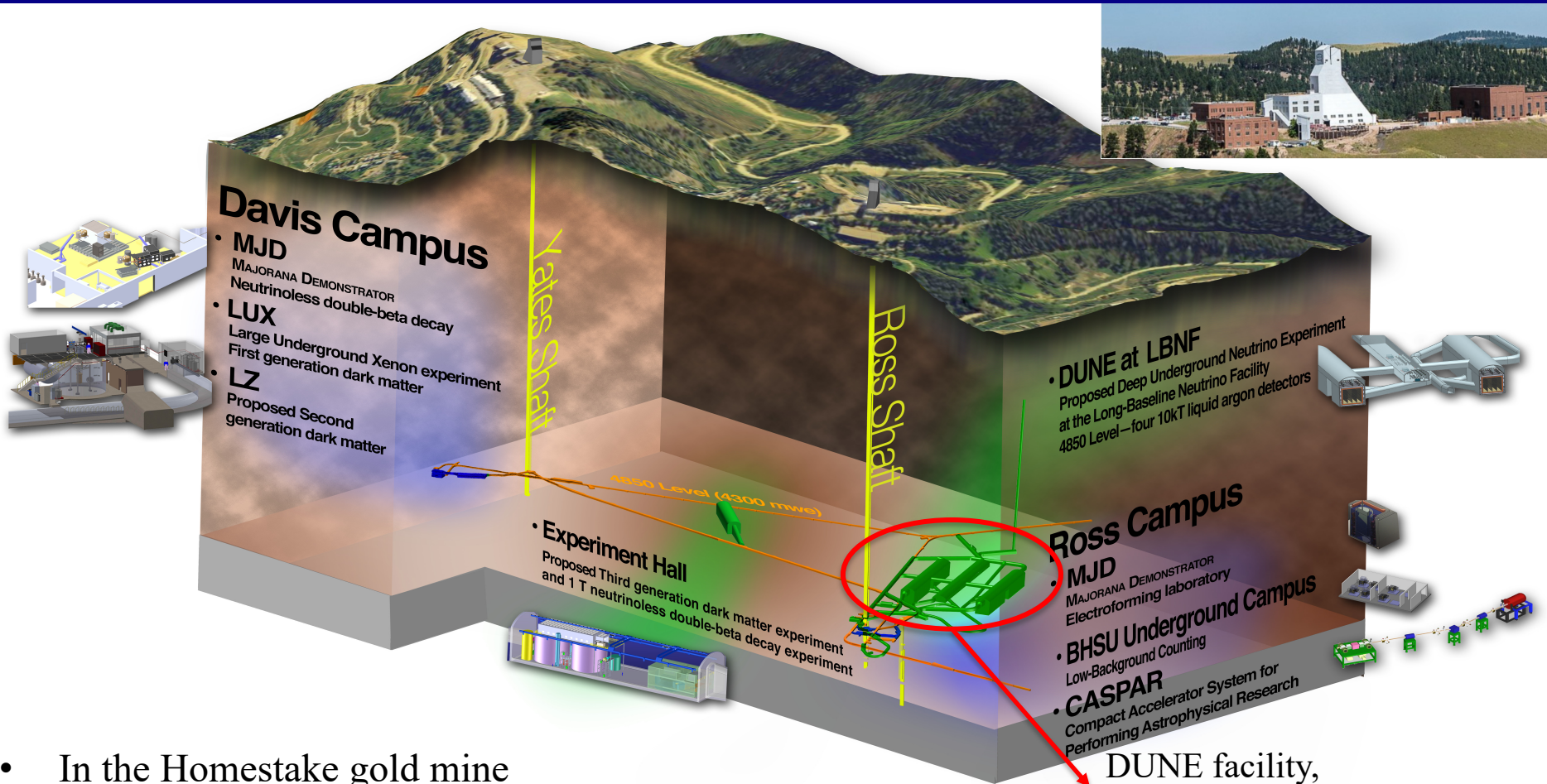


- Proton beam
  - Proton Improvement Plan-II (PIP-II)
  - 1.2 MW, upgradeable to 2.4 MW
  - Accelerated to 60-120 GeV by FNAL accelerator complex
  - Bent down at 5.8°, to reach Sanford
- Horns/beam line designed to maximize CP violation sensitivity



PIP-II Injector Test cryomodule

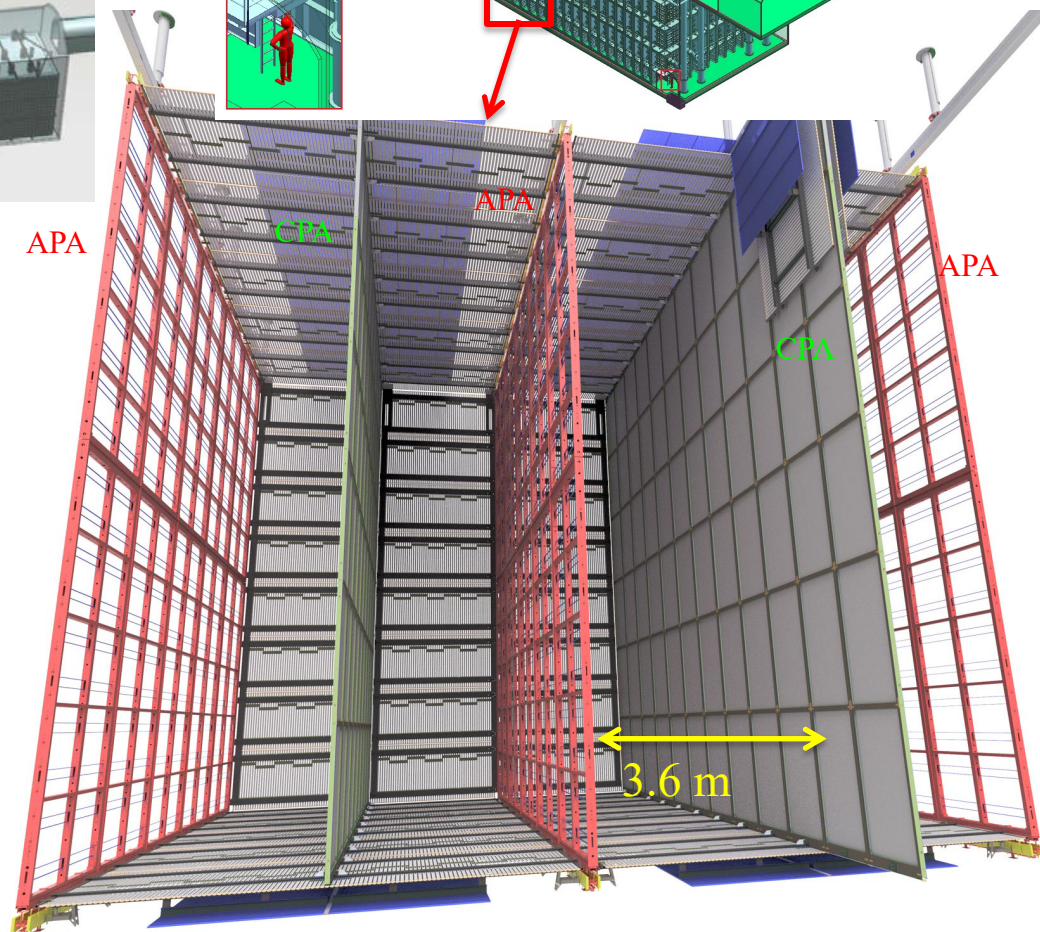
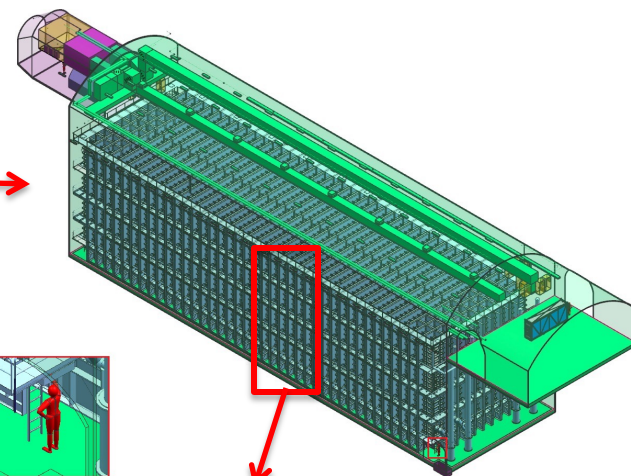
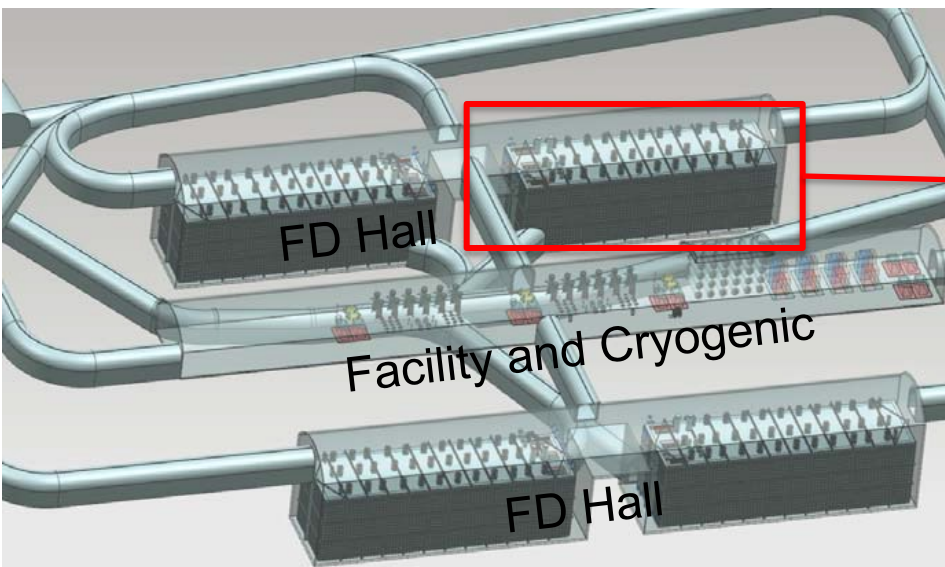
# Sanford Underground Research Facility (SURF) for Far Detector Lead, S. Dakota



- In the Homestake gold mine
- Home of Ray Davis's solar neutrino experiment

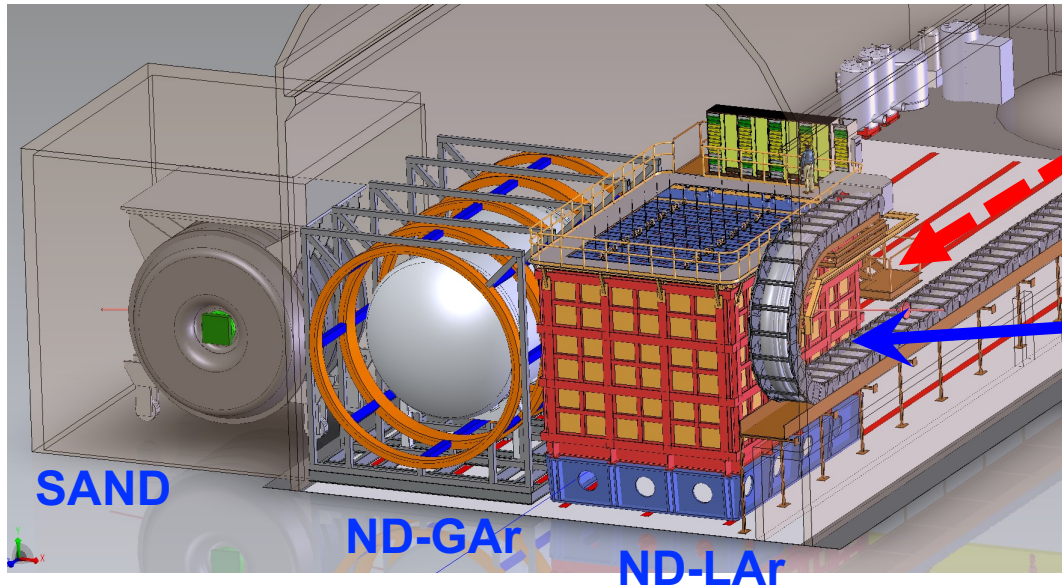


# Far Detectors: Liquid Argon Time Projection Chamber (LArTPC)



- Four 17-kt modules deployed in stages
- Single Phase LArTPC: all wire planes immersed in liquid argon
- First module will be single phase:
  - 18m x 19m x 66m
  - Drift distance: 3.6 m, wire pitch: 5 mm

# Near Detector Concept



ND-LAr and ND-GAr move off-axis to receive different beam fluxes for flux and cross sections disentangling (DUNE-PRISM)

beam  
direction

- Reference Design of DUNE Near Detector:

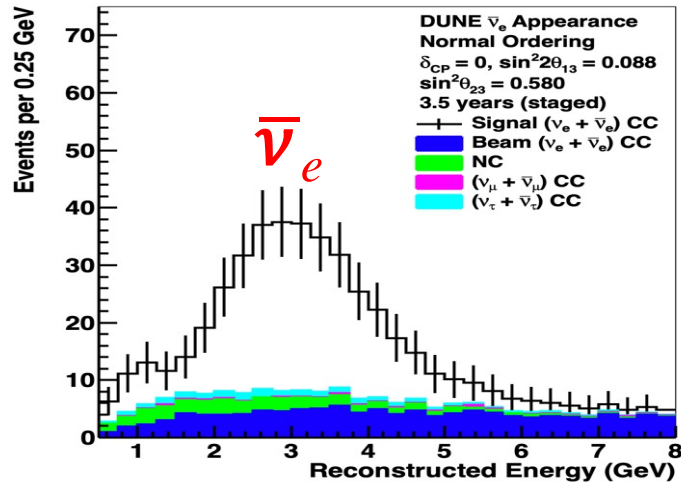
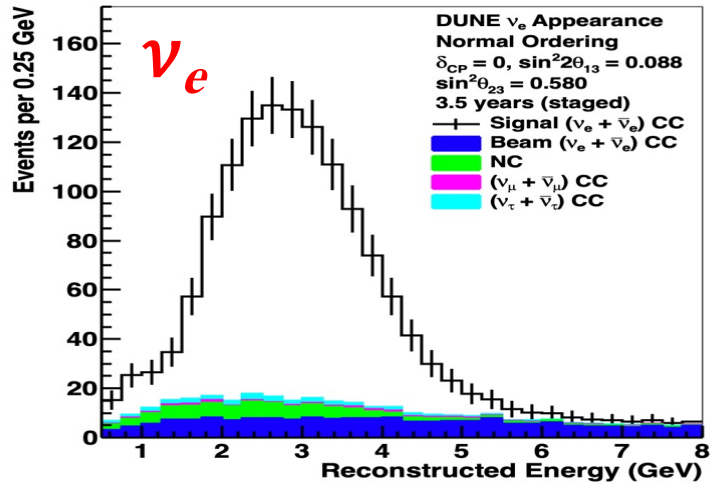
- ND-LAr: LArTPC with pixelated readout
  - Primary target and most similar to FD
- ND-GAr: High Pressure GAr TPC + ECAL + magnet
  - Constrains nuclear interaction model; muon spectrometer
- SAND (System for on-Axis Neutrino Detection): Tracker surrounded by ECAL and magnet
  - Monitors on-axis beam spectrum

## ND Hall location

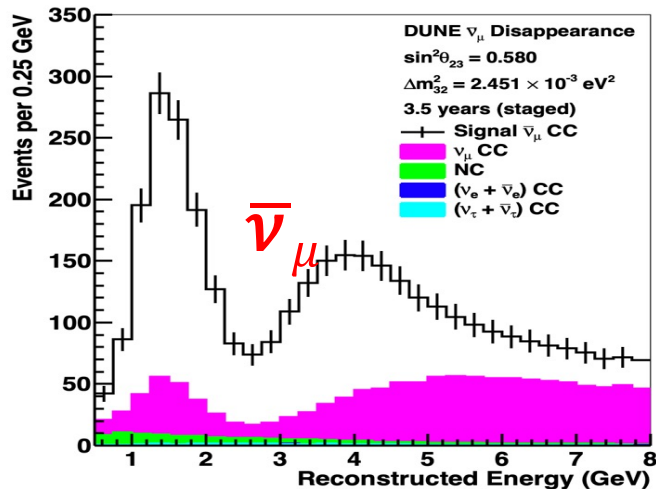
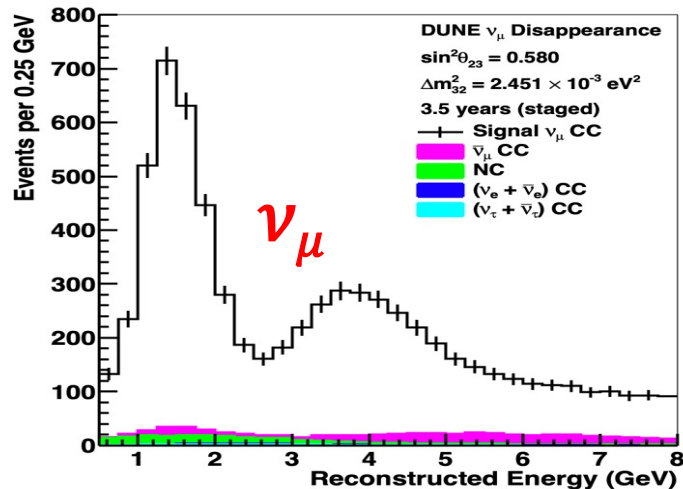
- 574 m from neutrino beam target
- Underground

# DUNE Oscillation Physics

- $\nu_e$  appearance +  $\bar{\nu}_\mu$  disappearance: Decisive measurements to neutrino CP violation and Mass Ordering
- An order of magnitude more data than NOvA



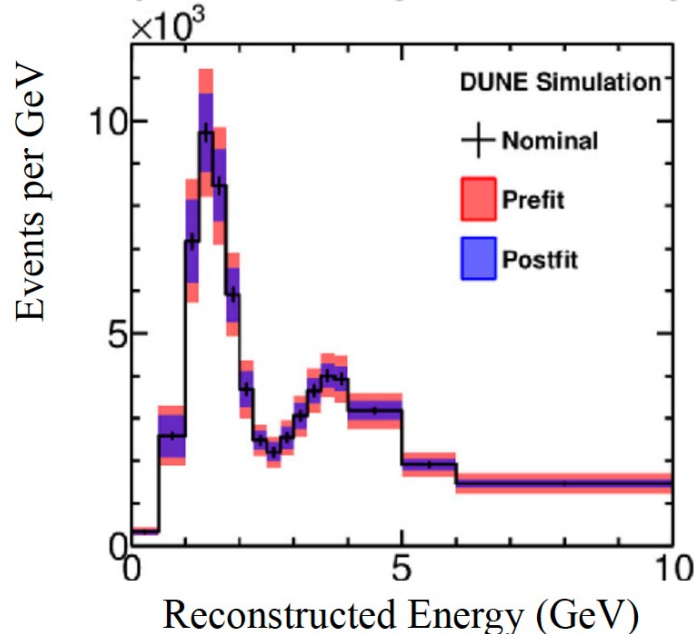
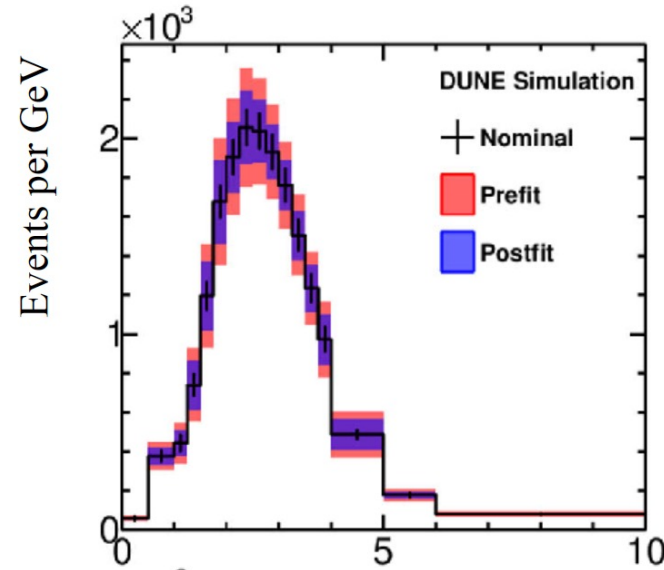
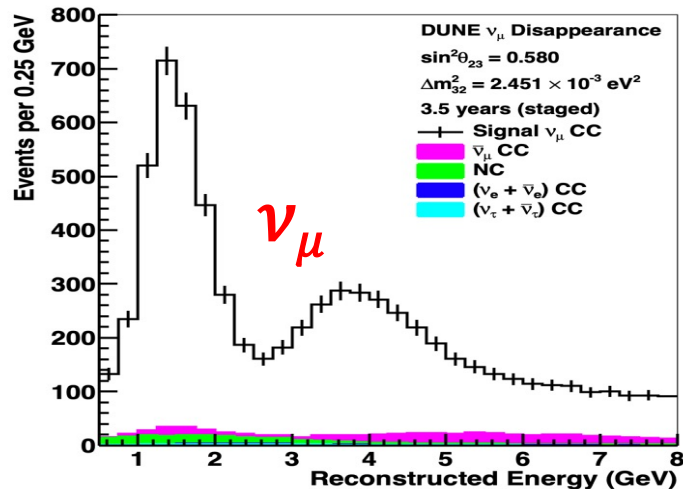
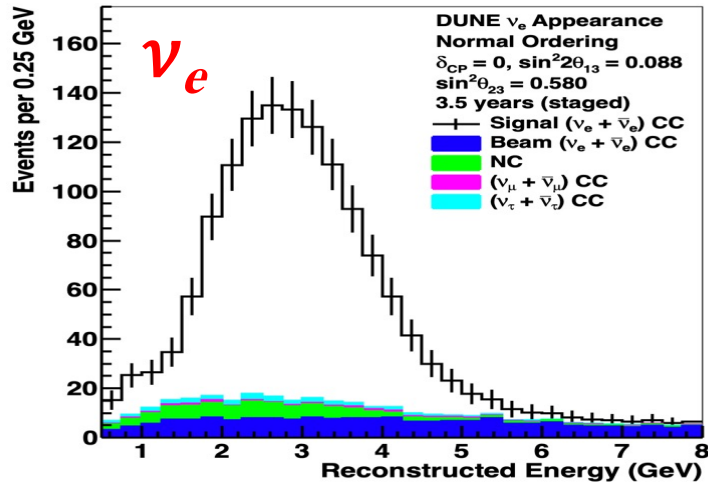
$\sim 1000 \nu_e \bar{\nu}_e$



$\sim 10000 \nu_\mu \bar{\nu}_\mu$

# DUNE Oscillation Physics

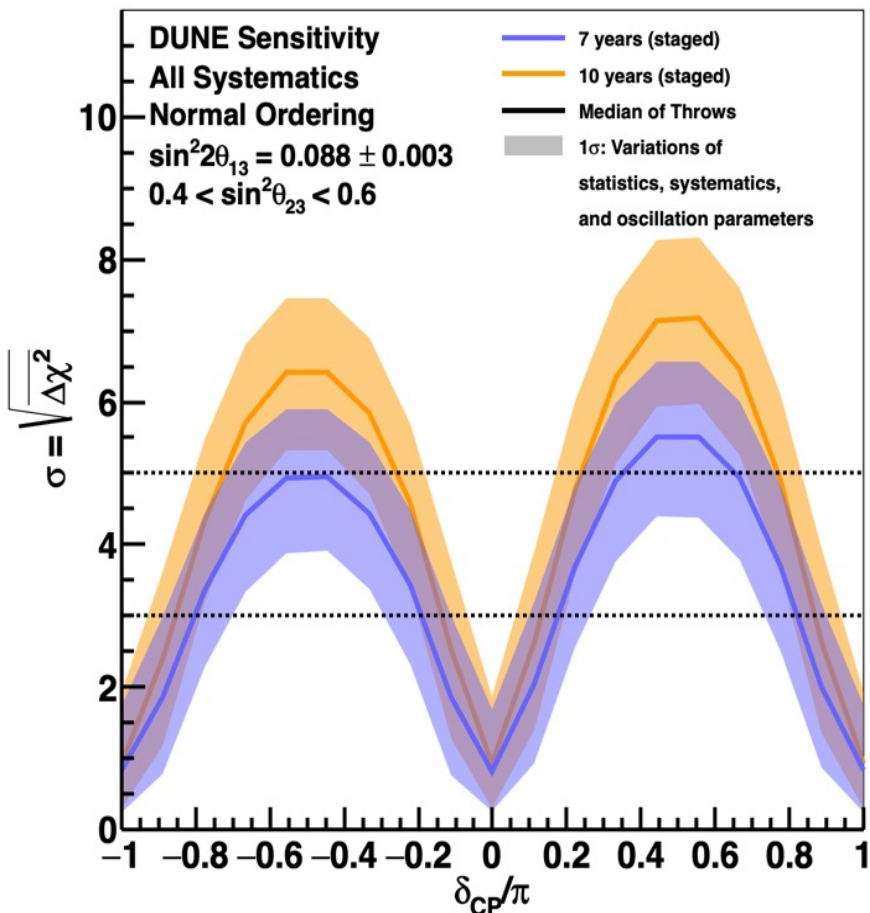
- $\nu_e$  appearance +  $\nu_\mu$  disappearance: Decisive measurements to neutrino CP violation ar
- An order of magnitude 1



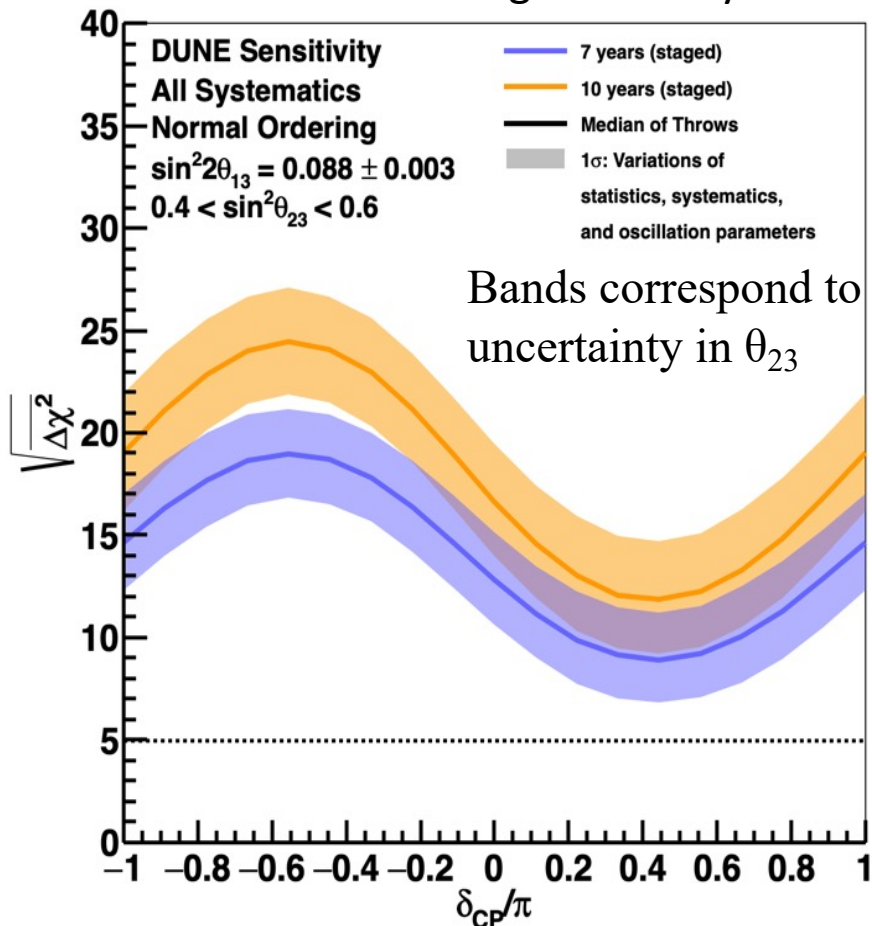
Oscillation fits:  
 detailed handling of  
 systematic  
 uncertainties + Near  
 Detector constraints

# CP violation and Mass Ordering at DUNE

## CPV Sensitivity



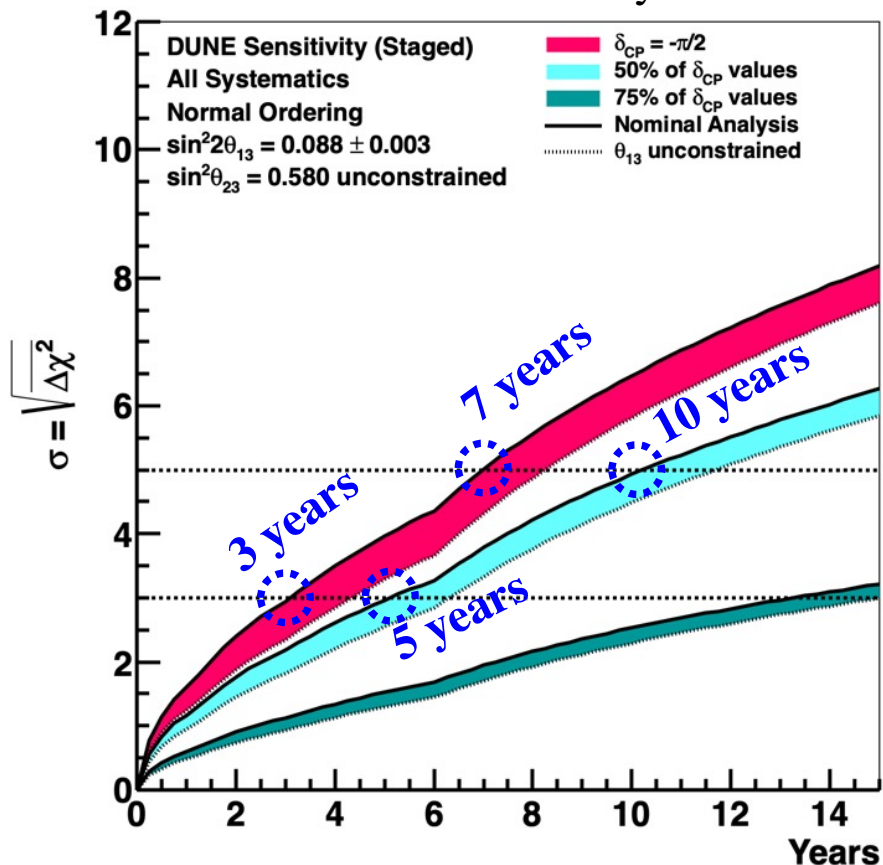
## Mass Ordering Sensitivity



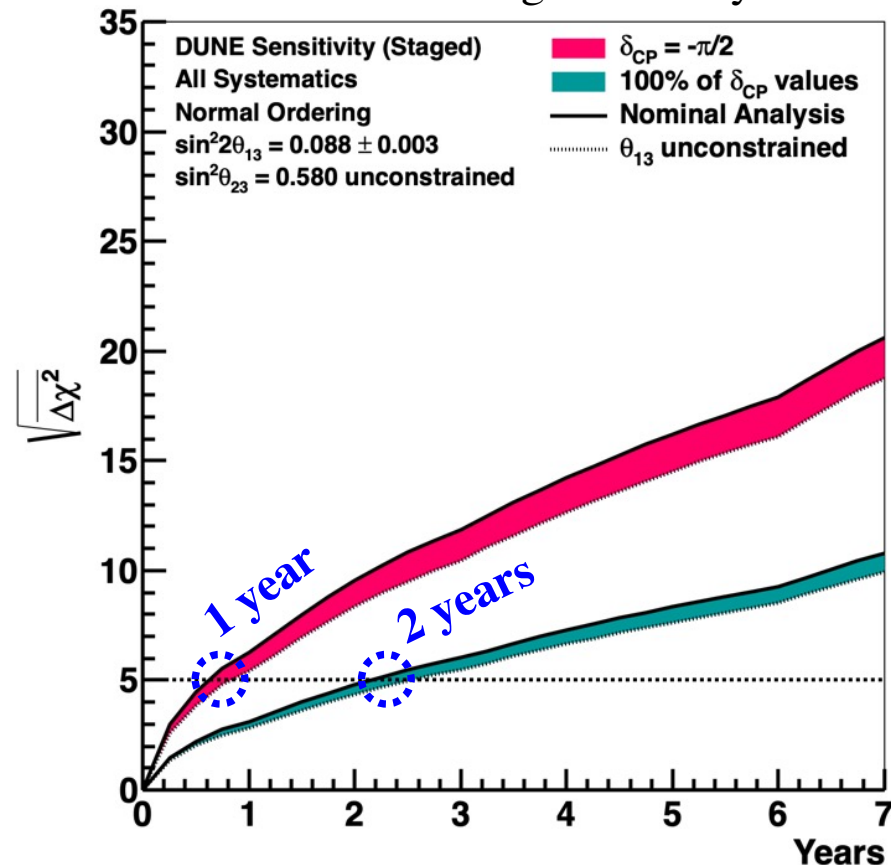
- $>5\sigma$  CPV discovery over a wide range of  $\delta_{CP}$
- $>5\sigma$  Mass Ordering determination for all  $\delta_{CP}$  values

# CP violation and Mass Ordering at DUNE

CPV sensitivity



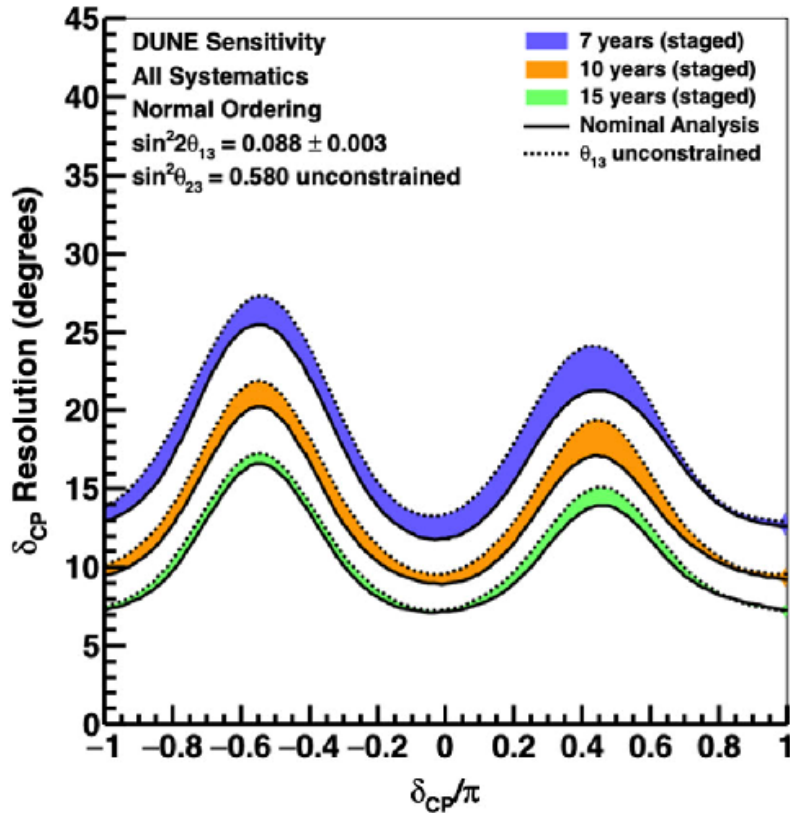
Mass ordering sensitivity



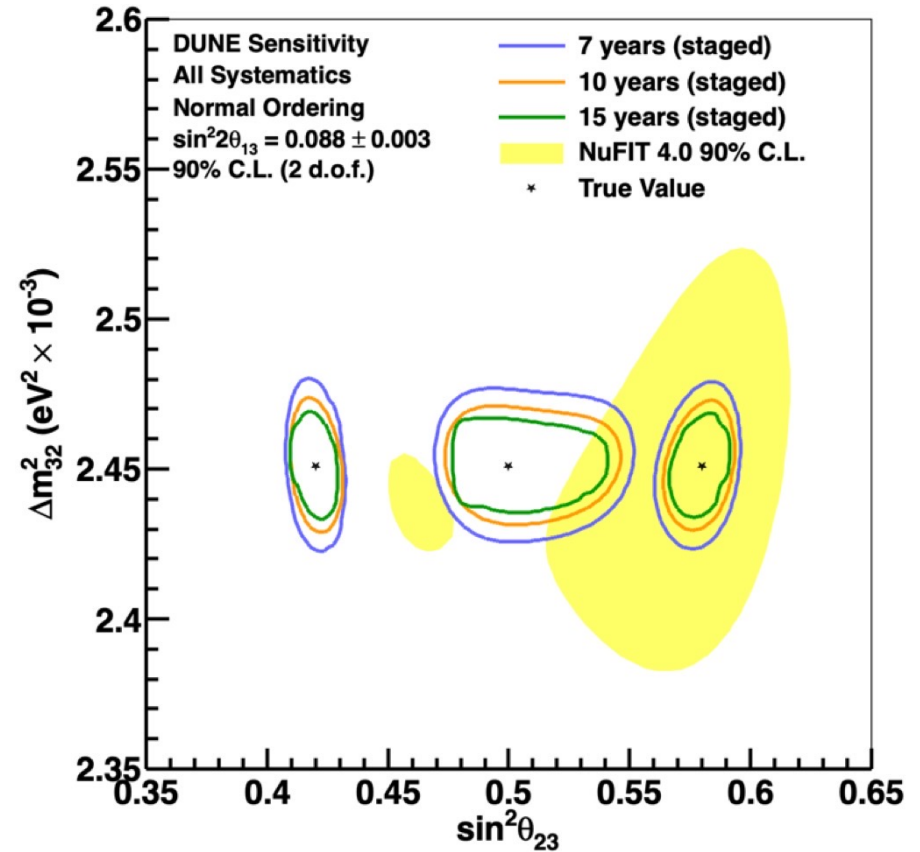
Significant milestones throughout beam-physics program

DUNE Technical Design Report (TDR): arXiv:2002.03005

# Parameter Measurement



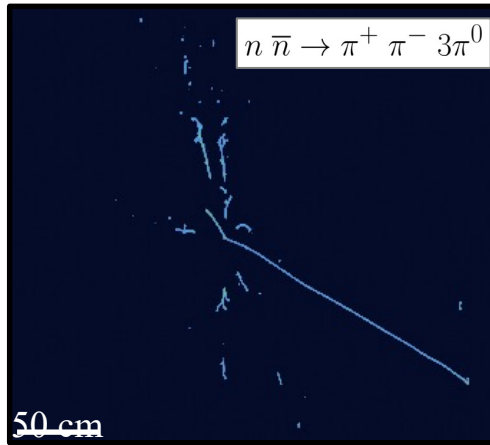
Resolution on  $\delta_{CP}$  over full range



Significant improvement in atmospheric parameters and octant of  $\theta_{23}$

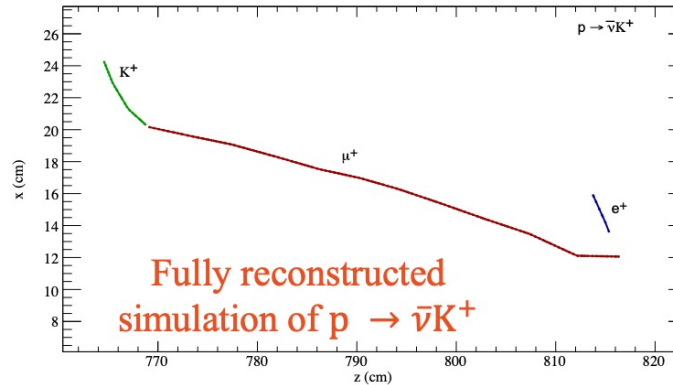
# Beyond Standard Model (BSM) Physics

## FD: $n - \bar{n}$ oscillation



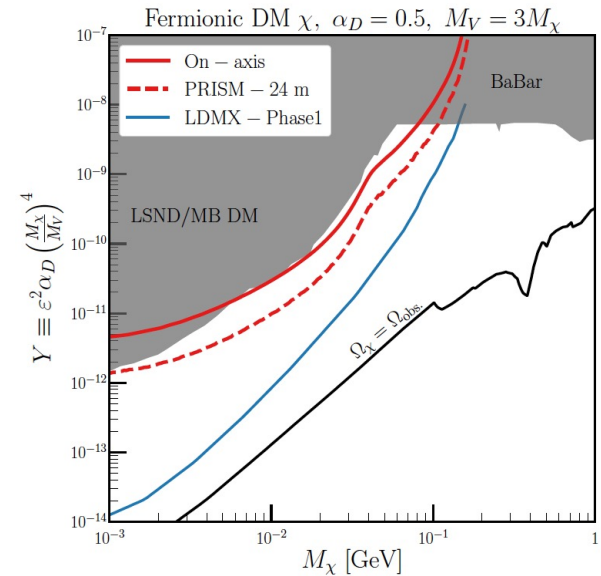
Free-neutron-equivalent sensitivity:  
 $\tau_{\text{free,osc}} > 5.5 \times 10^8 \text{ s}$  (90% C.L.)

## FD: Proton Decays



0.5 bkg events for 400 kt-yr, 30%  
 signal efficiency  
 Sensitivity (no signal):  $\tau/B >$   
 $1.3 \times 10^{34} \text{ yr}$  (90% C.L.)

## ND: Low-Mass Dark Matter



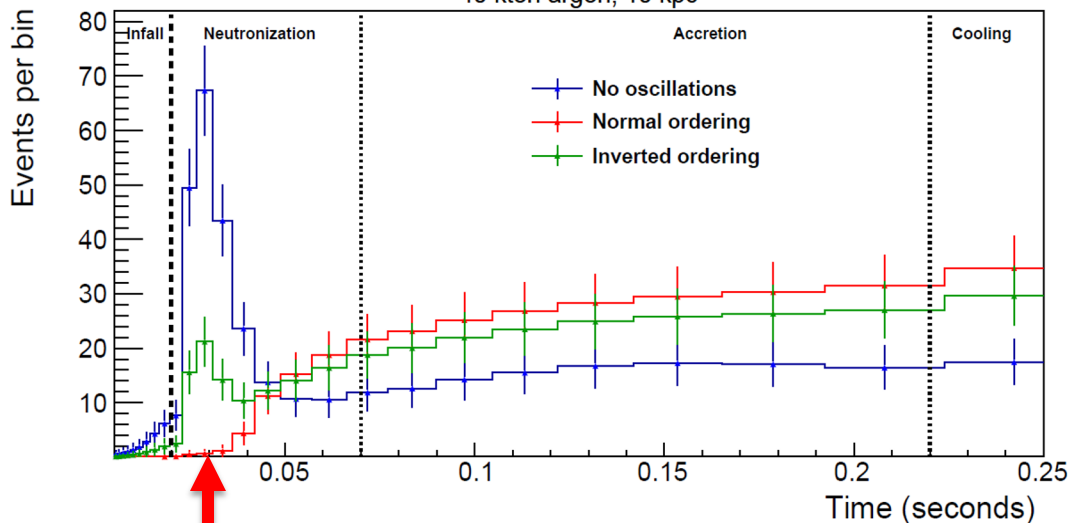
- FD : Large volume, deep underground, superior  $K/\pi$  reconstruction
- ND: High beam power, highly capable detectors
- Proton Decay,  $n - \bar{n}$  oscillation, NSI, Dark Matter, Sterile Neutrinos, Non-Unitarity, CPT Violation, etc

# Supernova Neutrino Burst and Solar Neutrinos

- Supernova Neutrino Burst (SNB)
  - Sensitive to neutronization ( $\nu_e$ ) in core collapse supernova  $\rightarrow$  solve neutrino mass ordering
  - $\nu$ -e elastic scattering could provide directionality, prompt pointing to supernova
  - Large statistics: for  $\sim 10$  kpc, Expect  $\sim 3,000$   $\nu_e$  in 10 seconds
- Also sensitive to solar neutrinos:  $^8\text{B}$  solar neutrinos and hep solar neutrinos

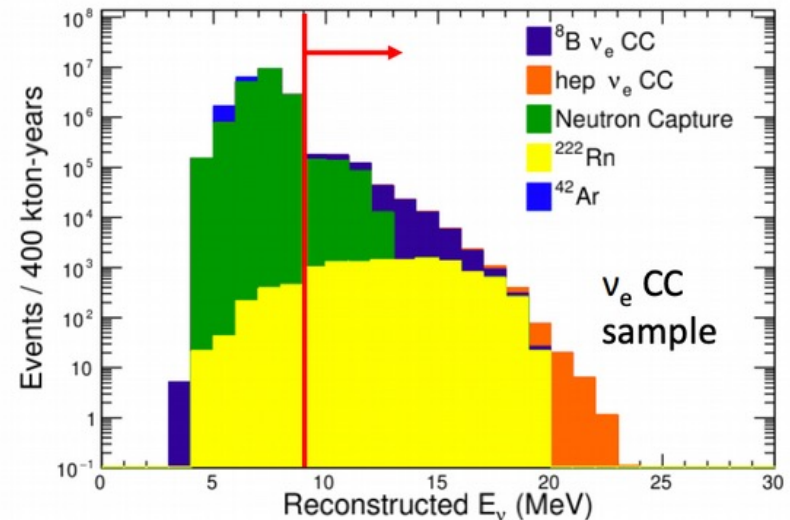
Number of supernova neutrinos vs. time

40 kton argon, 10 kpc



Neutronization: the initial neutrino burst in core collapse supernova, mostly  $\nu_e$

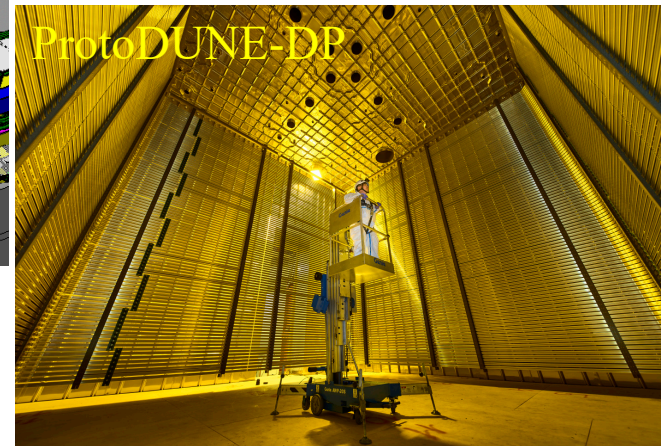
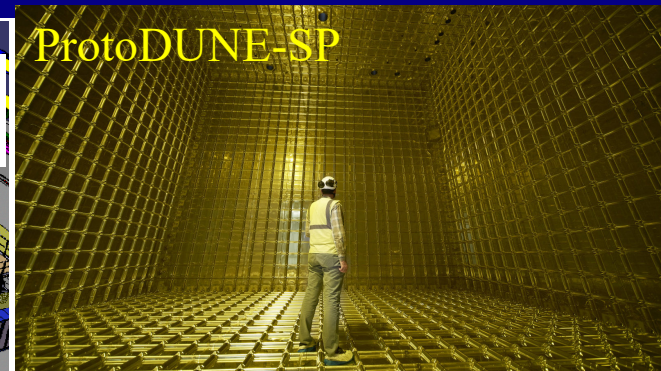
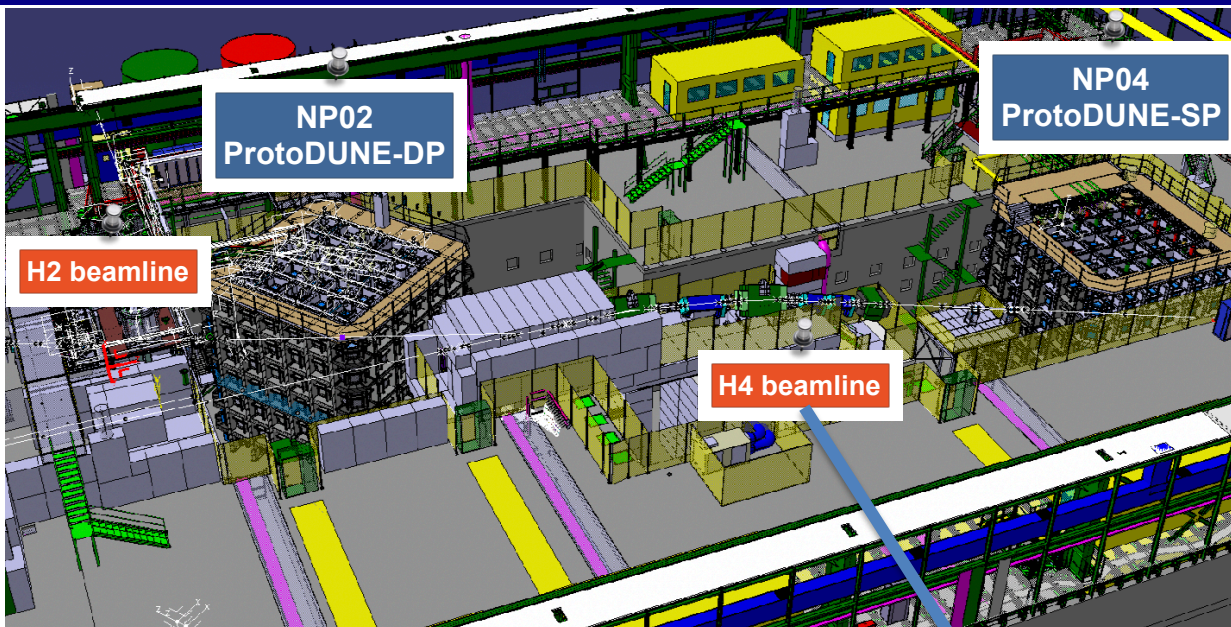
Solar Neutrinos



# DUNE: Schedule & Plans

- Far site construction is underway
- Near site preparation is also in progress
- 1st FD Module installation will start in 2024
- Neutrino beam available in late 20s
- Far detector physics data expected in the same timescale

# ProtoDUNE SP and DP at EHN1 (CERN)

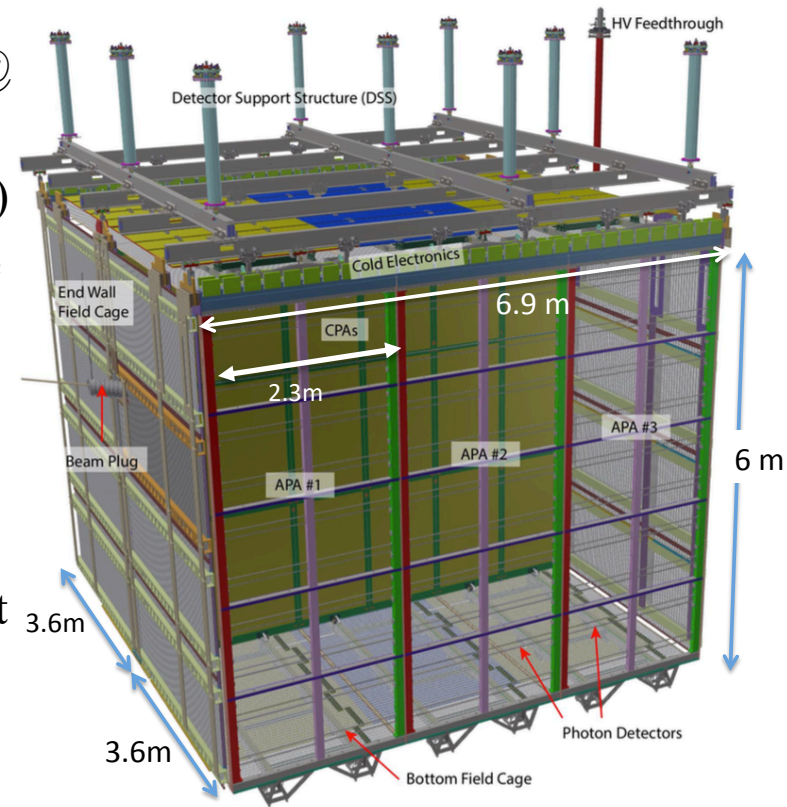


- ProtoDUNE-SP and DP are two large DUNE prototype detectors at CERN Neutrino Platform EHN1
- 770 tons LAr mass each
- Exposed to test beams H4(SP) and H2(DP), momentum-dependent beam composition contains  $e$ ,  $K^\pm$ ,  $\mu$ ,  $p$ ,  $\pi^\pm$
- Also take cosmic ray data

- H4-VLE beam line [Phys. Rev. Accel. Beams 22, 061003 (2019)]
- New tertiary, low-mom beam line; 2 secondary targets
- W for lower momenta (0-3 GeV/c); Cu for higher momenta (4-7 GeV/c)
- TOF and Cherenkov counters for PID

# ProtoDUNE-SP Detector

- TPC:
  - Two drift volumes, 3.6m drift distance in each @ 500V/cm
  - Active Volume: 6m (H) x 7m (L) x 2 x 3.6m (W)
  - Cathode Plane Assembly (CPA) on middle plane
  - Anode Plane Assemblies (APAs) on both sides
  - Cold electronics attached to the top of APAs
- Photon detectors (PDS):
  - SiPM readouts
  - Wavelength shifter converts VUV to visible light
  - 3 designs integrated into APA frame bars
- Cryogenic instrumentations: measure argon purity, temperature, liquid level and tag cosmic rays
- ProtoDUNE-SP Phase-I was operated Sept. 2018 – July 2020, Run-II data taking is under preparation
- First paper on ProtoDUNE-SP performance published: JINST 15 (2020) 12, P12004



#### CPA:

- 18 CPA modules
- HV=180 kV

#### APA:

- Each APA module: 6m high, 2.3m wide
- Two induction planes and one collection plane

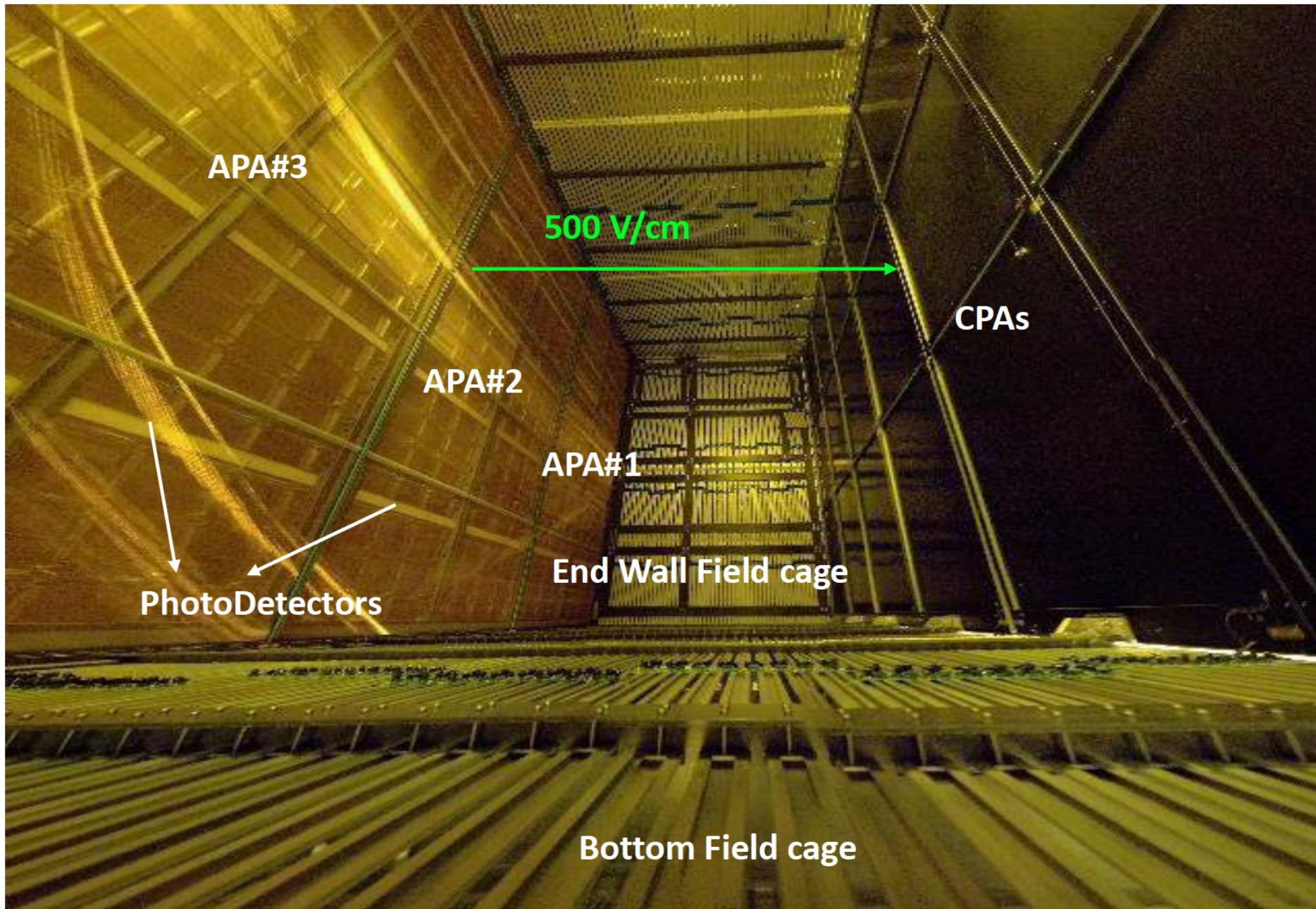
#### Cold electronics

- 2560 wires/APA, 15360 total wires

#### Field cage

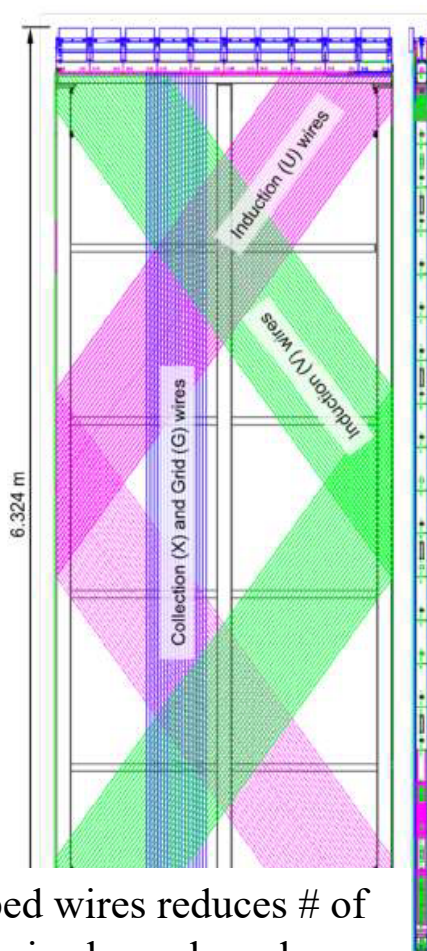
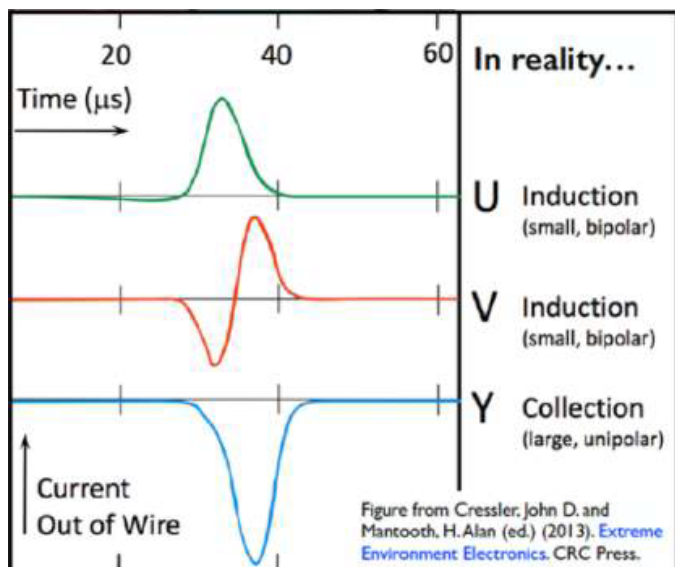
- Surrounds the open sides of the drift region to ensure uniform electric field

# ProtoDUNE-SP Field Cage



# ProtoDUNE-SP: Anode Plane Assembly (APA)

- APA: 3 wire planes (U/V,X) + 1 grid plane(G)
  - Grid plane prevents induction currents from drifting charge in drift volume
  - Induction wires (U, V): inclined at  $\pm 35.7^\circ$ , transparent to charges
  - Collection wires (X): collect charge forming unipolar signal
  - Grounding Mesh shields photon detectors

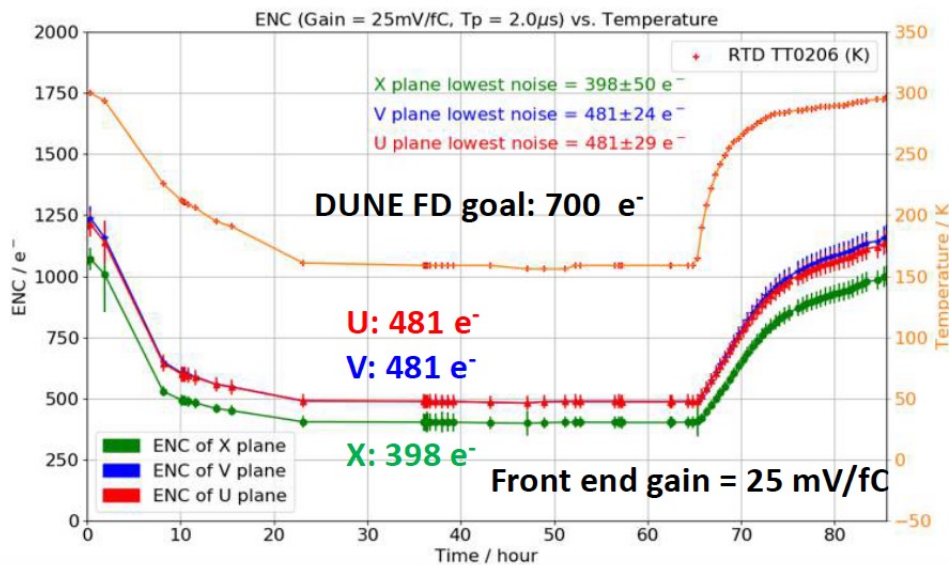
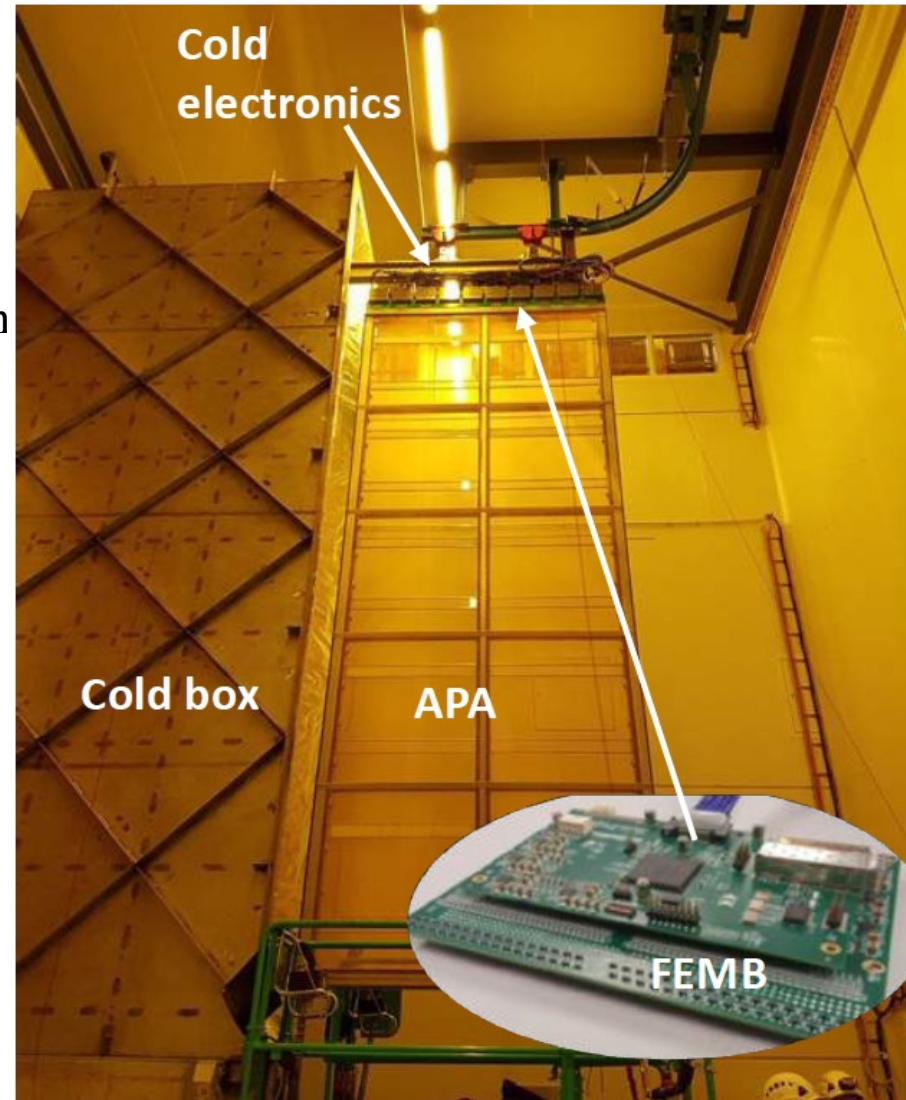


Wrapped wires reduces # of electronic channels and allows more active volume, all electronics on top



# Cold Electronics (CE)

- Cold Electronics (CE): Both Front-End and ADC ASICs submerged in liquid argon
- FEMB (Front End Mother Board) mounted on top of the APA
- Assembled APA and cold electronics tested in Cold Box (150K nitrogen gas) before installation
- Front-End ASIC worked well, R&D to improve ADC ASIC for DUNE

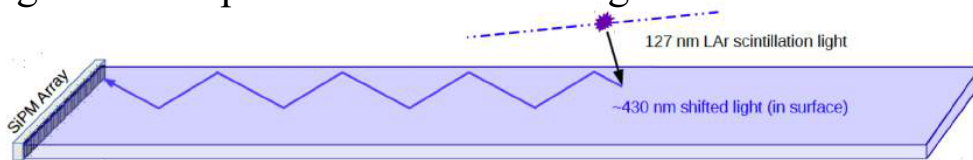


ENC (Equivalent Noise Charge): charge injected to detector capacitance which produces on the output side a signal with amplitude equals the output RMS noise

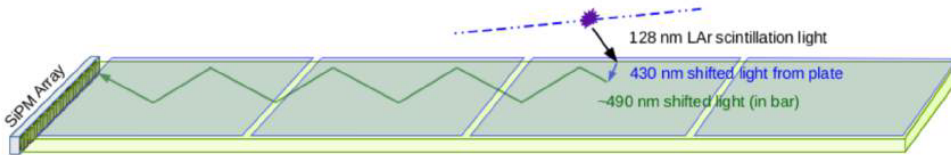
# Photon Detection System (PDS)

- LAr is excellent scintillating medium: 20,000 photons/MeV @ 500 V/cm, wavelength=128 nm
- Wavelength shifter converts VUV to visible light readout by SiPMs
- 3 PDS designs being tested in ProtoDUNE-SP:

Design 1: Dip-coated light guide (MIT and Fermilab): Acrylic light guide bar dip-coated with wavelength shifter

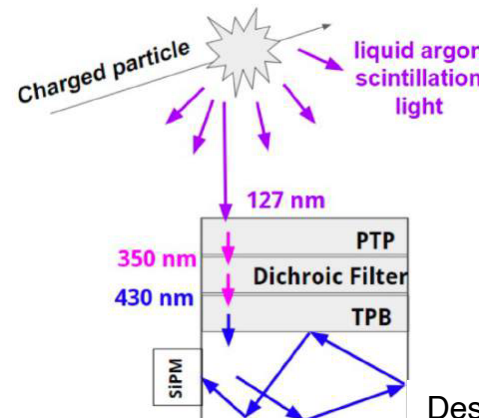


Design 2: Double-shift light guide (Indiana University): Wavelength shifting plates + wavelength shifting light guide

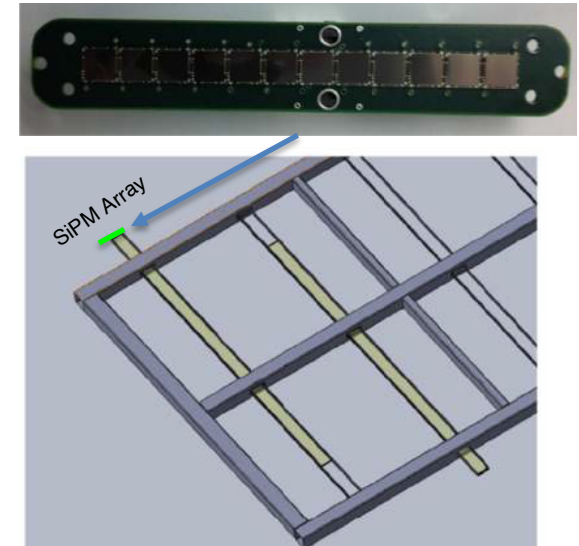


Design 3: ARAPUCA (Campinas University and Fermilab):

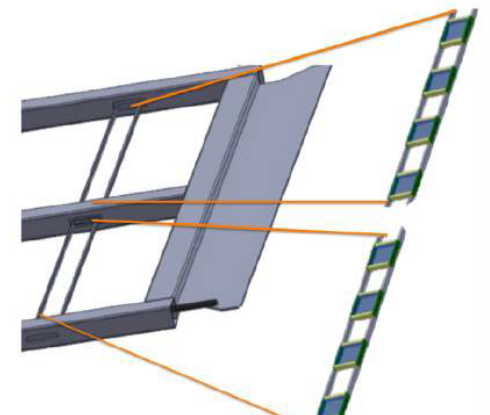
Light trapped and wavelength-shifted by dichroic filter, 5 ~10x light yield increase



SiPM Array



Design 1&2 PDS module inserted APA frame

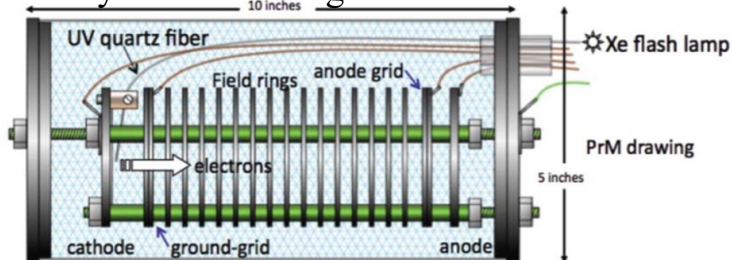


Design 3 PDS module inserted APA frame

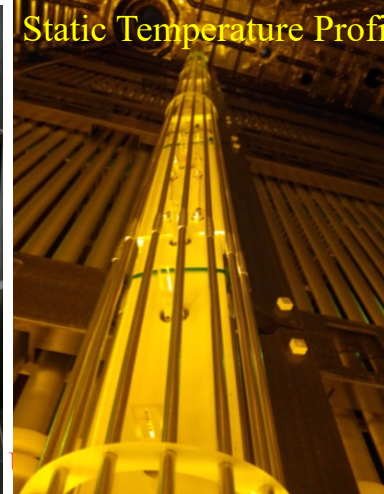
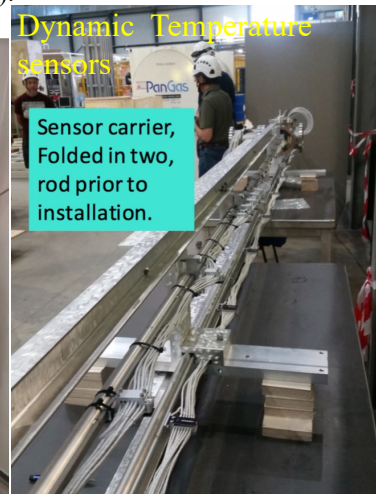
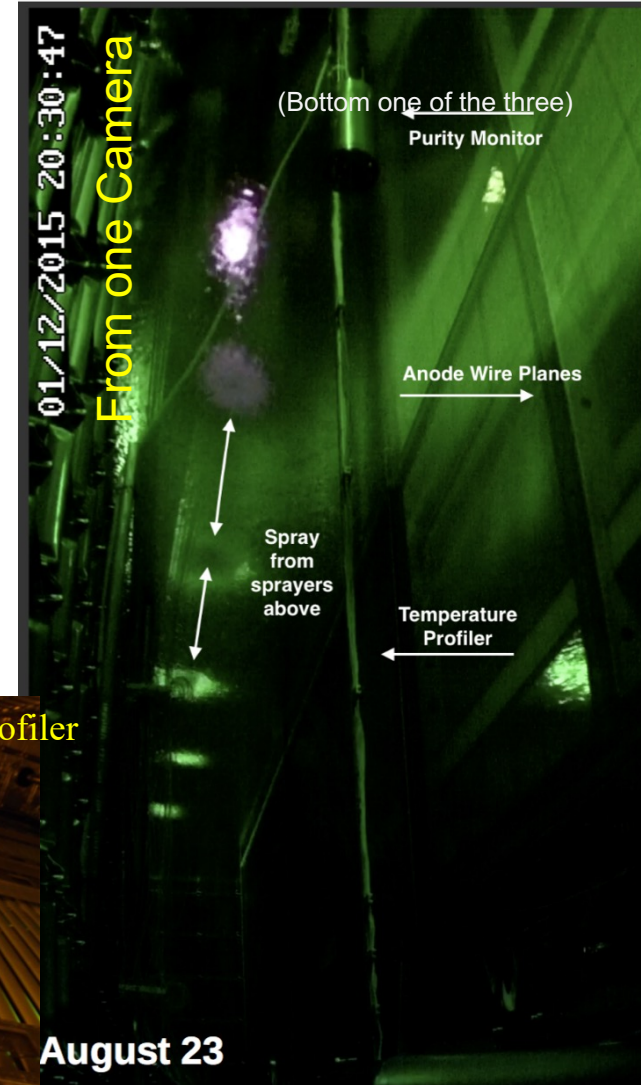
# Detector Instrumentation and Cosmic Ray Trigger

- Purity monitors (PrM): electron lifetime (LAr purity) measurement
- Gas analyzers analyzers: check argon gas purity
- Temperature sensors: Static and Dynamic sensors to measure temperature maps
- LAr level meters: keep LAr level constant
- Cameras: Observe visible for detector operation
- Cosmic ray tagger (CRT): scintillator panels upstream/downstream

Purity Monitor Design

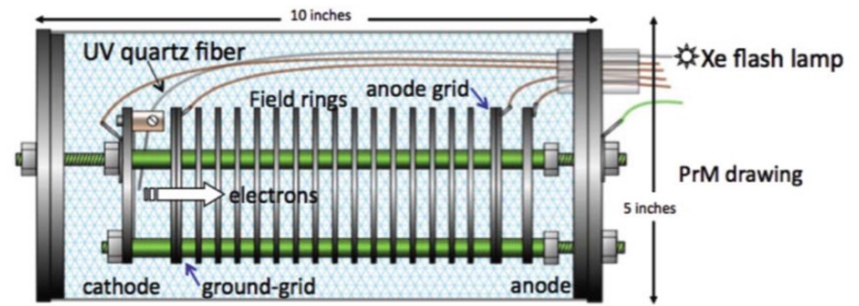


M. Adamowski et al., JINST 9, P07005 (2014).



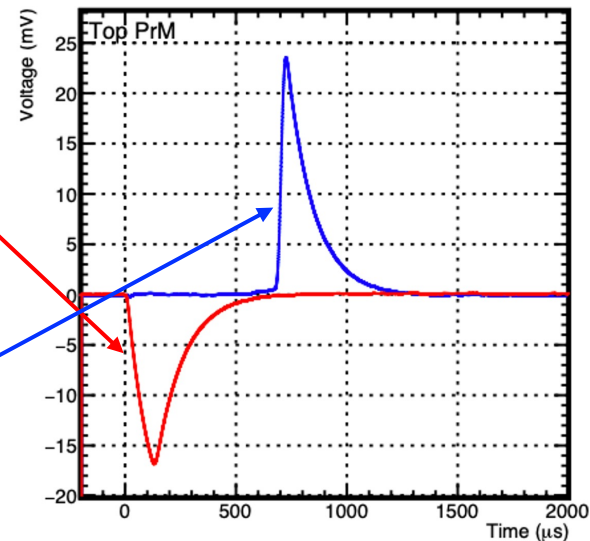
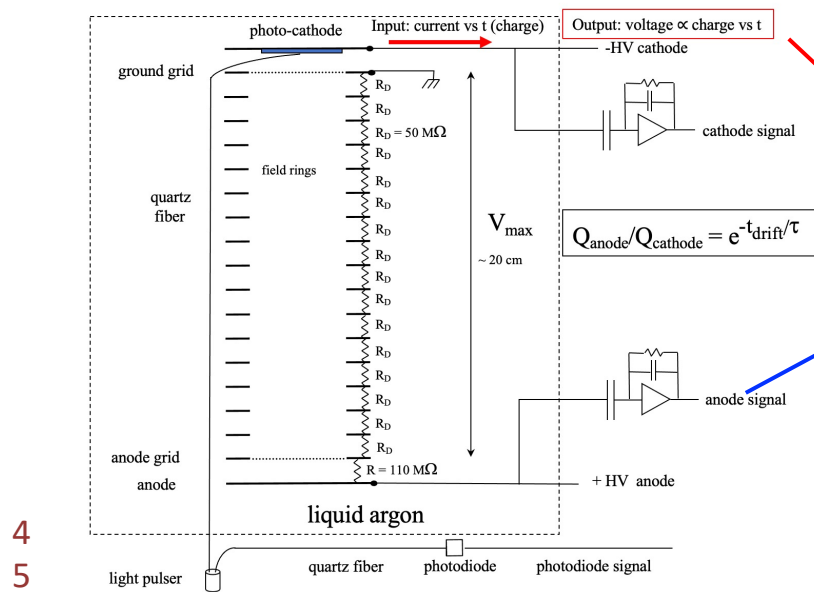
# Purity Monitors

- ProtoDUNE-SP equips 3 Purity monitors (PrM): Miniature TPC measuring drifting electron lifetime with photoelectrons.
- UV from Xenon flash lamp to generate photoelectrons on PrM gold photocathode
- Use anode-to-cathode charge ratio to measure drift electron lifetime:



M. Adamowski et al., JINST 9, P07005 (2014).

$$Q_{\text{anode}}/Q_{\text{cathode}} = e^{-t_{\text{drift}}/\tau}$$



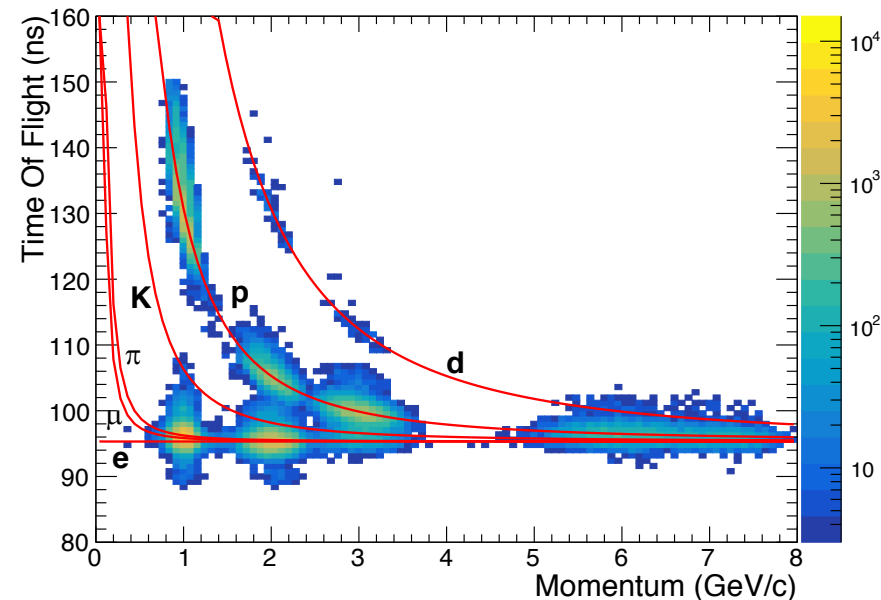
Purity monitor **Cathode** and **anode** signals in ProtoDUNE-SP

# Collected beam events: Oct-Dec 2018

Data taking time, total running time

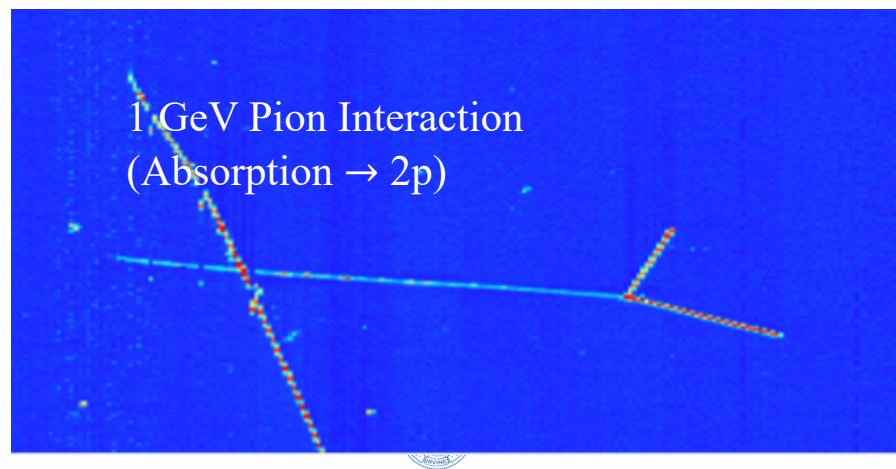
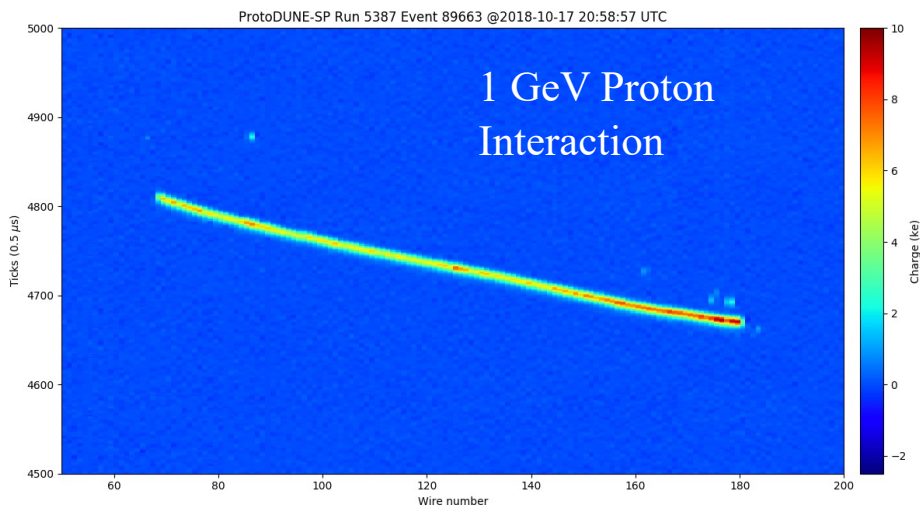
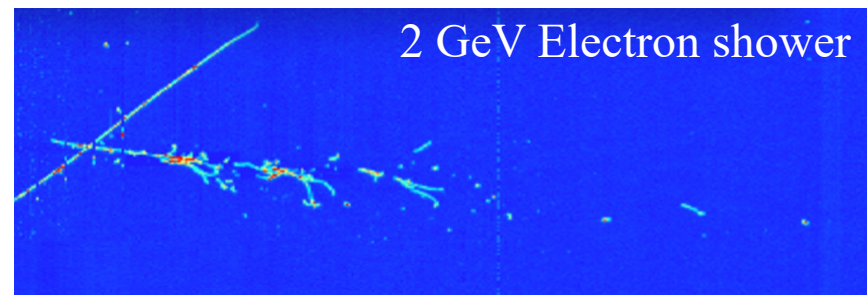
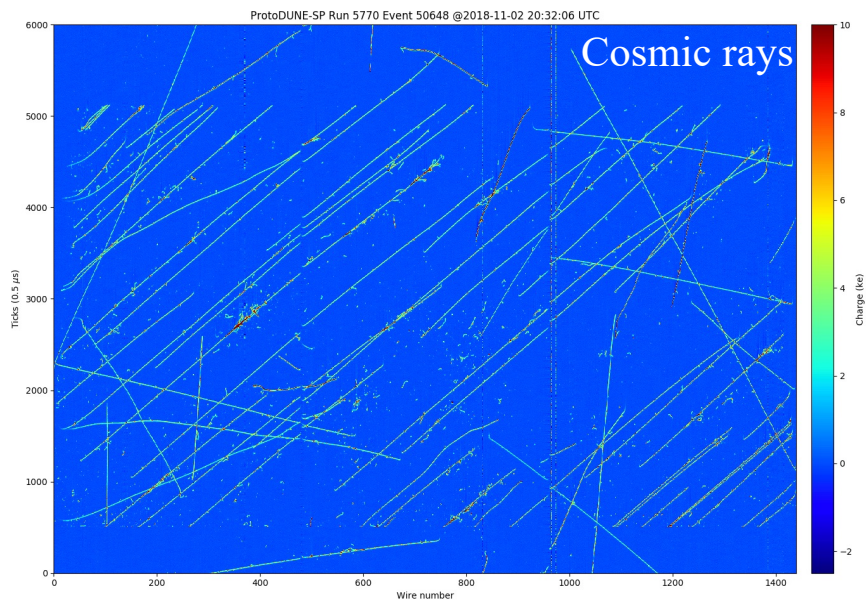
Momentum (GeV/c)	Total Triggers Recorded (K)	Total Triggers Expected (K)	Expected Pi trig. (K)	Expected Proton Trig. (K)	Expected Electron Trig. (K)	Expected Kaon Trig. (K)
0.3	269	242	0	0	242	0
0.5	340	299	1.5	1.5	296	0
1	1089	1064	382	420	262	0
2	728	639	333	128	173	5
3	568	519	284	107	113	15
6	702	689	394	70	197	28
7	477	472	299	51	98	24
All momenta	4173	3924	1693.5	777.5	1381	72

- Large statistics pion, proton, electron and kaon data at 1, 2, 3, 6, 7 GeV, data
- Beamline Time of Flight (TOF) and Cherenkov measurements for beam particle ID
- First paper on ProtoDUNE-SP performance published: JINST 15 (2020) 12, P12004

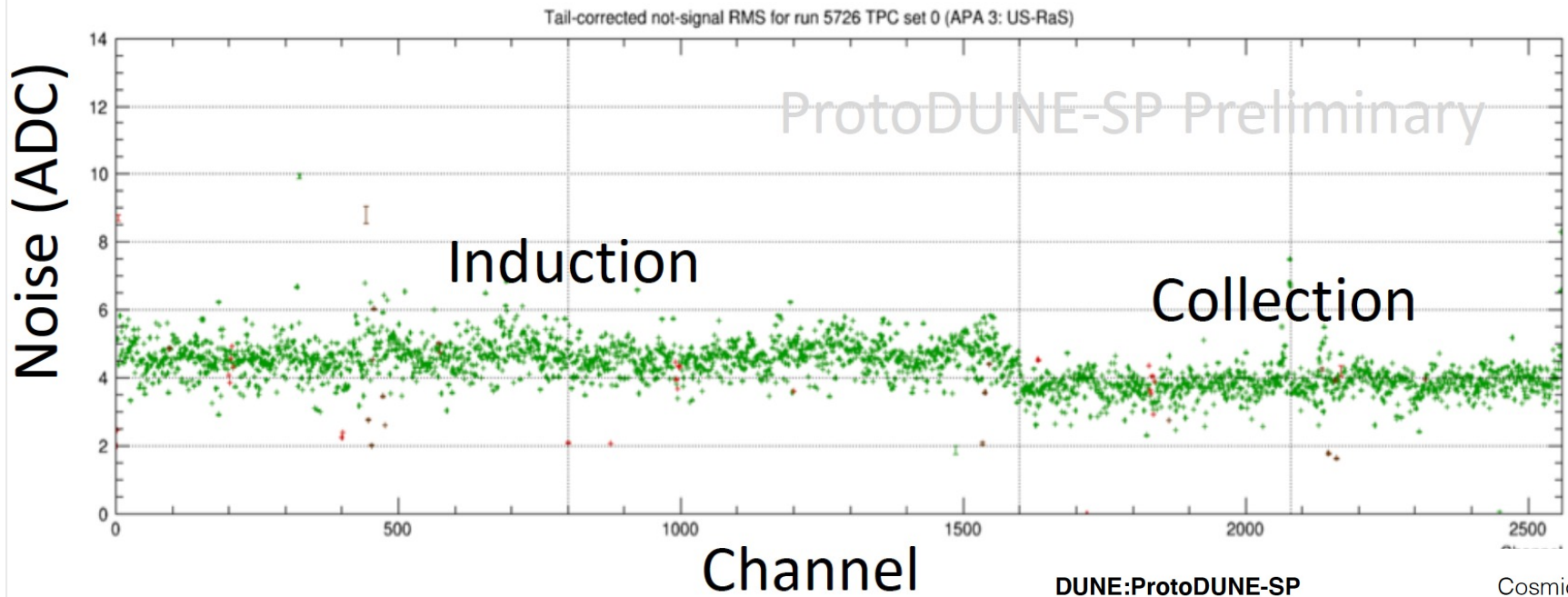


# Event Displays in ProtoDUNE-SP Data

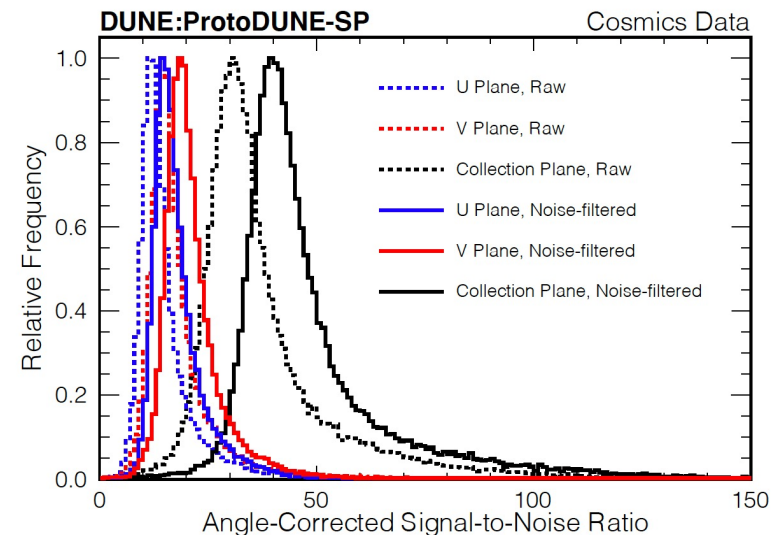
Resolution and data quality excellent → Liquid argon has high purity, Electronic noise under control



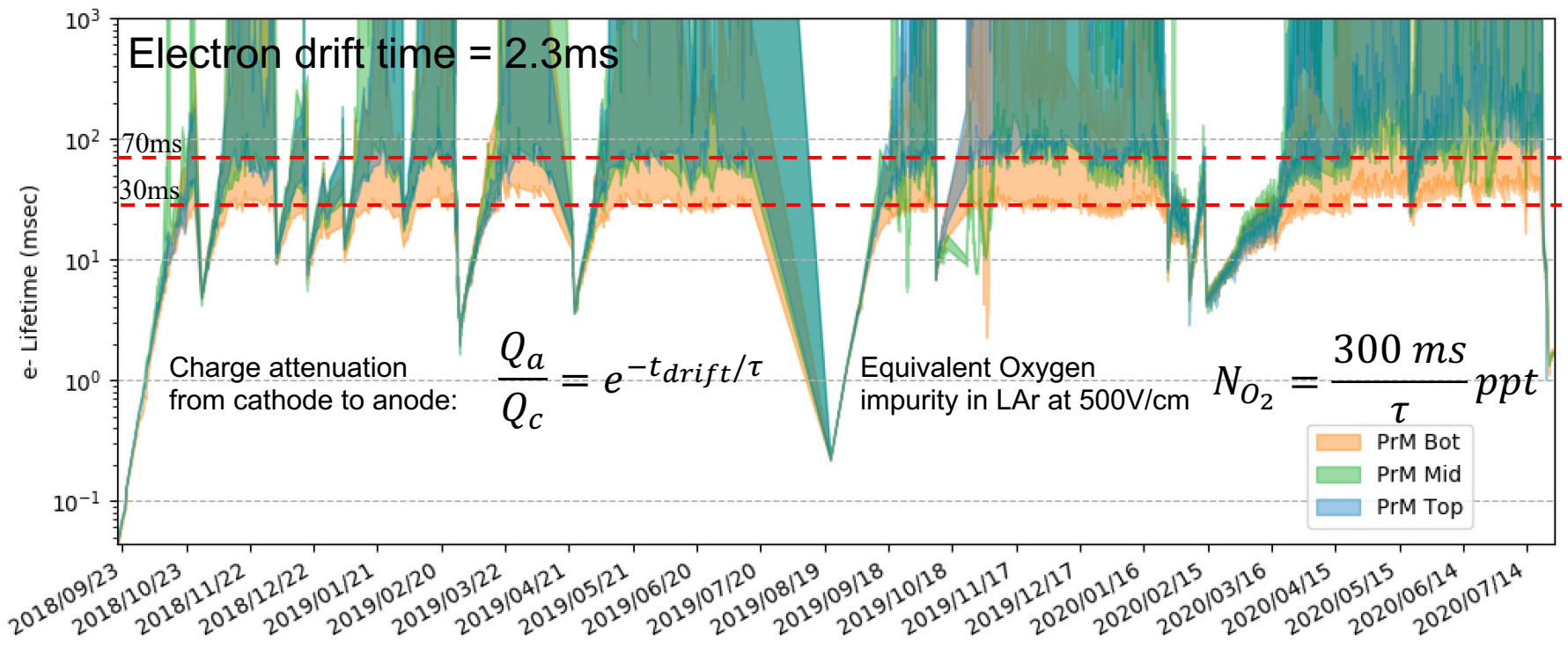
# Electronic noise and S/N ratios



- Electronic noise level measured by pedestal ENC (equivalent noise charge) before noise filtering: Collection (X): 550 e<sup>-</sup>, Induction: 650 e<sup>-</sup> (DUNE goal <1000 e<sup>-</sup>)
- Noise filter reduces both by ~100 e<sup>-</sup>
- Noise-filtered signal-to-noise ratio measured by cosmic muons: Collection: 48.7:1, Induction : 21.2:1



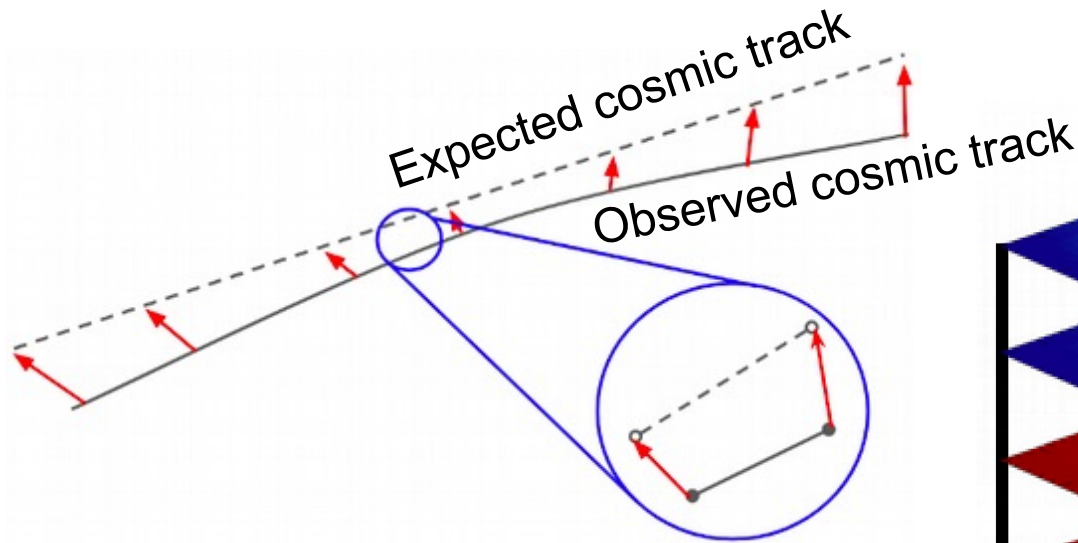
# Drift electron lifetime (LAr Purity)



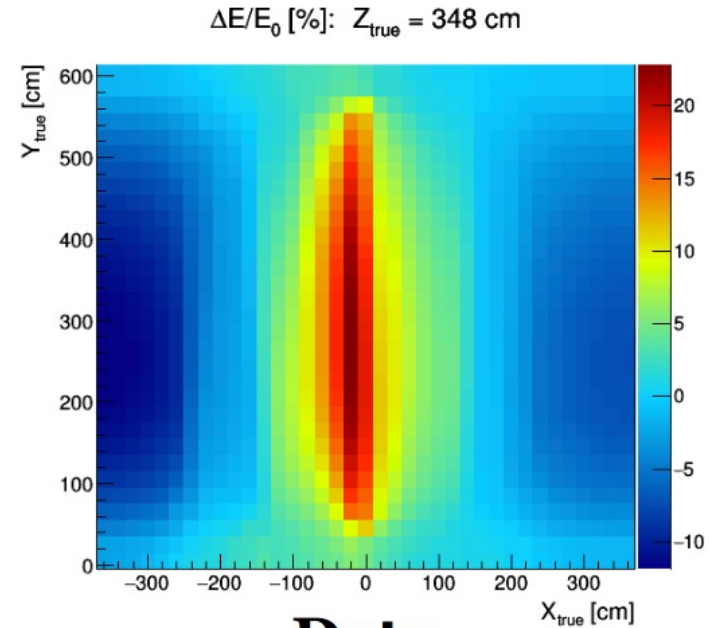
- Drift electron lifetime ( $\tau$ ): average drift time of electrons before captured by LAr impurities
- Key component of LArTPC calibration - corrects charge loss caused by LAr impurities
- Electron lifetime measured by purity monitors (small TPCs which measure e-lifetime with photoelectrons from a UV light source)
- Validated with cosmic ray tagger data.
- High LAr purity and electron lifetime (>30ms) achieved at ProtoDUNE-SP

# Space Charge Effect Correction with cosmic rays

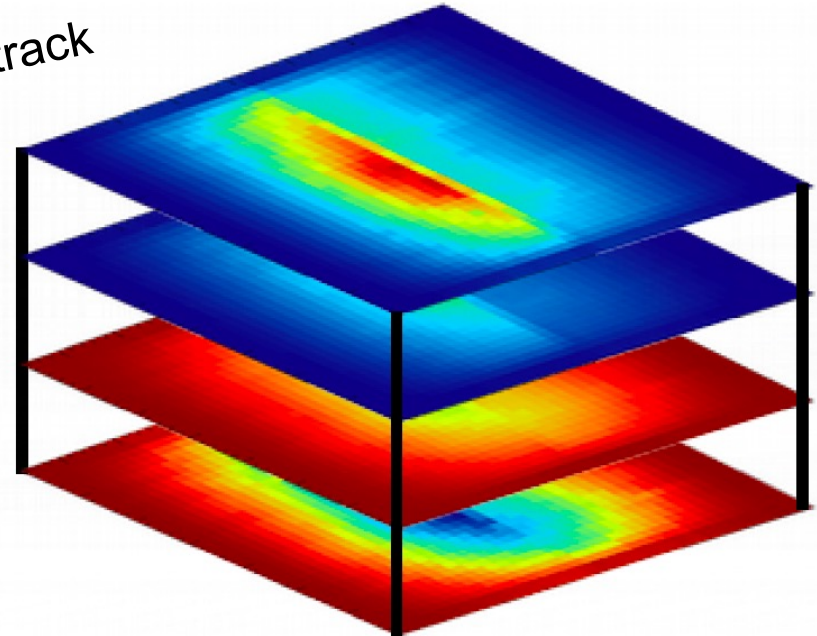
- Space Charge Effect (SCE): E-field distortions due to accumulation of slow drifting ions induced by cosmic rays
- Key effect to charge and position calibration for on-surface LArTPC experiments
- Solve for E-field distortion from spatial distortion observed in cosmic ray tracks
- Map and correct E-field for calibration  $\sim +20\%$  at cathode,  $\sim -10\%$  at anode due to SCE



(Michael Mooney, ICHEP20)

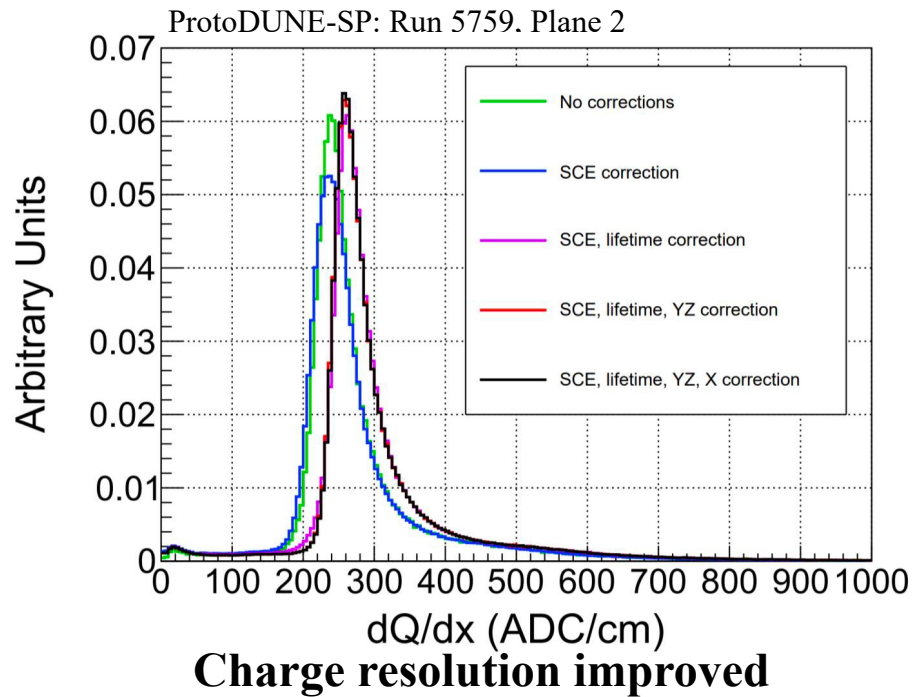


**Data**

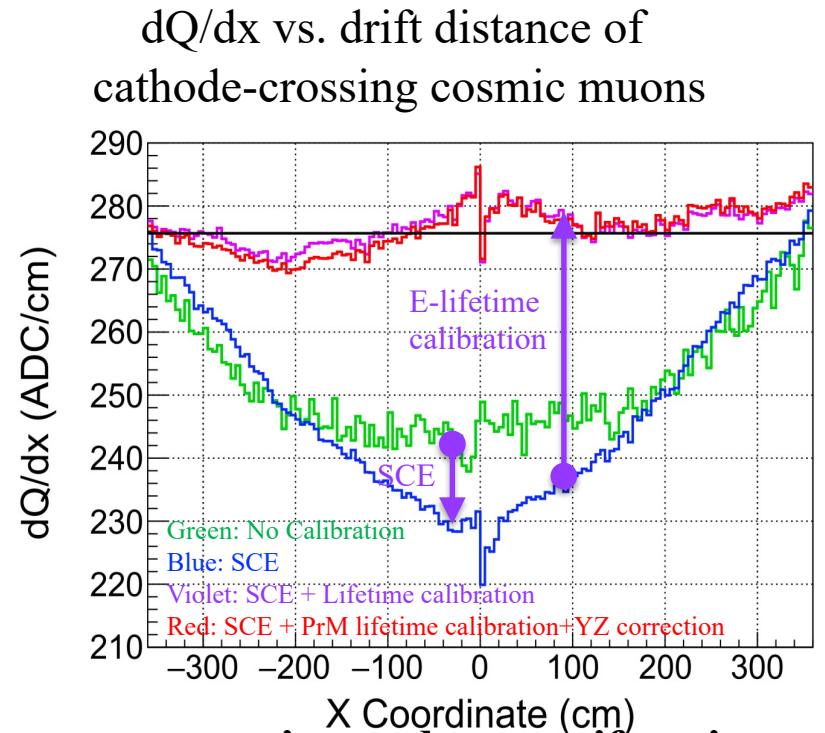


# TPC Calibration Scheme

- Electron lifetime calibrated with purity monitors (validated with cosmic ray tagger data)
- Space charge effect corrected with cosmic rays
- Position calibration based on cosmic rays
- Absolute energy calibration: stopping muons in cosmic rays
- Other calibration methods under development: Ar39, neutron source, laser, radioactive source (Bezawada, Huang, Dvornikov and Fani's talk in NuTel21)

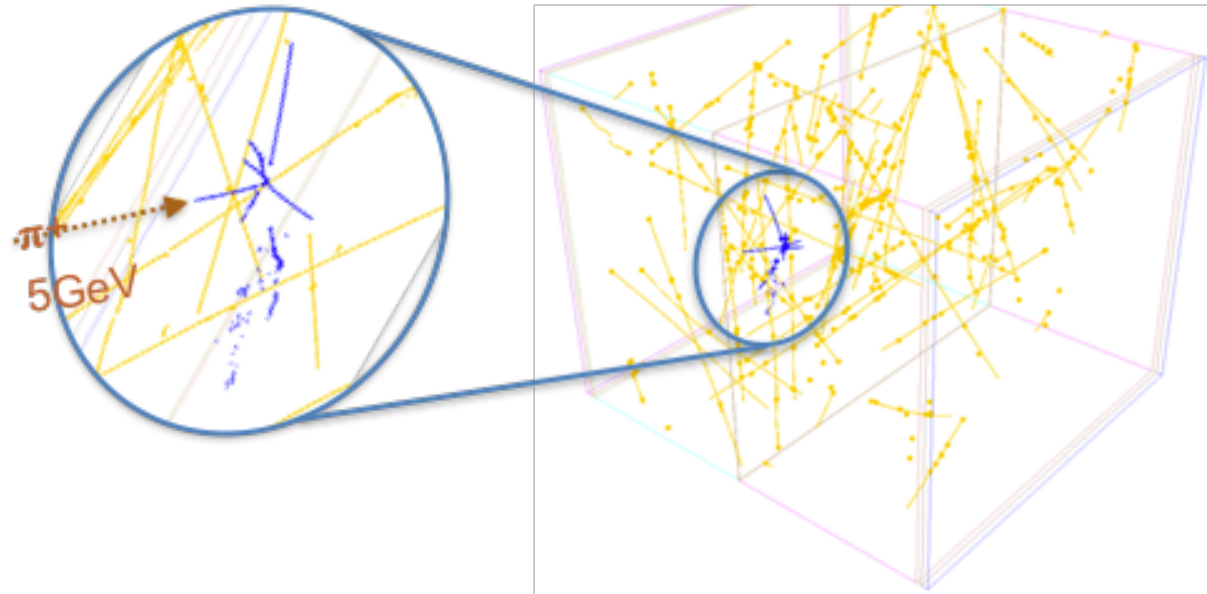


(Graham Chambers-Wall, Fermilab User's meeting 2020)

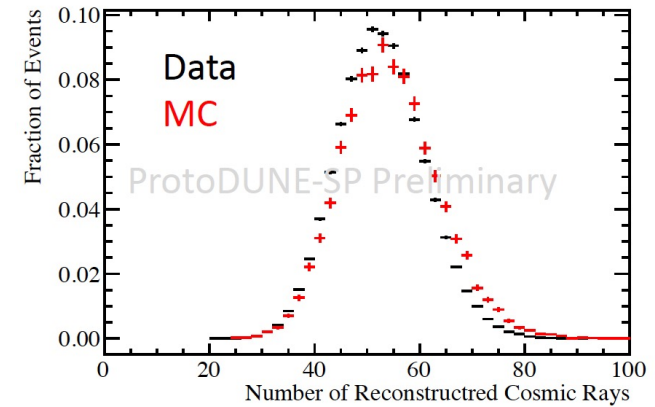


**Charge attenuation and non-uniformity on TPC signal mostly corrected**

# Beam Event and Cosmic Ray Reconstruction



Number of reconstructed cosmic ray tracks in the 3 ms readout window



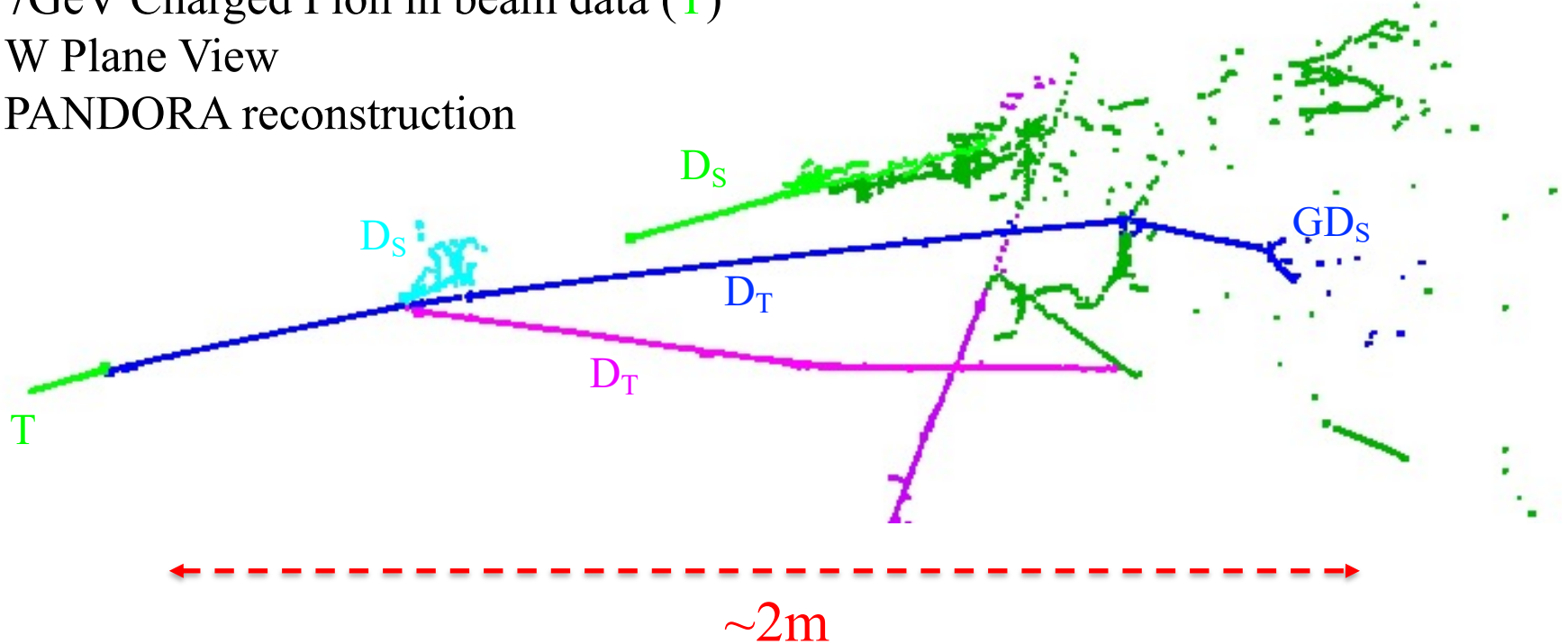
- PANDORA pattern recognition (Eur. Phys. J. C 78, no.1, 82 (2018)) to reconstruct and classify beam events and cosmic muon tracks in 3 ms TPC readout window
- Subsequent off-line analysis deals with beam events and cosmic rays separately

# Beam Event Reconstruction in Data

7GeV Charged Pion in beam data (T)

W Plane View

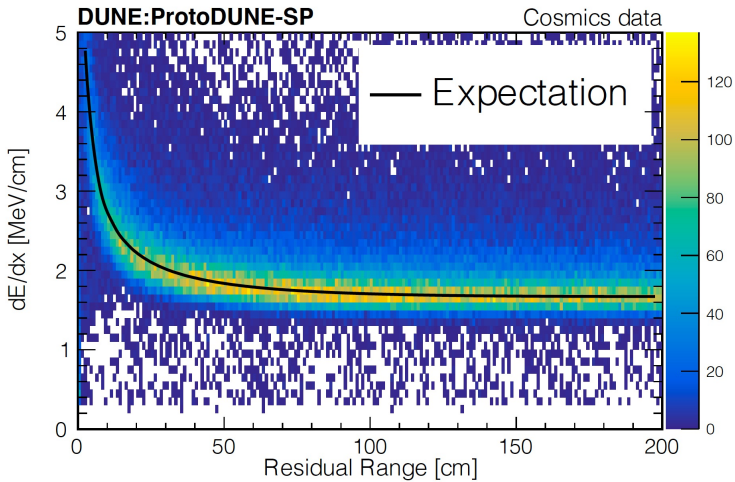
PANDORA reconstruction



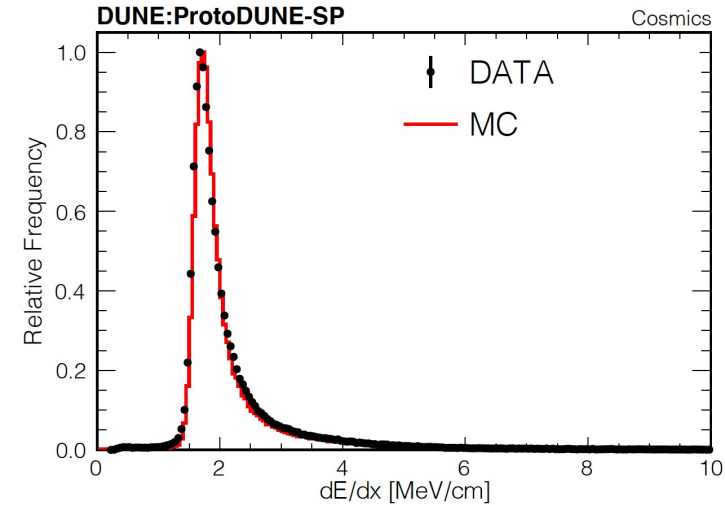
TPC reconstruction  
chain tested with real  
test beam data

T = Trigger Parent Particle from test beam  
D<sub>T</sub> = Daughter Track  
D<sub>S</sub> = Daughter Shower  
G D<sub>T</sub> = Granddaughter Track  
G D<sub>S</sub> = Granddaughter Shower

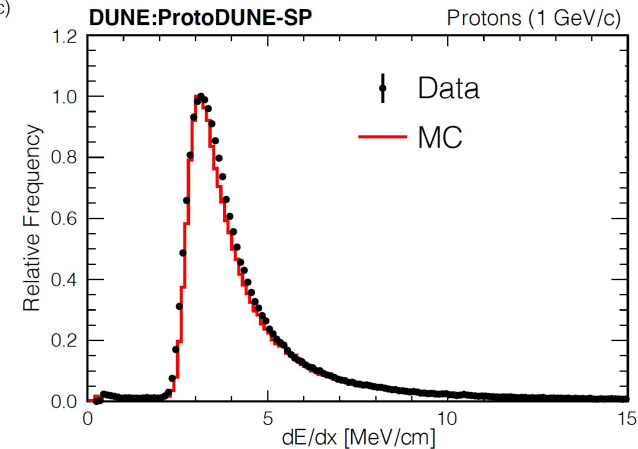
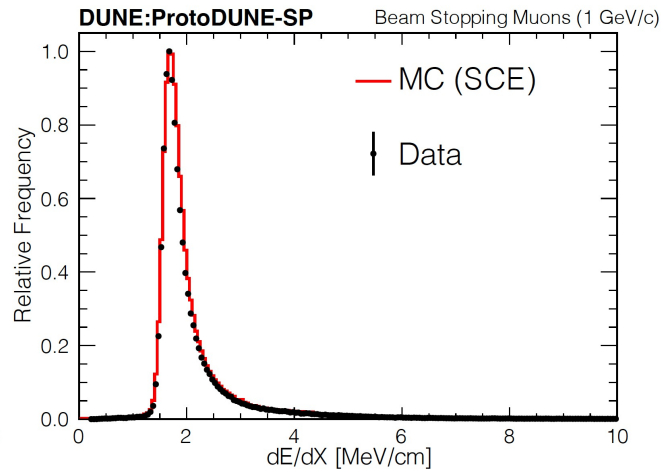
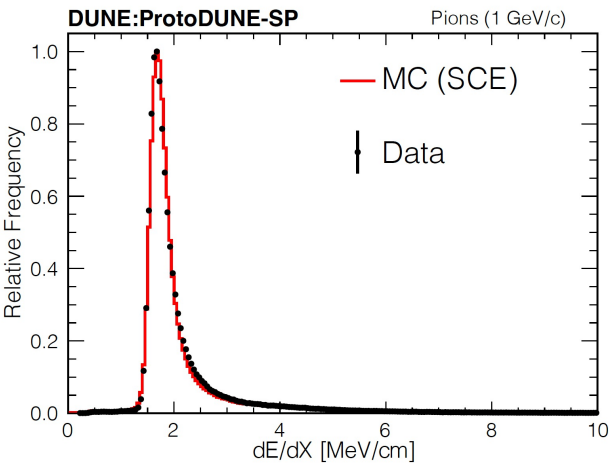
# dE/dx Reconstruction



Use stopping muons in cosmic ray data to determine absolute dE/dx scale



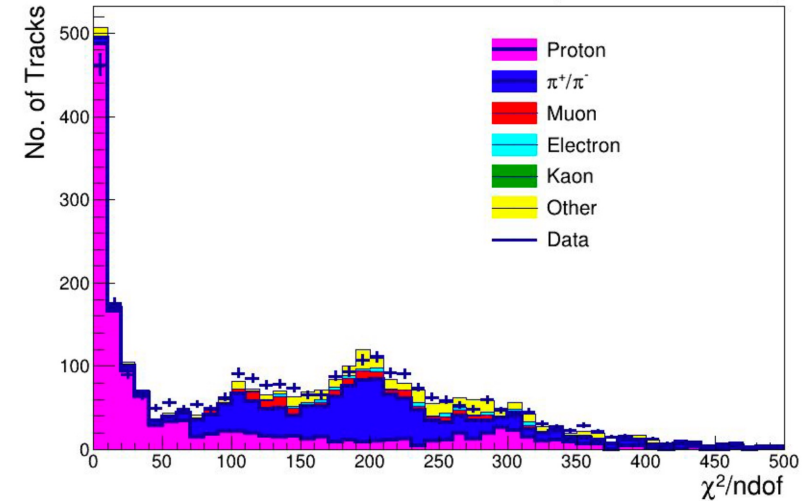
Same stopping muon absolute calibration works well for beam data



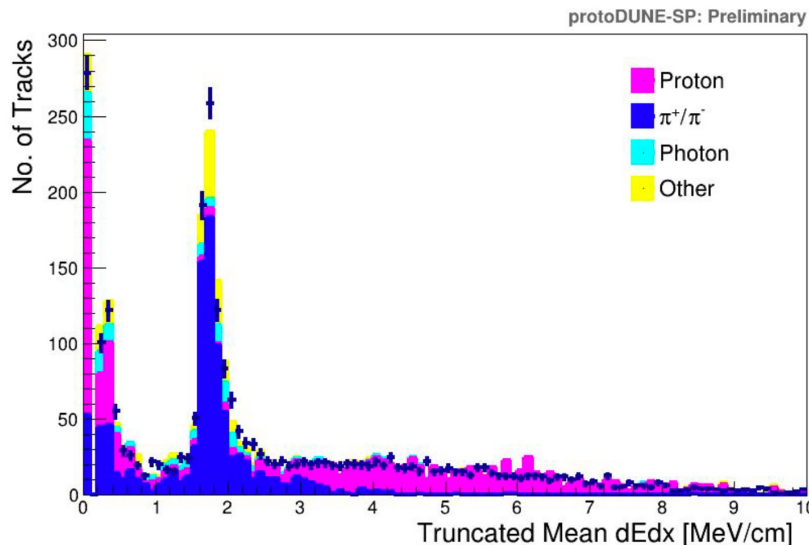
# Particle Identification (PID)

- Well understood and calibrated detector response for different types of particles
- Developed traditional  $dE/dx/\chi^2$ -based particle identification and deep-learning (CNN) based particle identification
- EM-shower and proton identification purity  $\sim 90\%$
- PID distributions show good data/MC consistency

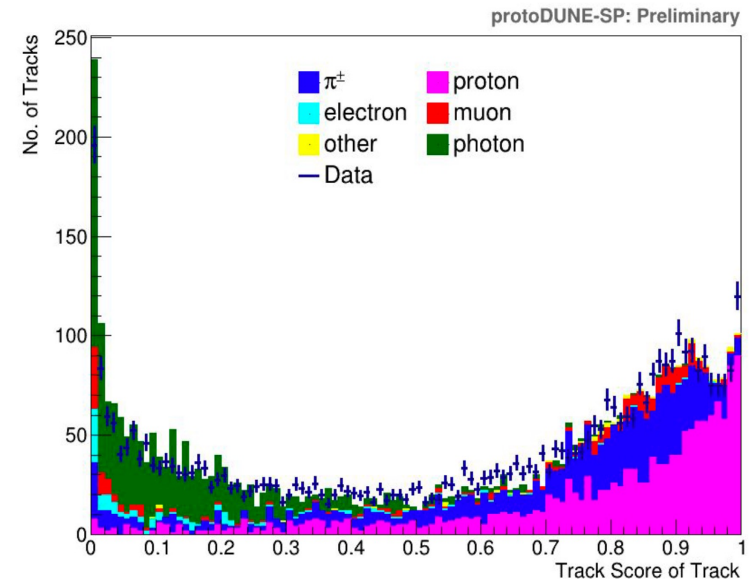
## $dE/dx \chi^2$ for Proton-Pion identification



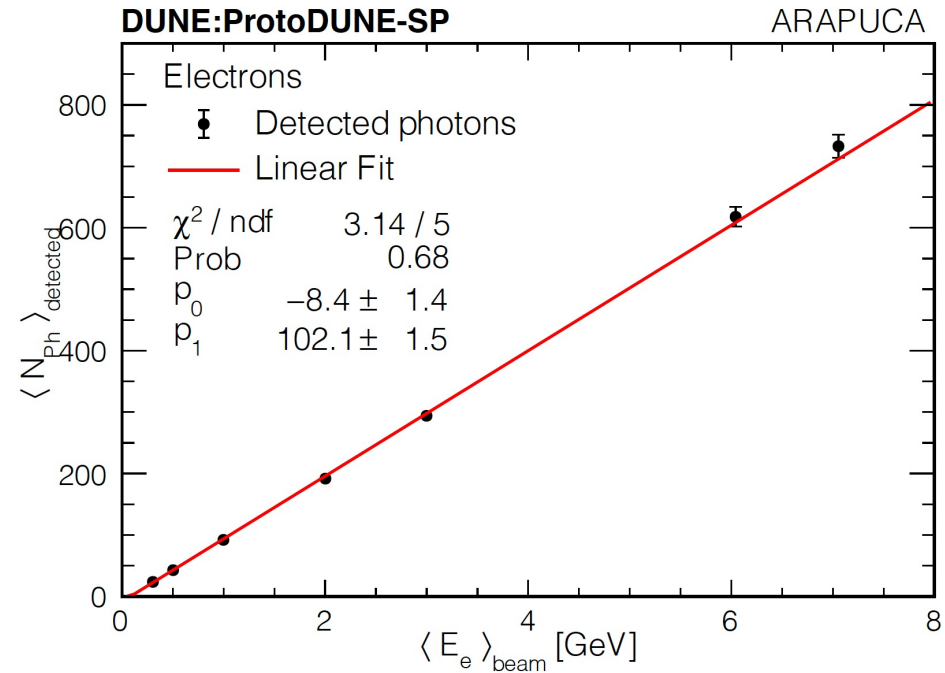
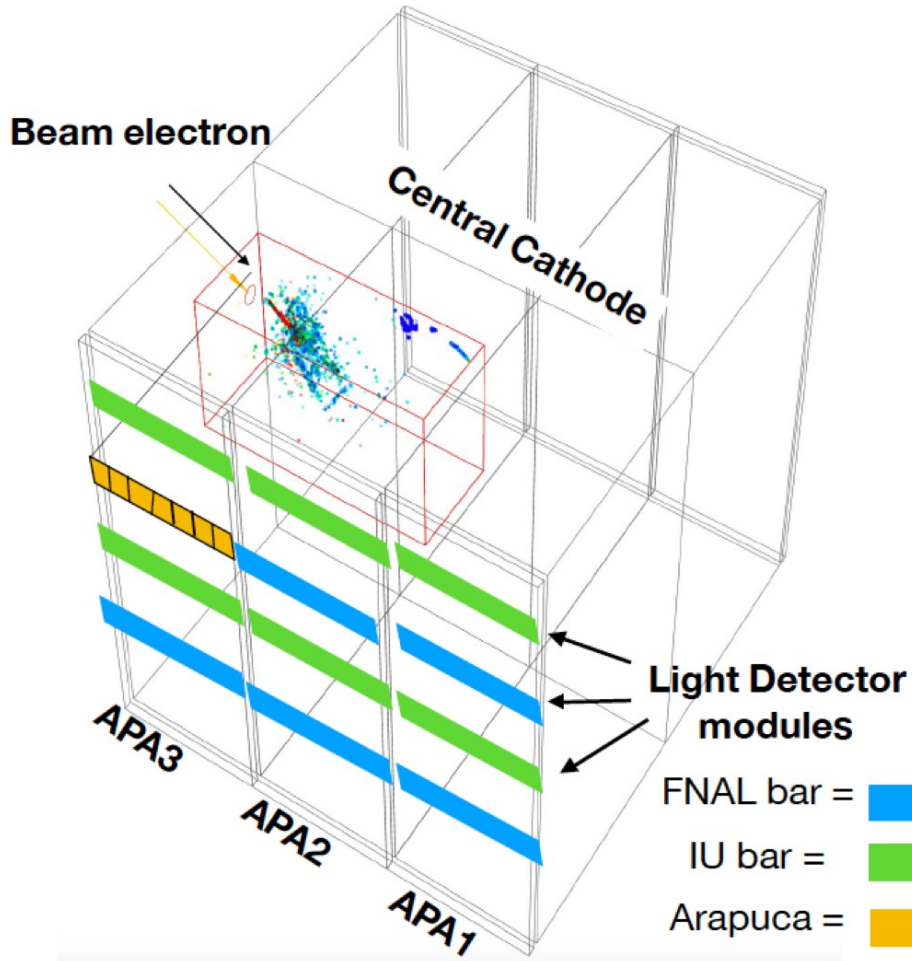
## $dE/dx$ for Proton-Pion identification



## CNN based shower-track separation



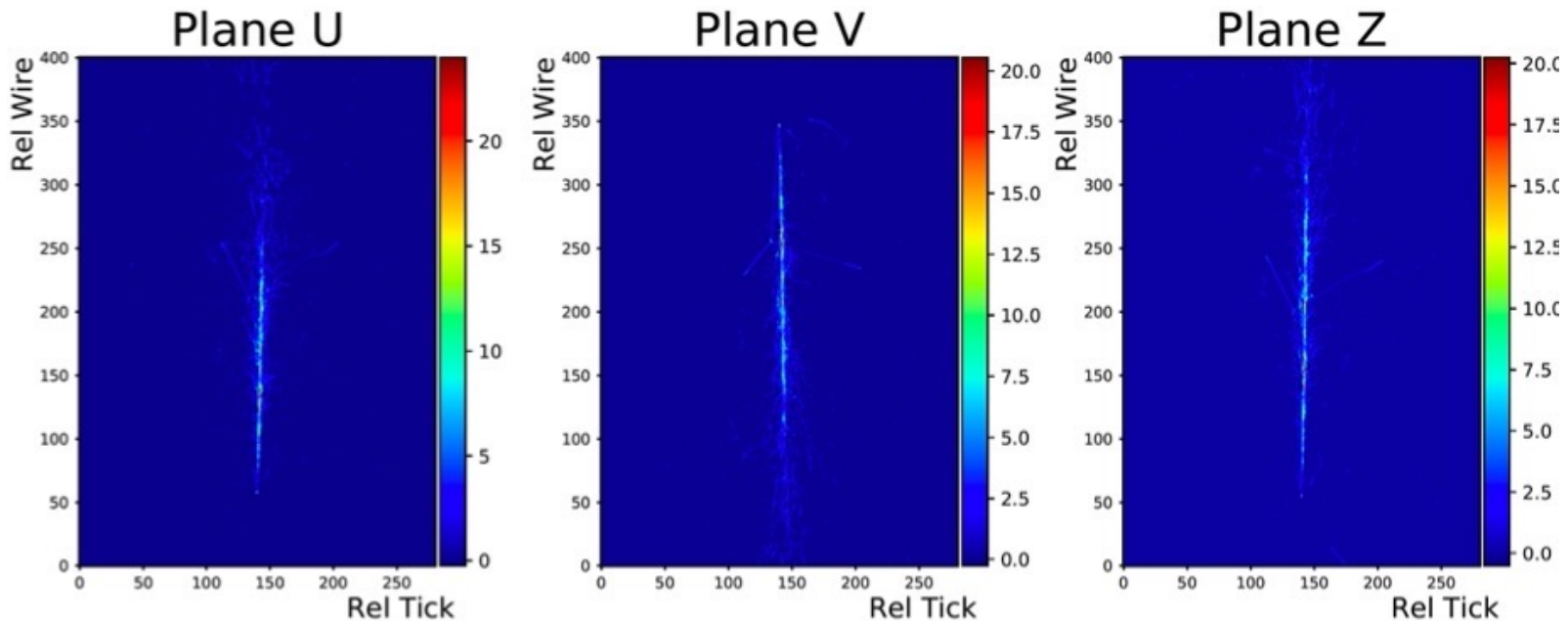
# Photon Detector Performance



- Good energy linearity for contained beam electrons in the detector
- Working on geometry, attenuation and efficiency corrections

# Convolutional Neural Network for Classification and Regression

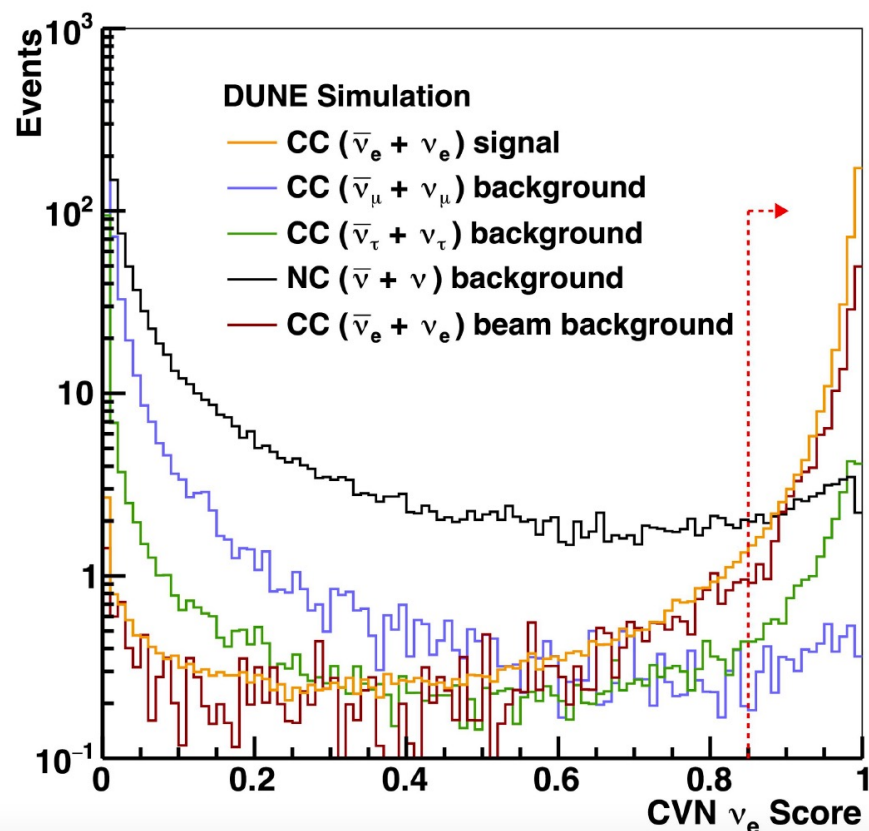
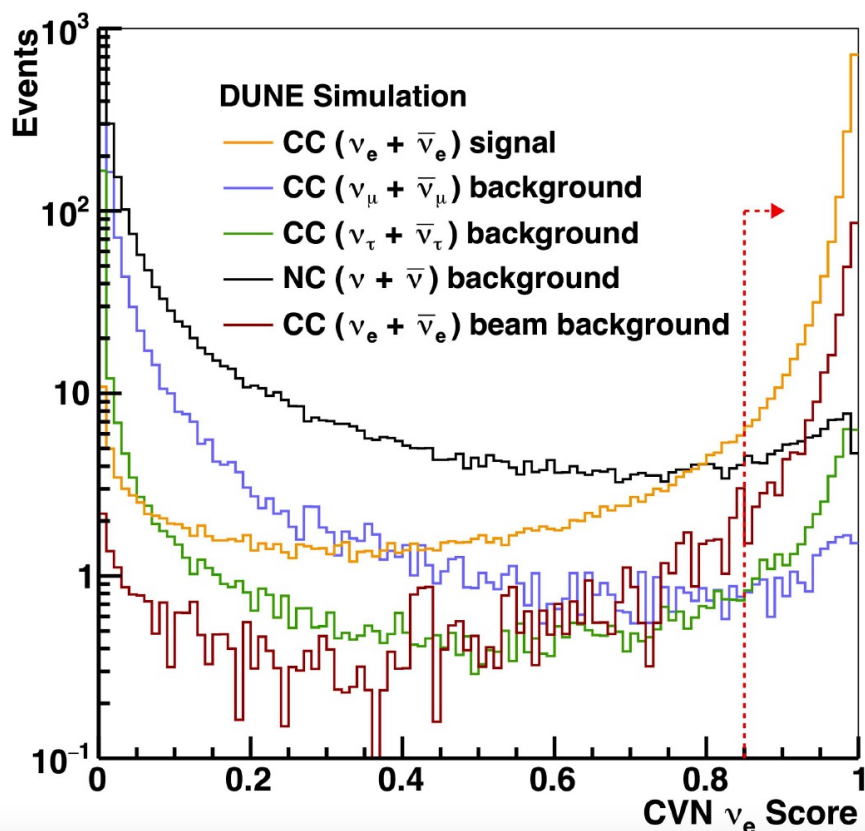
- LArTPC pixel maps for each event are either 3 x 2D images
- CNNs are neural networks specialized to taking images, using a set of translationally invariant filters
- Therefore, reconstructing DUNE events with CNNs is ideal application of deep learning techniques
- CNNs can be used for:
  1. Regression: fitting for particle energy, event energy, or event vertex
  2. Classification: Particle and event identification



*3 x 2-D images for a  $\nu_e$  CC event in DUNE FD simulation: Wire ID vs Time Tick for U, V and Z wire planes*

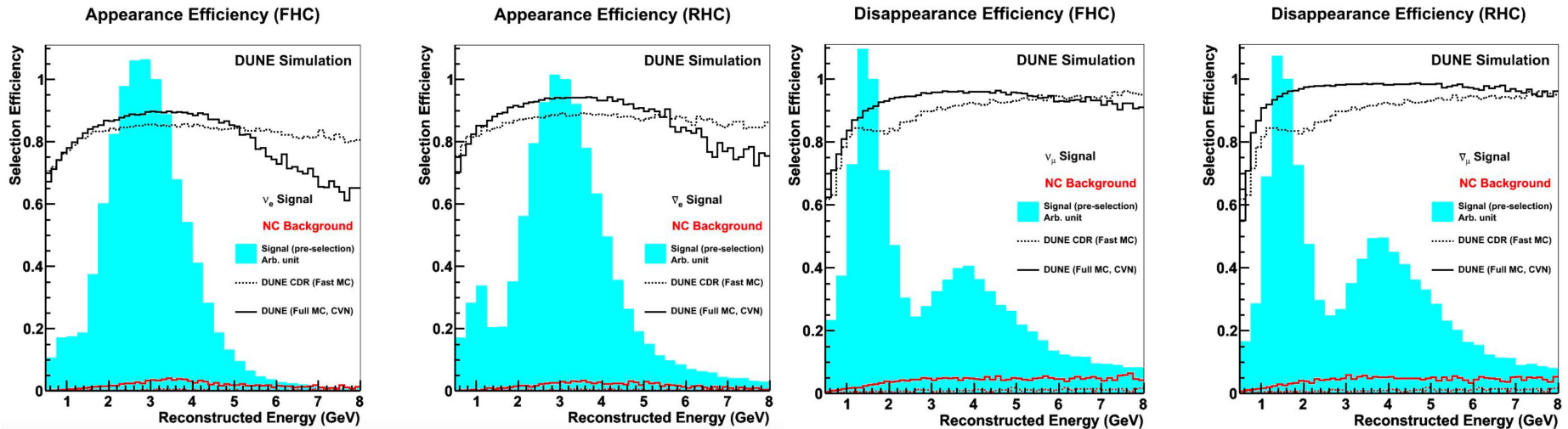
# Event Classification CNN identifiers in DUNE

- Classification Convolutional Neural Network has been implemented at DUNE for event identification (CVN)
- Identify  $\nu_\mu$ CC,  $\nu_e$ CC and NC events



# Event Classification CNN identifiers in DUNE

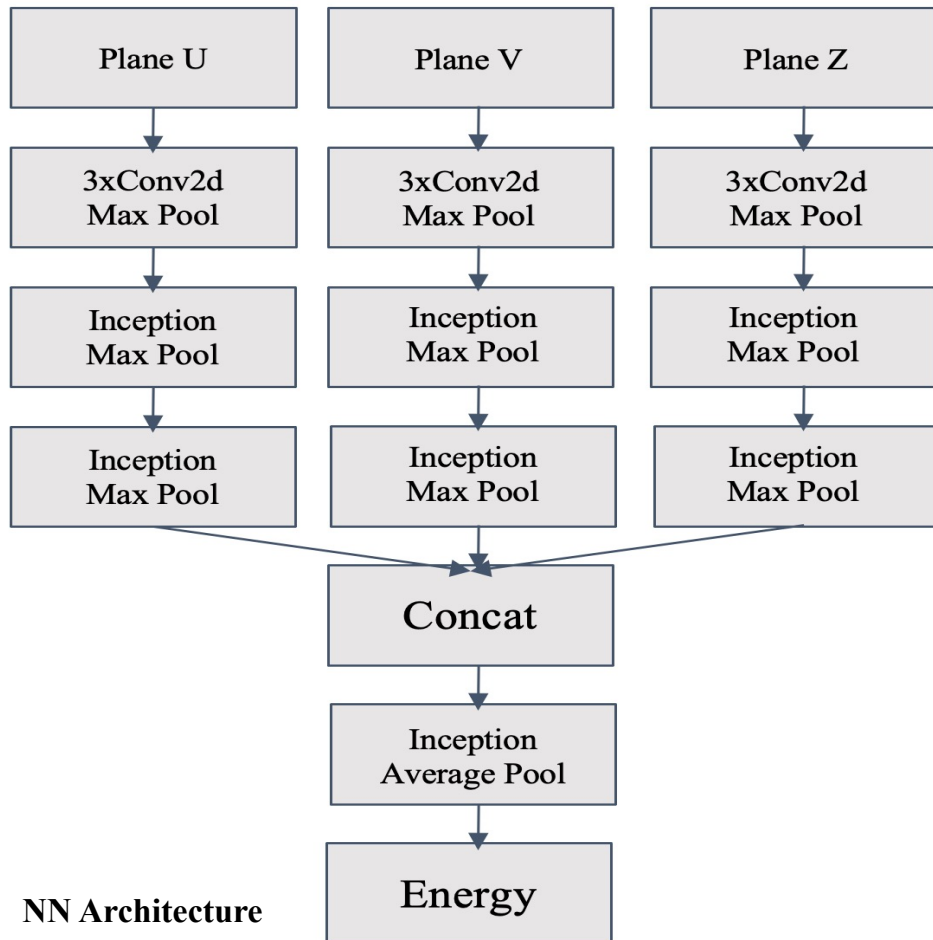
- Performance is better than DUNE CDR assumptions
- Paper published: Phys.Rev.D 102 (2020) 9, 092003



# Regression Convolutional Neural Network for Energy Reconstruction in DUNE

$$L(\mathbf{W}, \{(\mathbf{x}_i, y_i)\}_{i=1}^n) = \frac{1}{\sum_j^n \sqrt{\omega_j}} \sum_i^n \sqrt{\omega_i} L(\mathbf{W}, \mathbf{x}_i, y_i)$$

Loss function

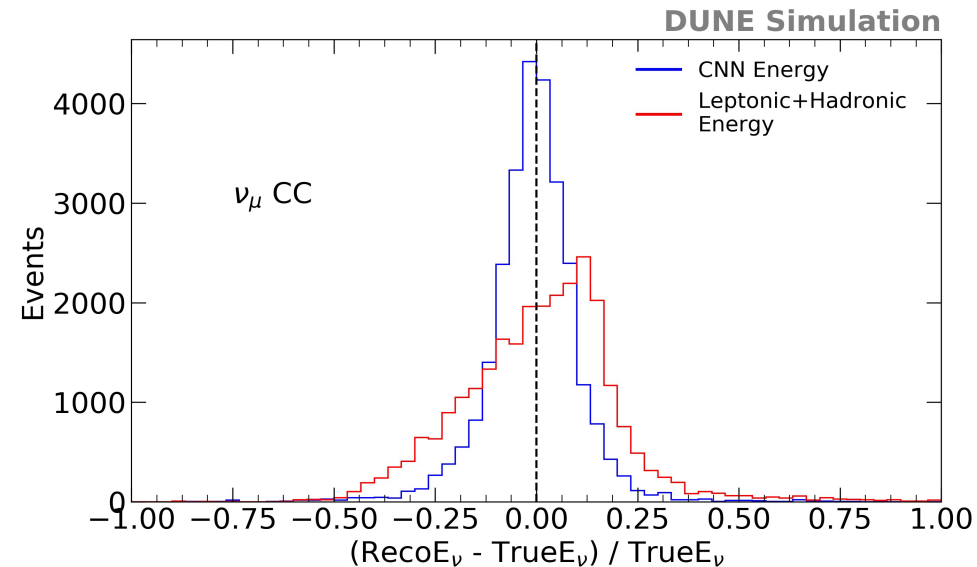
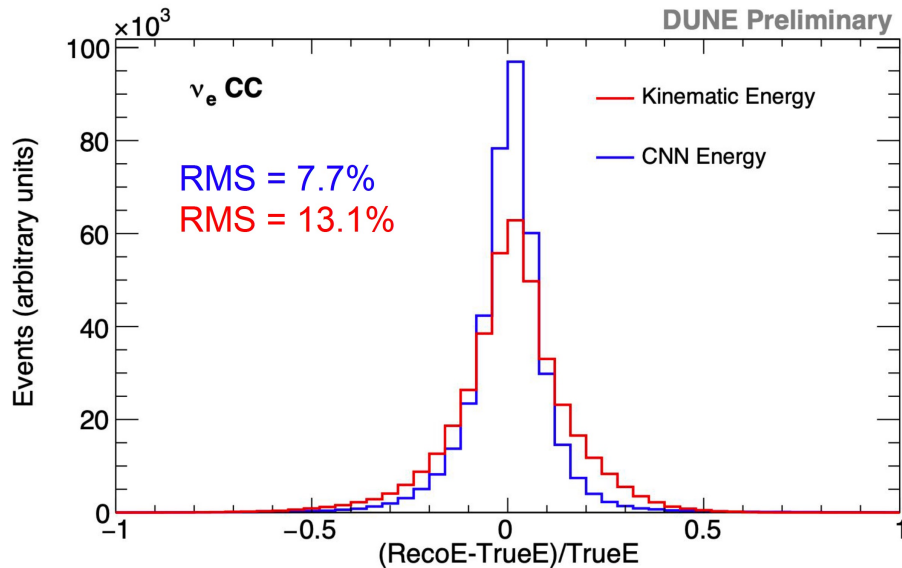


NN Architecture

- Provides appropriate surrogate to optimize energy resolution  $E_{\text{reco}} - E_{\text{true}} / E_{\text{true}}$
- Linear output unit for energy
- Optimize energy resolution and reduce impacts from outliers.
- Use hyperparameter optimization software SHERPA
- Weighted events by energy to reduce energy dependent bias

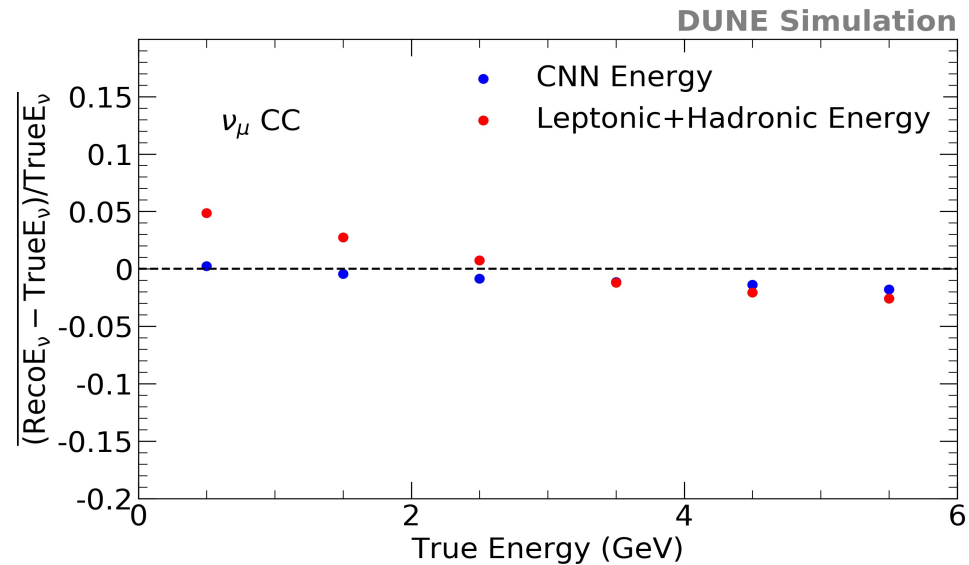
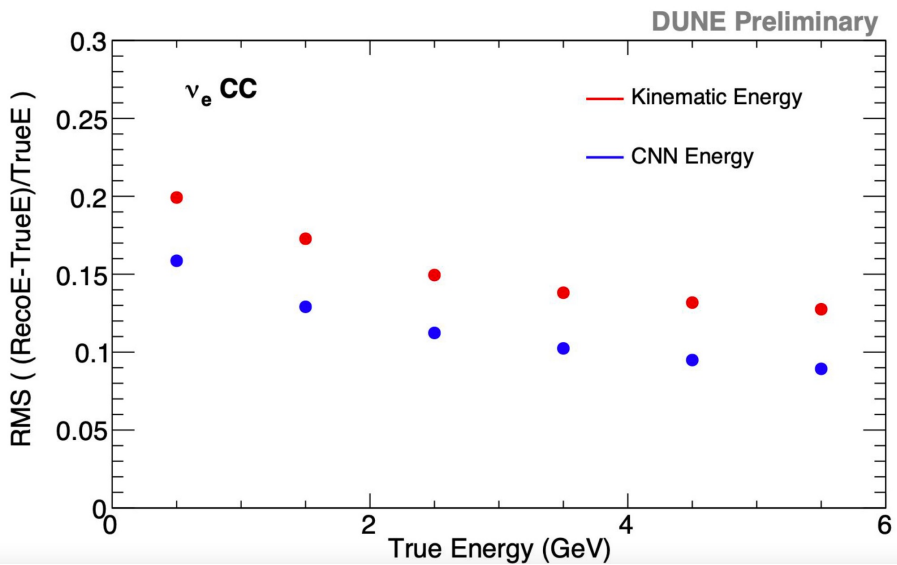
# $\nu_e$ CC and $\nu_\mu$ CC Event Energy

- Regression CNNs outperform kinematic energy based energy reconstruction ( $E(\nu) = E_{lep}^{cor} + E_{had}^{cor}$ )
- Better resolutions in all energy regions



# $\nu_e$ CC and $\nu_\mu$ CC Event Energy

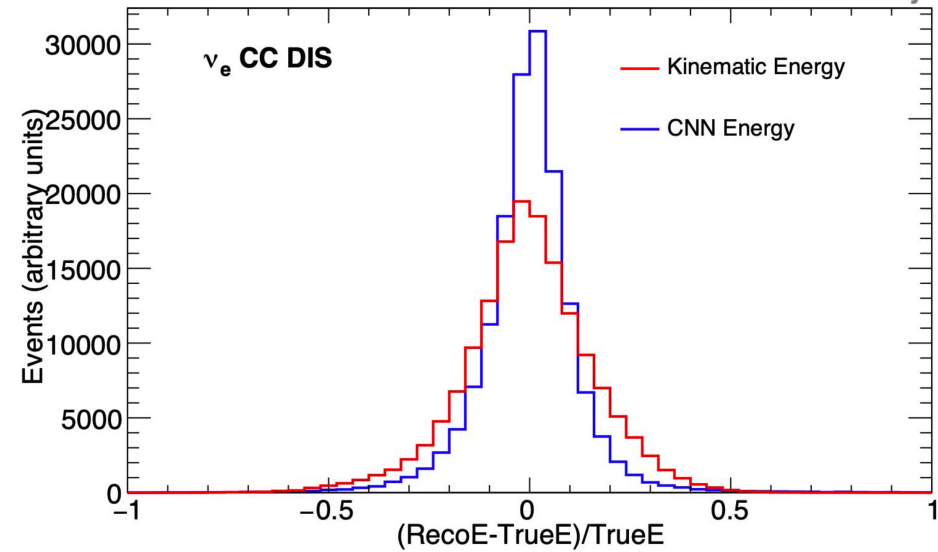
- Regression CNNs outperform kinematic energy based energy reconstruction ( $E(\nu) = E_{lep}^{cor} + E_{had}^{cor}$ )
- Better resolutions in all energy regions
- Less energy dependent bias



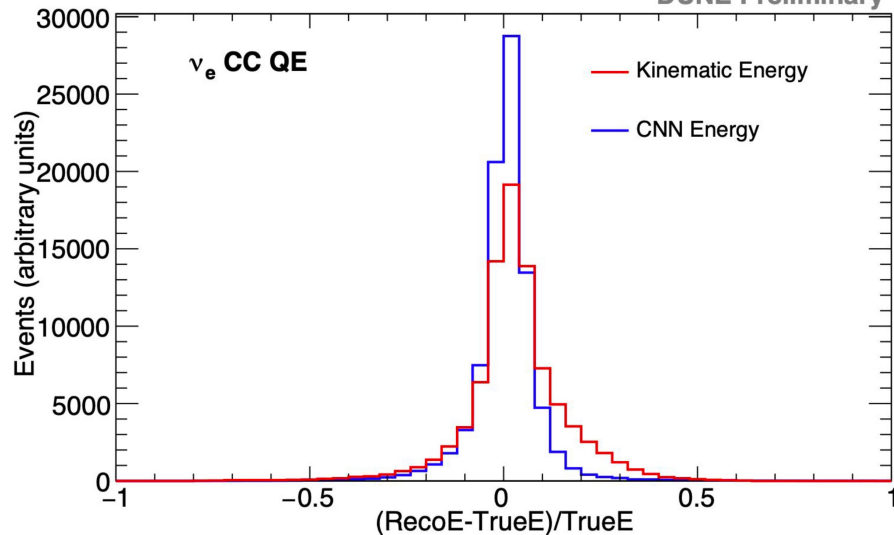
# $\nu_e$ CC and $\nu_\mu$ CC Event Energy

- CNNs are also robust against neutrino interaction modes, because of high number of degrees of freedom to fit to different types of interaction

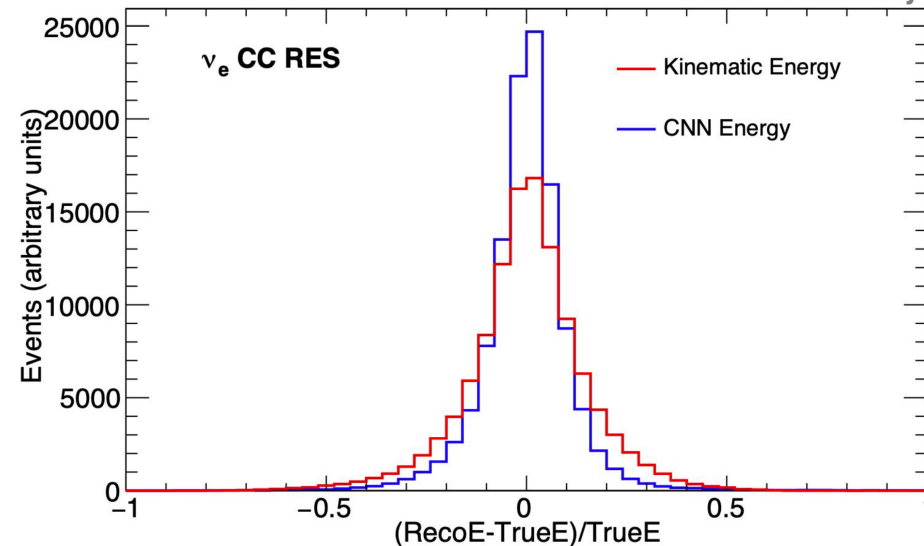
DUNE Preliminary



DUNE Preliminary

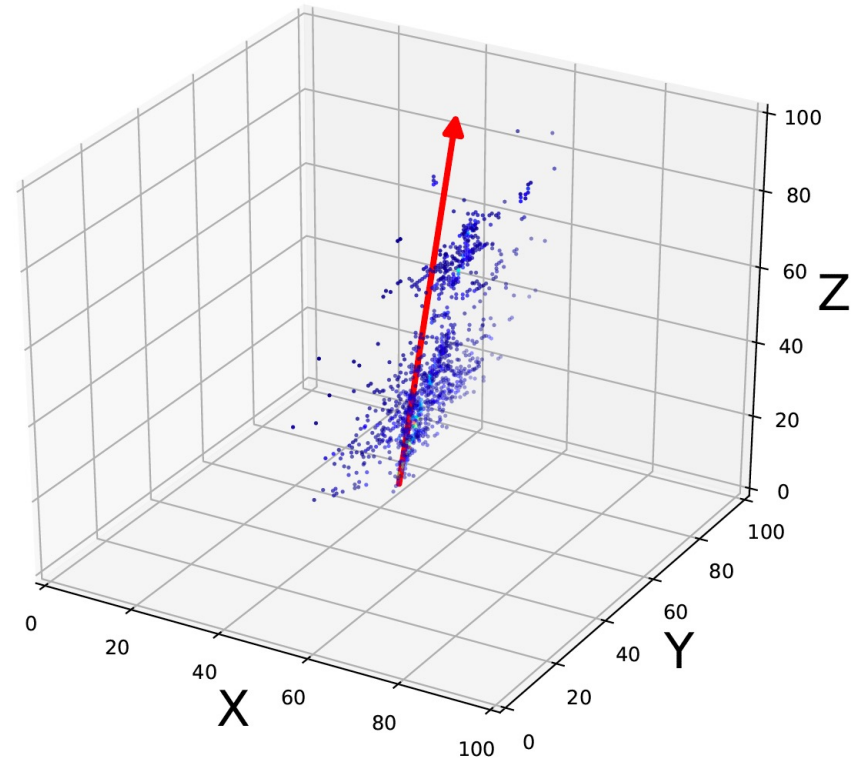
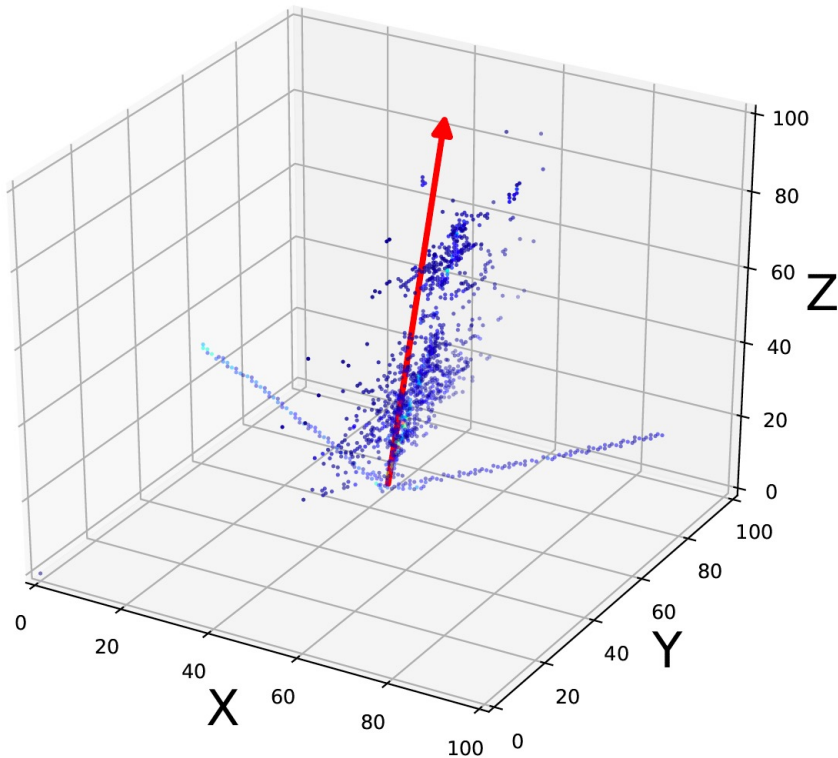


DUNE Preliminary



# Particle Direction Reconstruction

- Direction regression heavily dependent on 3-D geometry
- So we designed a 3-D CNN to reconstruct particle directions.
- 3-D image constructed from the 3x2D detector images

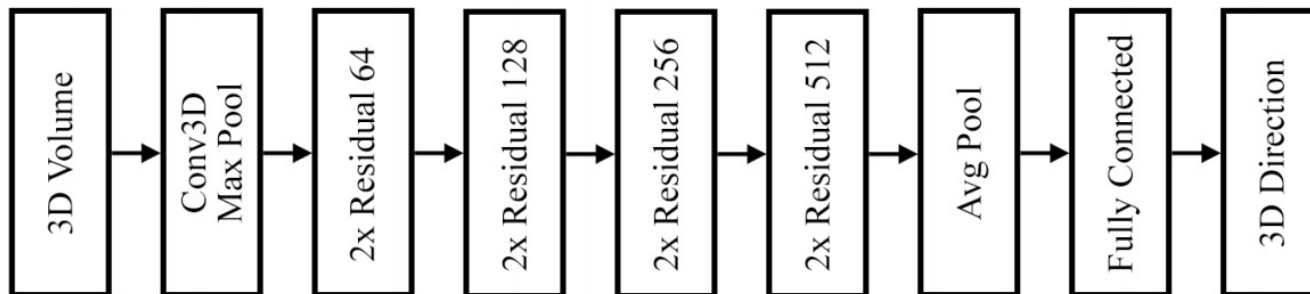


# Particle Direction Reconstruction

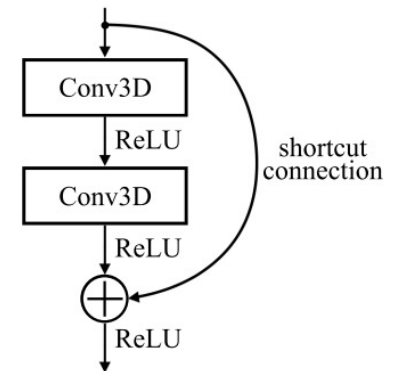
- To distinguish between exactly opposite directions, we defined relaxed cosine distance loss for better performance:

$$L_{\text{dir}} = \frac{1}{n} \sum_{i=1}^n \min \left( 1 + \frac{\vec{d}_{\text{True}}^i \cdot \vec{d}_{\text{Reco}}^i}{|\vec{d}_{\text{True}}^i| |\vec{d}_{\text{Reco}}^i|}, 1 - \frac{\vec{d}_{\text{True}}^i \cdot \vec{d}_{\text{Reco}}^i}{|\vec{d}_{\text{True}}^i| |\vec{d}_{\text{Reco}}^i|} \right)$$

- Architecture model built on a series of residual blocks and a linear layer to output 3-D direction vectors. A cosine distance metric used for training



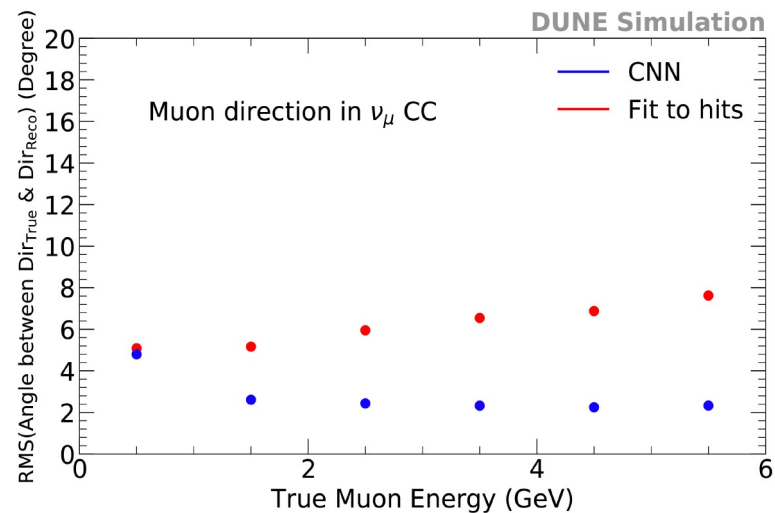
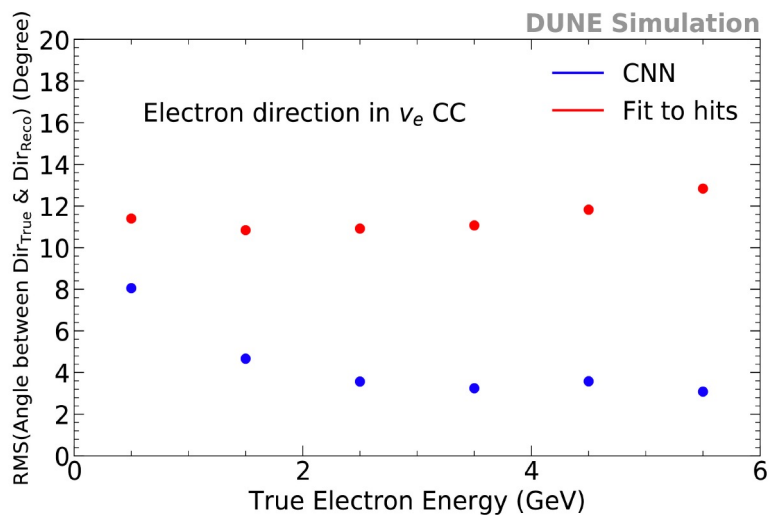
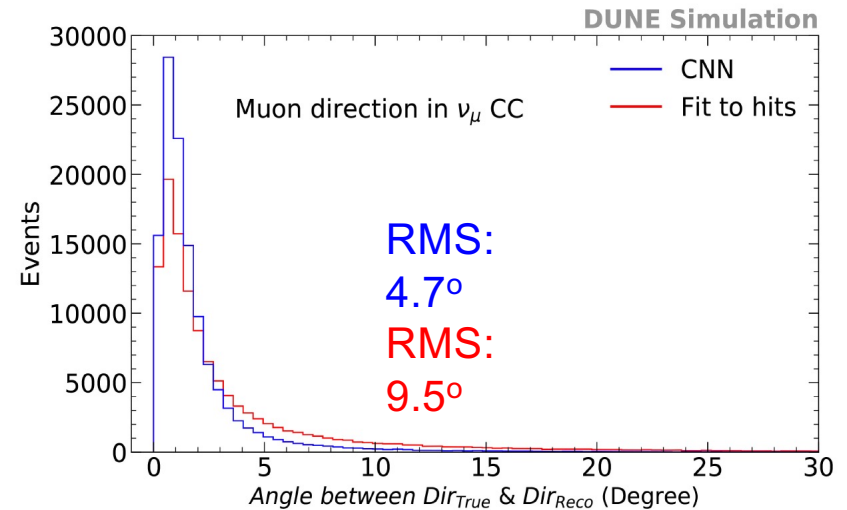
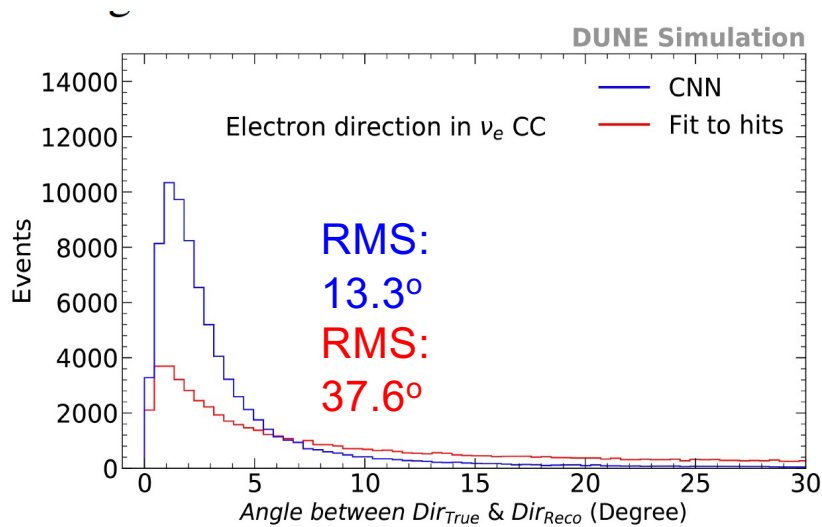
(a) Direction Regression



(b) Residual block

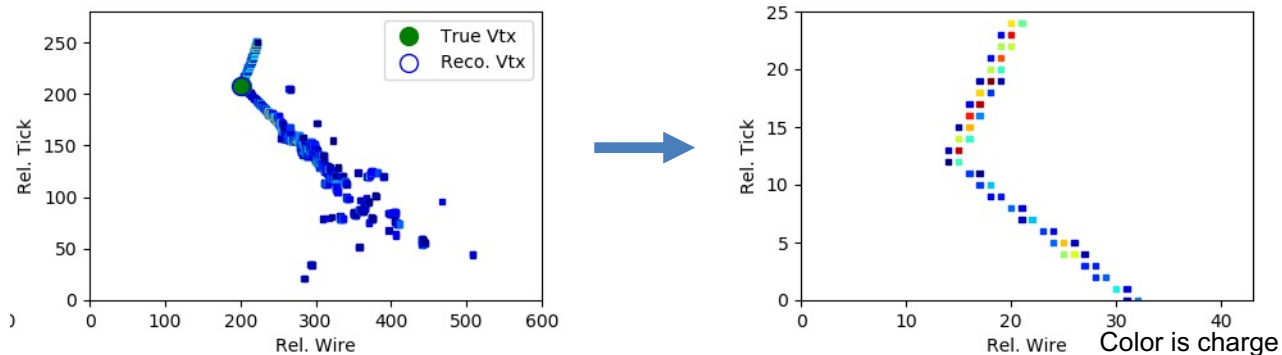
# Particle Direction Reconstruction

- Regression CNNs beat traditional fit-to-hits method with better electron and muon resolutions in all energy regions

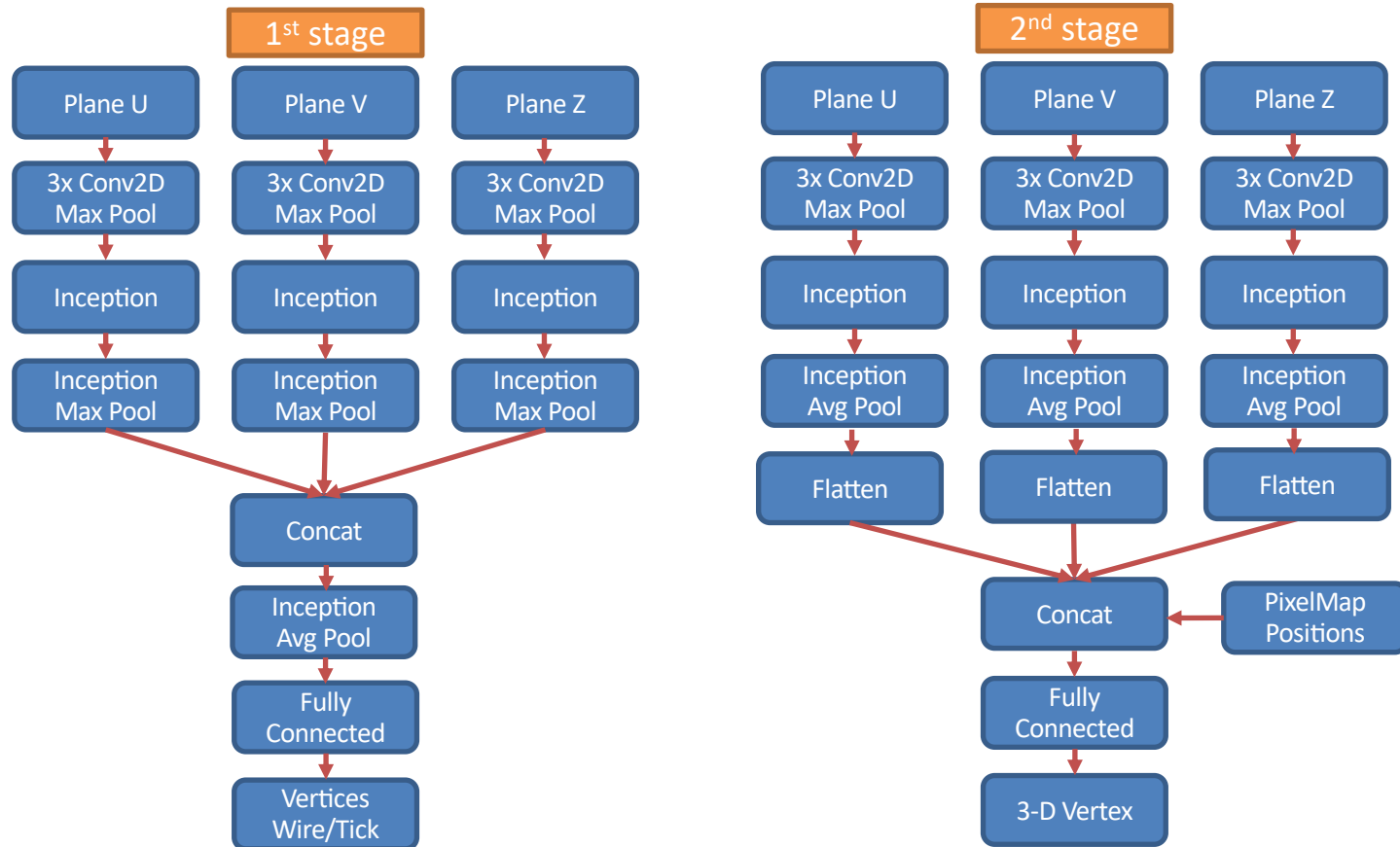


# Two stage training for Vertex

- The pixel map size (280x400) is too large for vertex training, to improve resolution we construct 2-stage architecture
- First stage: propose the vertex on each plane  $\rightarrow$  crop each view and make smaller pixel map
- Second stage: reconstruct the 3-D vertex with the smaller pixel map



# Vertex Regression CNN Architectures

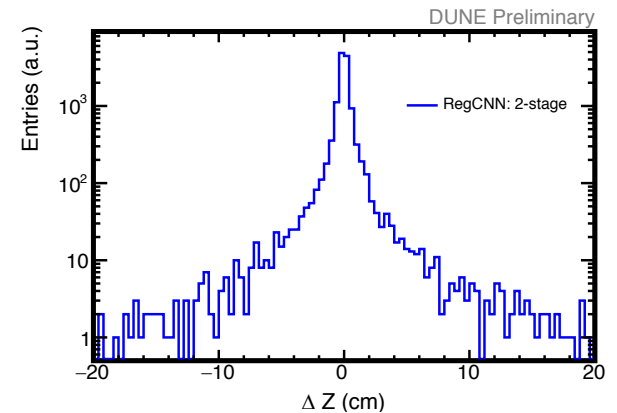
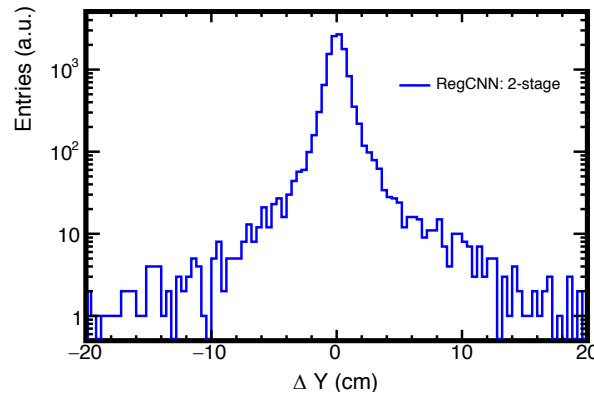
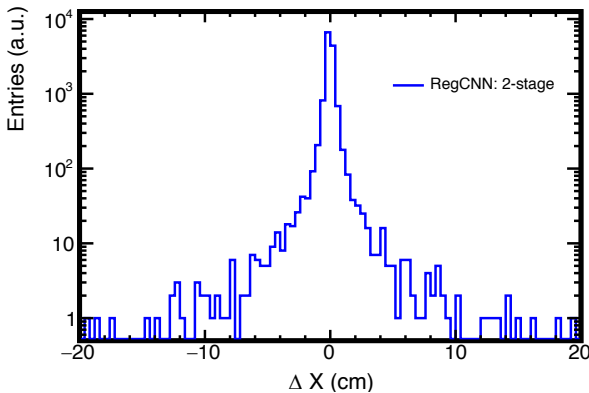
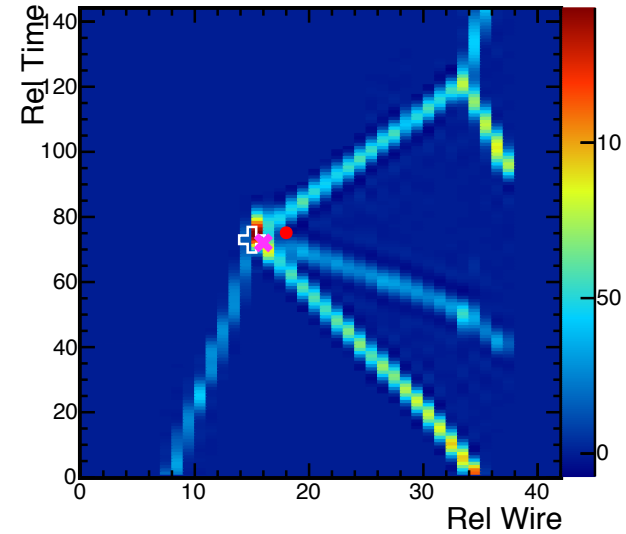
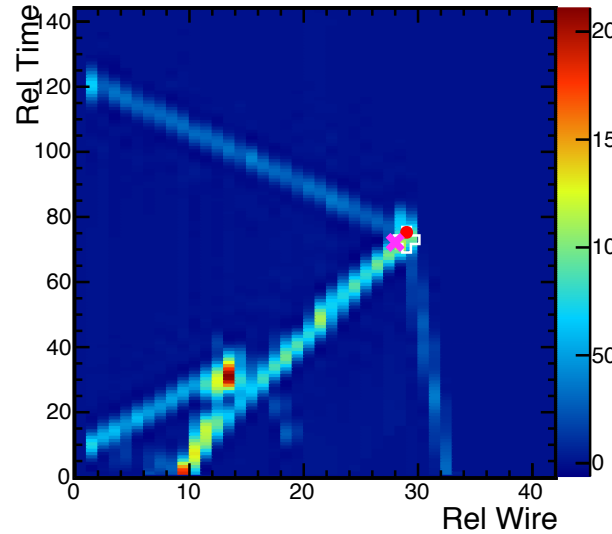
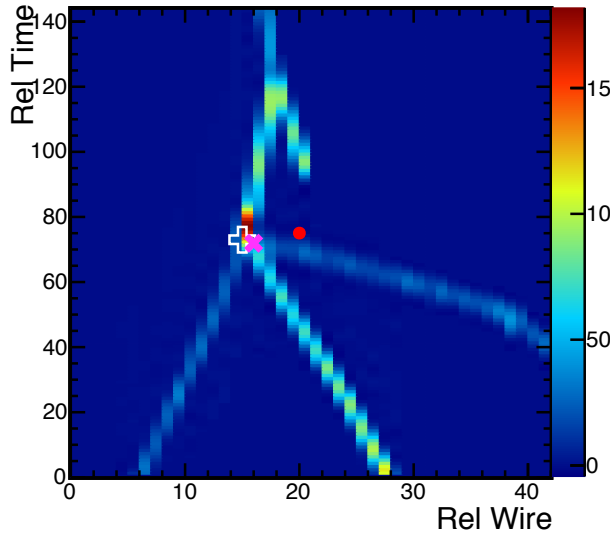


# Reconstructed 3-D Vertex at DUNE

+ true vertex  
U plane

× RegCNN vertex  
V plane

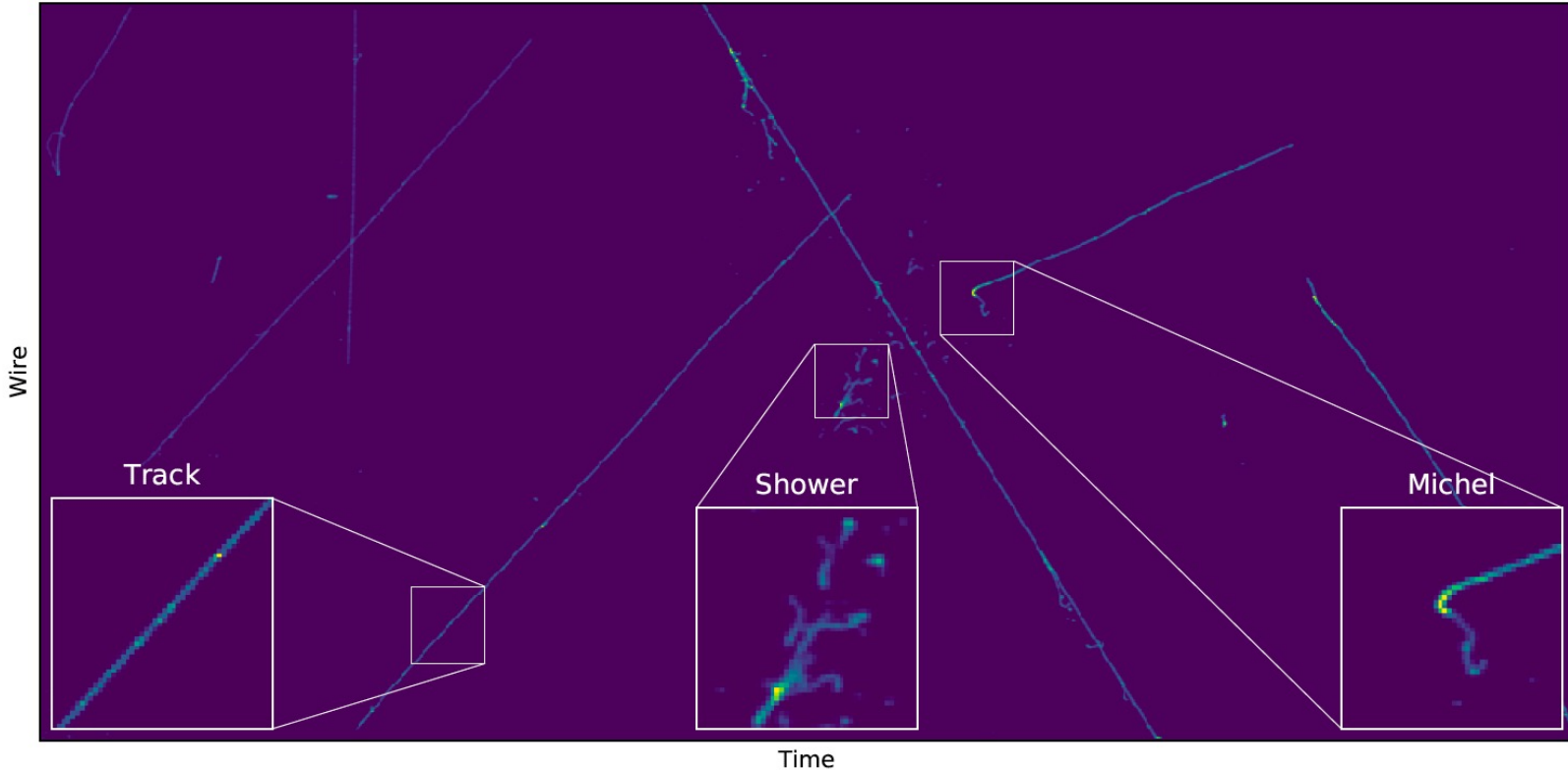
• Traditional vertex reconstruction  
Z plane



Vertex reconstructed by Regression CNN has better precision than traditional methods

# CNN for Shower/Track Separation in ProtoDUNE-SP

ProtoDUNE-SP Event with Example CNN Input Patches

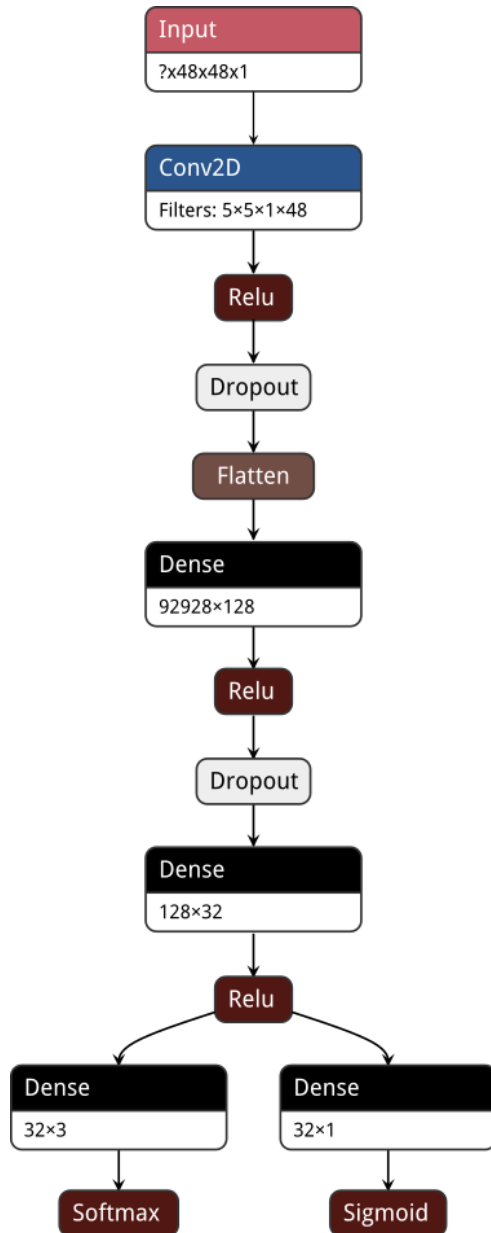


Use CNN to classify energy deposits (hits) from Shower, Track and Michel electrons

- Showers: Energy deposit pattern caused by electron, gamma, etc
- Tracks: Energy deposit pattern caused by muon, pion, etc
- Michel electrons: Low energy electron from muon decays

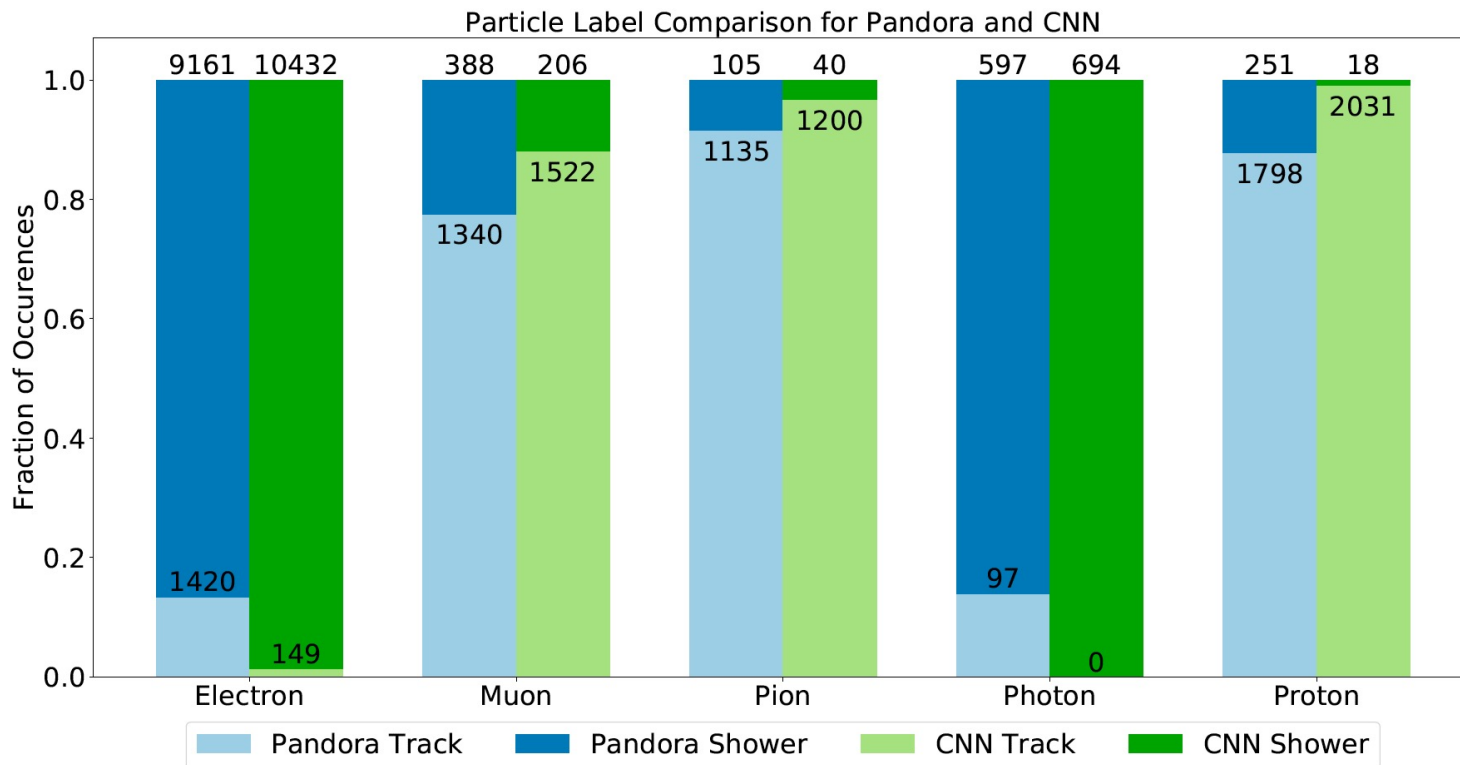
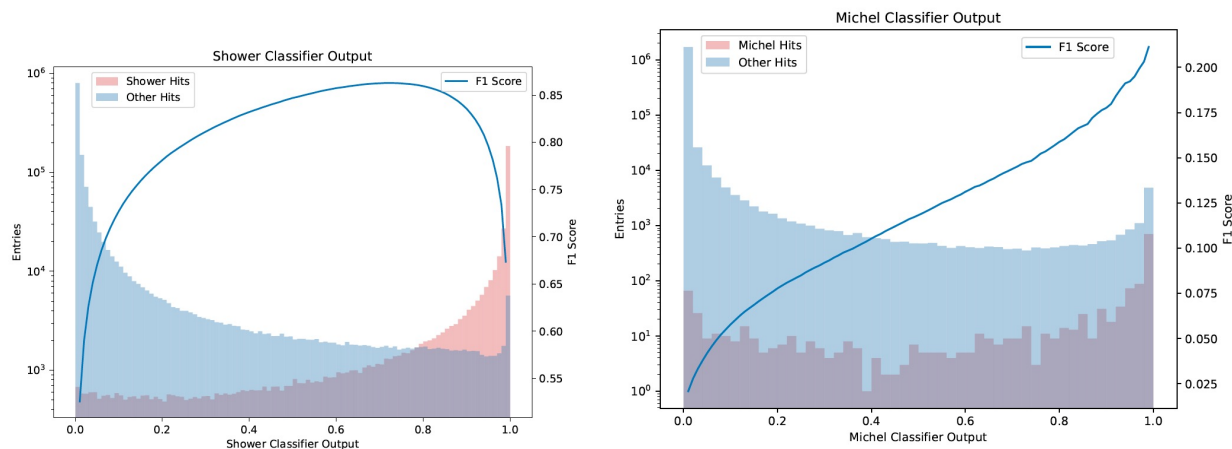
Can be used in clustering, PID, etc

# CNN architecture

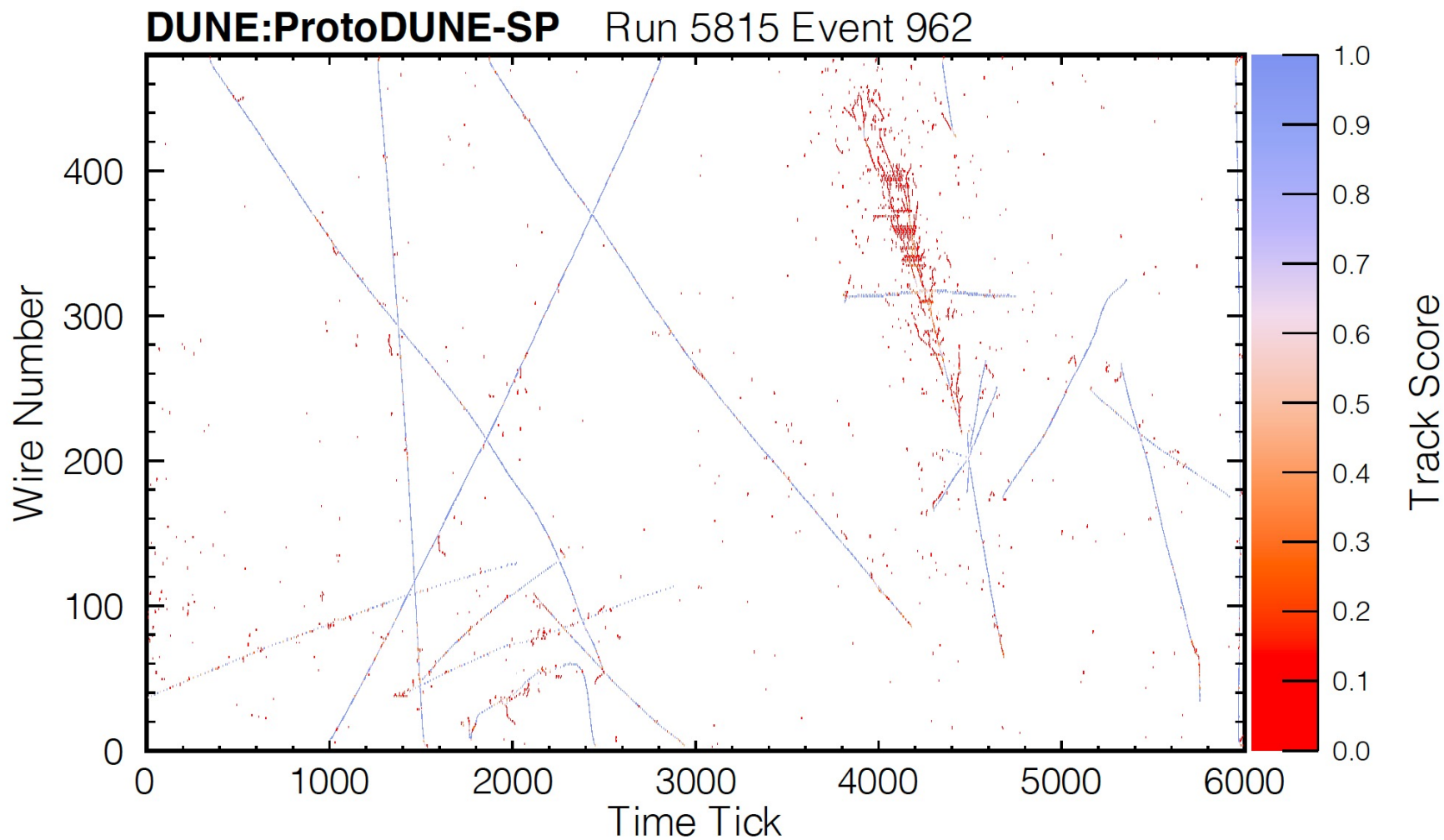


- The inputs are 48 pixel images centered on the reconstructed hit object to be classified
- A single convolutional layer is used to extract feature maps from the images
- These are processed by two dense layers before being split into two branches which classify the images
- The question mark in the input box denotes that images can be processed in parallel in a batch
- Output is the type of hit: from shower? Track? Michel electron?

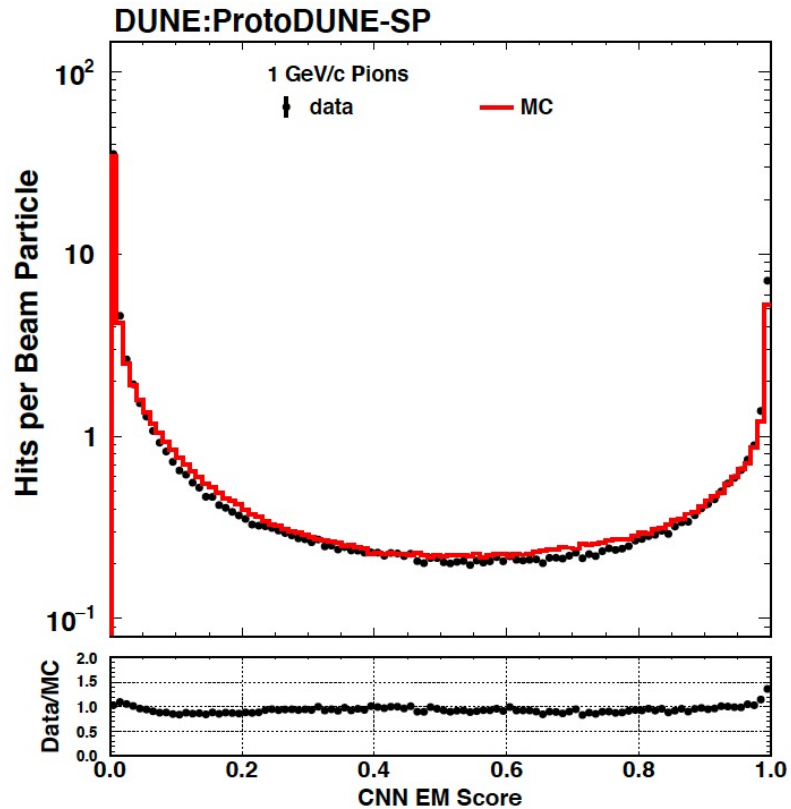
# Performance of Shower/Track CNN in MC



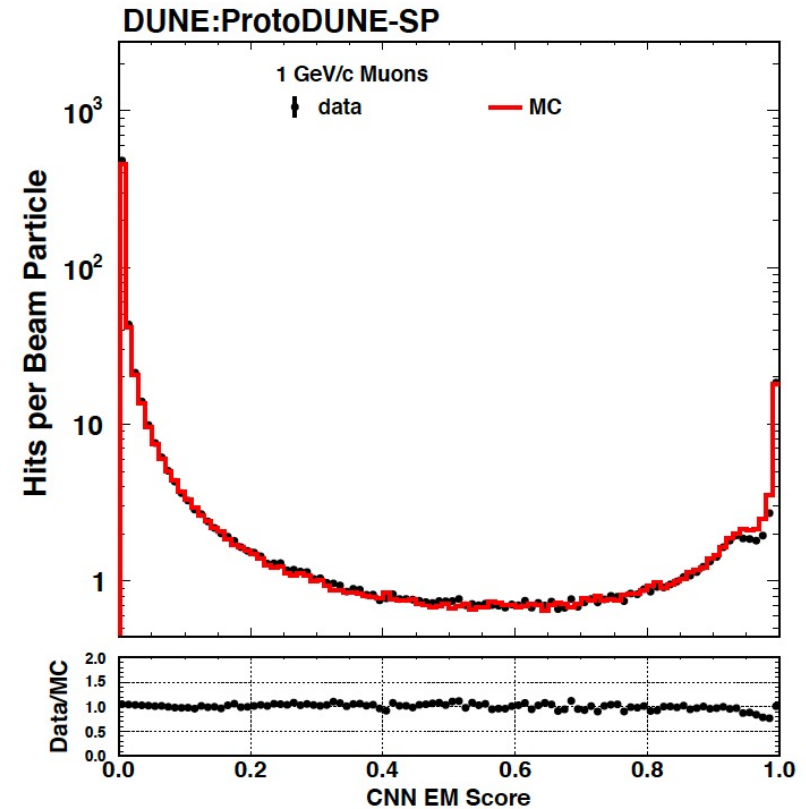
# Performance of Shower/Track CNN in Data



# Performance of Shower/Track CNN in Data



(a) pion



(b) muon

Shower classifier scores for different particle species in the ProtoDUNE-SP beam. The error bars on the data are statistical.

# Other Methods Being Developed at DUNE

- Sparse CNNs for Semantic Segmentation
  - Takes advantage of sparseness of hits in 3D pixelmaps
  - Has shown promise for identifying individual pixels as part of tracks or showers
- Graph Neural Networks (GNN) 
  - Breaks up hits into “graph” comprised as connected nodes with information such as geometry and energy composition
  - Feeds these graphs to a NN which labels individual nodes
  - Has shown promise in ProtoDUNE

# Summary

- NOvA new results
  - Precisely measured  $\sin^2\theta_{23} = 0.57+0.03-0.04$  and  $\Delta m_{23}^2 = (2.41+0.07-0.07)*10^{-3} \text{ eV}^2$
  - Exclude  $\delta_{\text{CP}}=\pi/2$  in IH at  $> 3\sigma$
  - Disfavor (NH,  $\delta_{\text{CP}}=3\pi/2$ ) at  $\sim 2\sigma$
- With the full dataset and an upgraded beam, can reach  $3\sigma$  hierarchy sensitivity for 30-50% of  $\delta$  values

- DUNE Collaboration has been established as an international scientific priority in next decade:
  - Decisive measurements to CP violation, Mass Ordering and Octant of  $\theta_{23}$
  - Also Nucleon decay, Astroparticle physics, BSM ...
- Technical Design Report for DUNE FD complete, Conceptual Design Report for DUNE ND under review
- ProtoDUNEs successfully operating at CERN, first results released

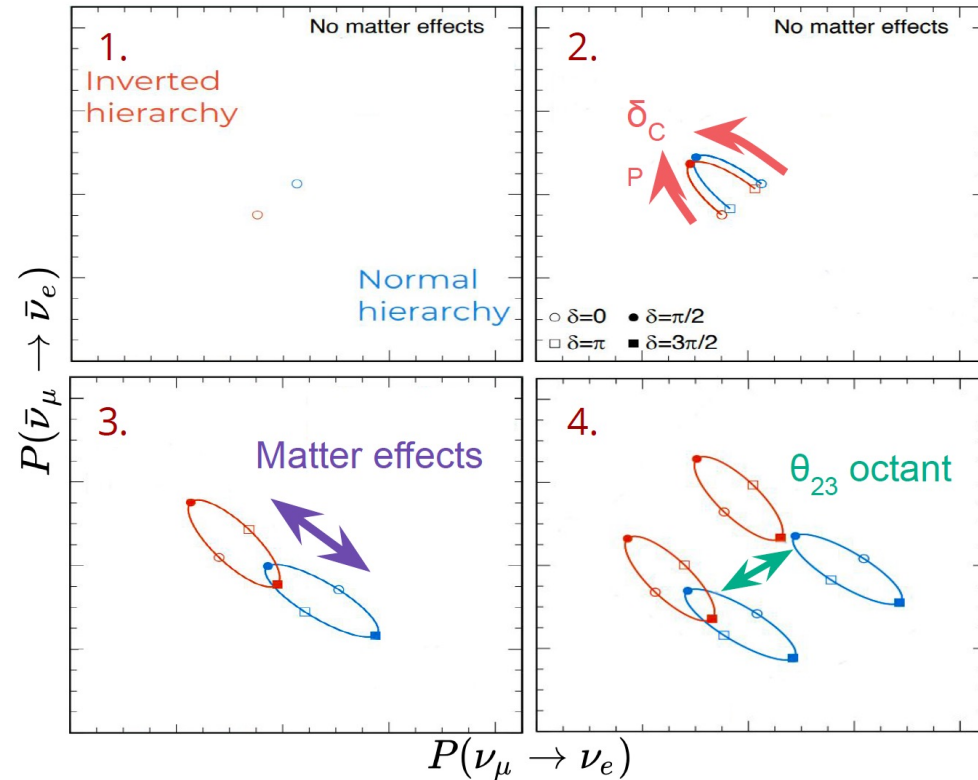
- Machine Learning in NOvA and DUNE:
  - NOvA published physics results with deep-learning algorithms
  - Many deep-learning algorithms developed in NOvA and DUNE
  - Developing full AI/ML based reconstruction chains at NOvA and DUNE
  - Machine learning also enhance oscillation parameter inference

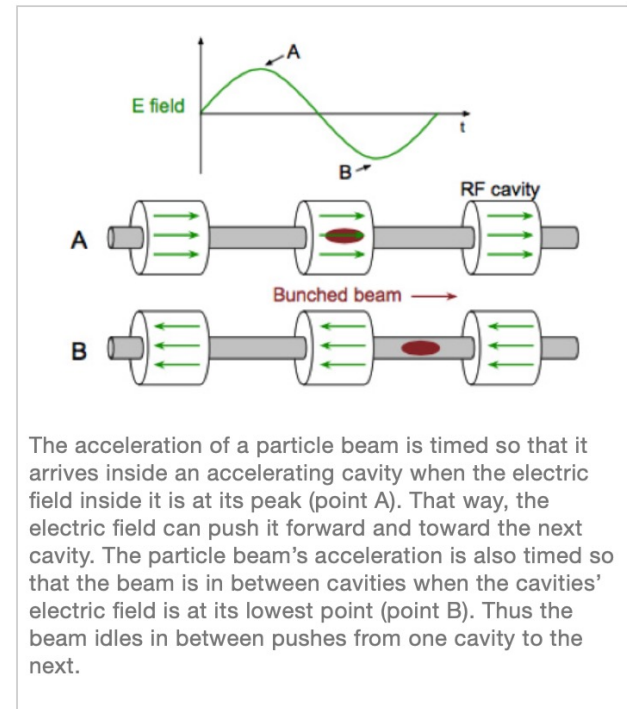
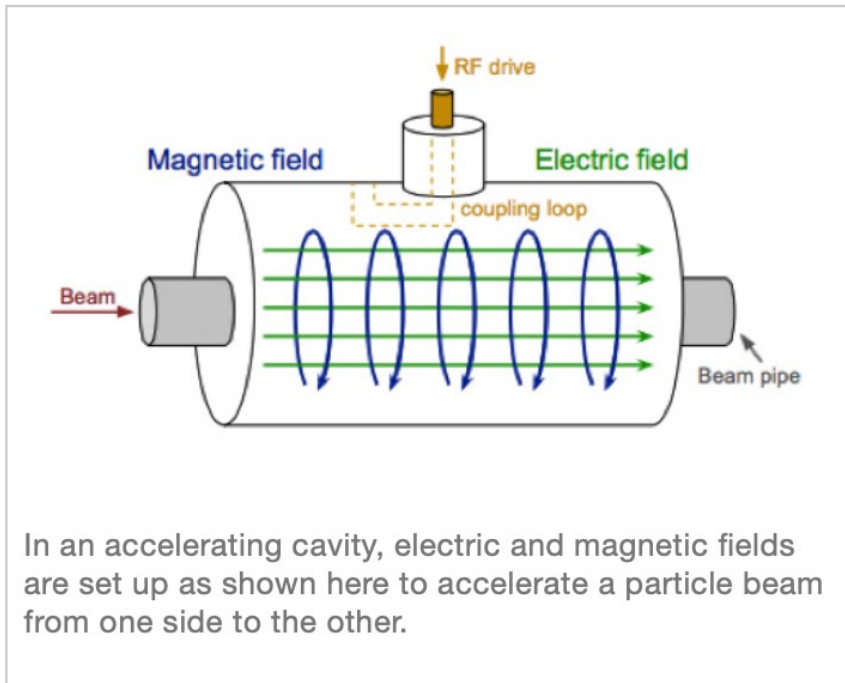
*Thank you!*

# *Backup*

# Appearance $\nu_e$ vs anti- $\nu_e$

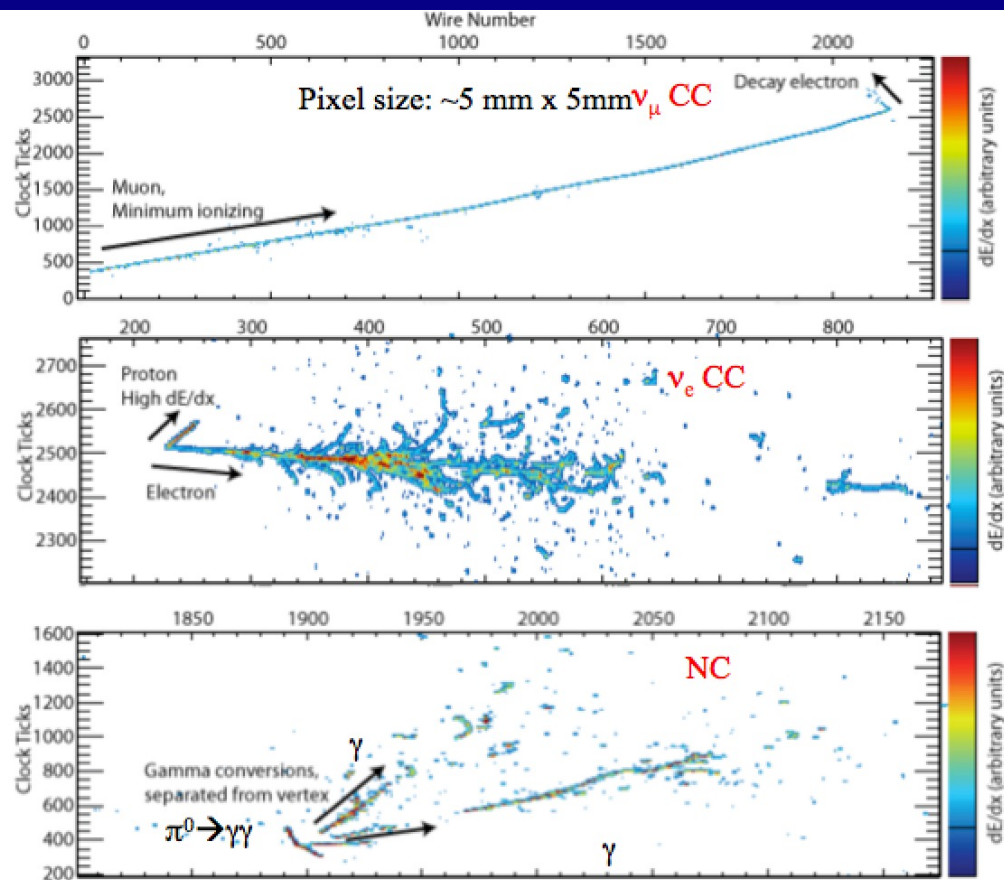
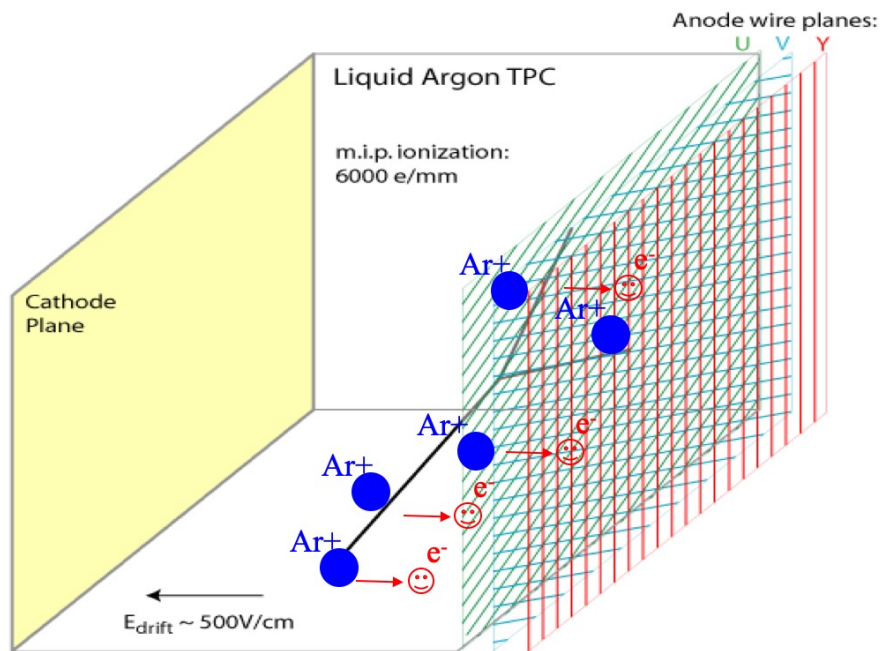
1. Inverted hierarchy gives a **slight suppression** in both.
2. **CP violation** causes **opposite effects** in neutrinos and antineutrinos.
3. **Matter effects** also produce **opposite effects** in neutrinos and antineutrinos.
4. The **octant of  $\theta_{23}$**  causes either a **suppression** or **enhancement**.





A resonant cavity allows us to set up a radio-frequency (RF) standing wave inside it with significant voltage and minimal power loss. The first figure shows an example of a cavity with electric and magnetic field lines that result from exciting the cavity with an RF source. Both fields oscillate sinusoidally, reversing direction during each cycle as shown in the second figure. The bunched beam is present in the cavity only when the electric field is oriented to provide an acceleration. The oscillations make it possible for the standing wave to reach substantial potentials. By stringing cavities together, we can achieve on more than a million volts for each pass of the beam around the accelerator.

# Far Detectors: Liquid Argon Time Projection Chamber (LArTPC)



Event display in LArTPC (MicroBooNE MC)

- High resolution 3D track reconstruction
  - Charged particle tracks ionize argon atoms
  - Ionized electrons drift to anode wires ( $\sim$ ms) for XY-coordinate
  - Electron drift time projected for Z-coordinate
  - Ionizing electrons drift long distances, impurity atoms attract electrons  $\rightarrow$  liquid argon purity is essential to signal detection
- Argon scintillation light ( $\sim$ ns) detected by photon detectors, providing  $t_0$

**Table 1.** Fundamental properties of common WLS materials used in LAr detectors: peak emission wavelength ( $\lambda_{em}$ ), PLQY, re-emission lifetime ( $\tau$ ), refractive index ( $n$ ), vapour pressure ( $p_{sat}$ ), and approximate sublimation temperature ( $T_m$ ).

Wavelength Shifter	$\lambda_{em}$ [nm]	PLQY @ 128 nm	$\tau$ [ns]	$n$	$p_{sat}$ [mbar]	$T_m$ [°C]	Comment
TPB	430	0.6 [25]–2 [26]	2	1.7	$10^{-11}$	204	
p-Terphenyl	350	0.82 [27]	1	1.65		213	PLQY @ 254 nm
bis-MSB	440	0.75–1 [28,29]	1.5	1.7		180	PLQY rel. to TPB
pyrene	470	0.64 [30]	155	1.8	$6 \cdot 10^{-6}$	150	PLQY @ 260 nm
PEN	420	0.4–0.8 [31]	20	1.75	–	270	PLQY rel. to TPB

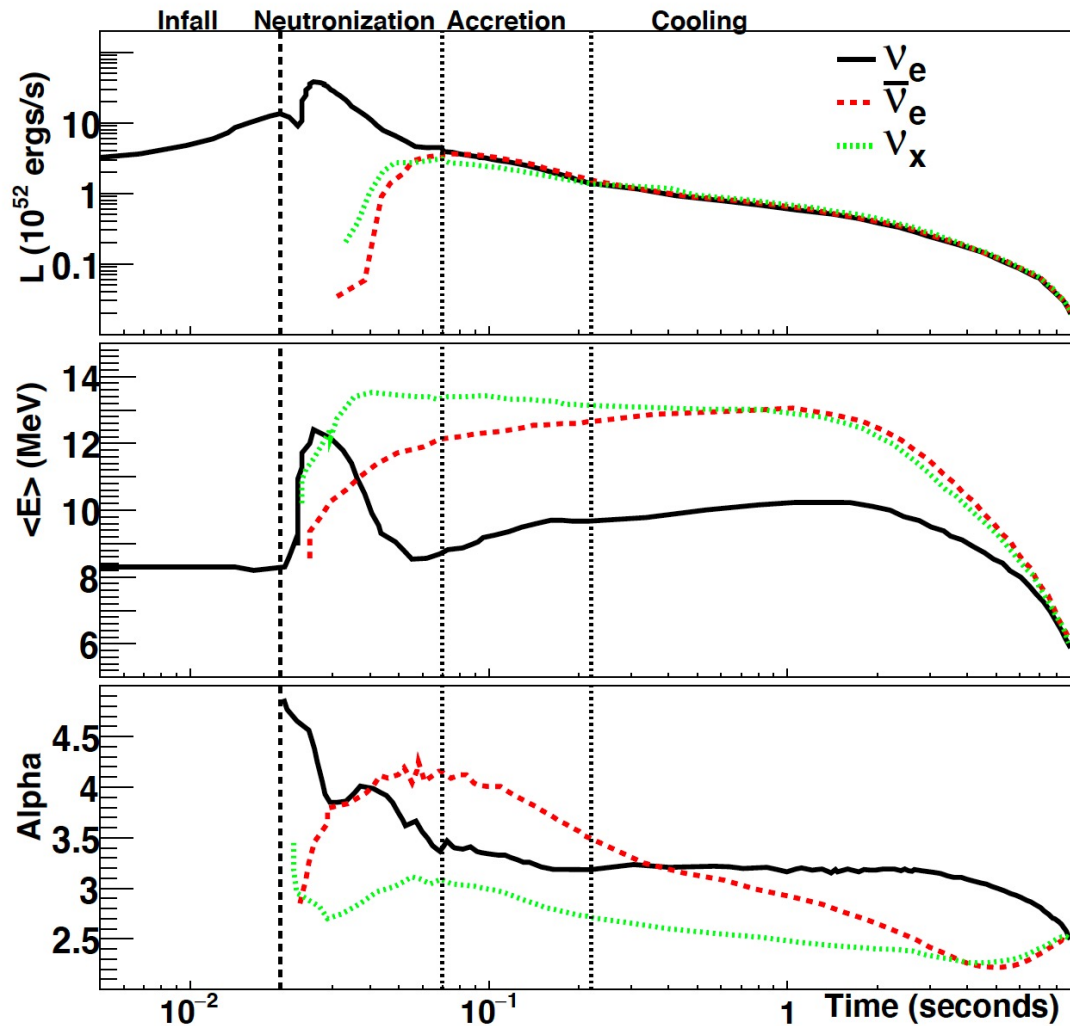


Figure 7.1: Expected time-dependent signal for a specific flux model for an electron-capture supernova [249] at 10 kpc. No oscillations are assumed. The top plot shows the luminosity as a function of time, the second plot shows average neutrino energy, and the third plot shows the  $\alpha$  (pinching) parameter. The vertical dashed line at 0.02 seconds indicates the time of core bounce, and the vertical lines indicate different eras in the supernova evolution. The leftmost time interval indicates the infall period. The next interval, from core bounce to 50 ms, is the neutronization burst era, in which the flux is composed primarily of  $\nu_e$ . The next period, from 50 to 200 ms, is the accretion period. The final era, from 0.2 to 9 seconds, is the proto-neutron-star cooling period. The general features are qualitatively similar for most core-collapse supernovae.